공학박사학위논문

Development of Oxime Palladacycle Resin, Ionic Liquid Resin, and Core–Shell-Type Resin Designed for Efficient C-C Coupling and Peptide Synthesis

효과적인 탄소-탄소 결합 반응과 펩타이드 합성을 위하여 고안된 옥심 팔라다싸이클 수지, 이온성 액체 수지, 코어-쉘 타입 수지 개발

2013년 2월

서울대학교 대학원

화학생물공학부

조 홍 준

효과적인 탄소-탄소 결합 반응과 펩타이드 합성을 위하여 고안된 옥심 팔라다싸이클 수지, 이온성 액체 수지, 코어–쉘 타입 수지 개발

Development of Oxime Palladacycle Resin, Ionic Liquid Resin and Core–Shell-type Resin Designed for Efficient C-C Coupling and Peptide Synthesis

지도 교수 이 윤 식

이 논문을 공학박사 학위논문으로 제출함

2013년 2월

서울대학교 대학원

화학생물공학부

조 홍 준

조홍준의 공학박사 학위논문을 인준함

2013년 2월

위 원 장 김 영 규 (인)

부위원장 이 윤 식 (인)

위 원 백 승 걸 (인)

위 원 공 영 태 (인)

위 원 이 상 영 (인)

Abstract

Development of Oxime Palladacycle resin, Ionic Liquid resin, and Core–Shell-Type resin Designed for Solid-phase Peptide Synthesis and C-C coupling

Hong-Jun Cho

School of Chemical and Biological Engineering

The Graduate School

Seoul National University

Polymer support is a very useful tool for organic synthesis and chemical process. A polymer support on which metal or organic catalyst are immobilized has been used as a heterogeneous catalyst and a functionalized polymer support with linker has been used in SPPS and SPOS. Because the polymer support is mostly insoluble in solvents, it can be easily isolated from the reaction media by simple filtration and reused many times. Furthermore, it is possible to design simple chemical processes through repeating reaction and filtration. Despite these advantages, there are several

limitations in using polymer support because the reaction occurs between a solid and a liquid interface. Therefore, the development of highly efficient polymer supports still remains a challenge in SPPS and heterogeneous catalyst fields.

In this thesis, three different types of polymer supports were developed for efficient Suzuki coupling reaction and SPPS: palladated oxime resins, ionic liquid resins, and core–shell-type resin.

In the first part, various oxime derived palladacycle resins were prepared as a heterogeneous catalyst for Suzuki coupling reaction of aryl halide with arylboronic acid. Unlike Kaiser oxime resin, electron-rich oxime resins afforded efficient and stable environment to form a palladium complex. The electron-richness of oxime ligand could be controlled by the number of methoxy group. The electronic effect of oxime ligand on C-C coupling reactions of activated and deactivated aryl halide (Cl, Br, I) with arylboronic acid were studied with the oxime palladacycle resins. The most electron-rich oxime resin catalyzed Suzuki coupling reaction in high yield and displayed high turnover number without severe leaching of palladium. In reusability test, two methoxy substituted oxime palladacycle resin could be reused during 5 cycles maintaining good catalytic activity for C-C coupling.

In the second part, ionic liquid (IL) resins with an ionic liquid environment on polymer support were prepared by immobilizing ionic liquid spacers on polystyrene (PS) resin. The properties of IL resins were dramatically changed as the anions of IL were exchanged. The performance of IL resins for solid-phase peptide synthesis

(SPPS) was evaluated by measuring coupling kinetics of the first amino acid and synthesizing several peptides on IL resins. Initial loading of amino acids were performed very efficiently on IL resins with PF_6^- and $TFSI^-$ anions. They also achieved higher purity in the synthesis of difficult sequences peptide than that of AM PS resin.

In the third part, a simple, mild and inexpensive bi-phasic functionalization approach is attempted for preparing an ideal core–shell-type resin. The core–shell-type architecture was constructed by coupling Fmoc-OSu to the amino groups on the shell layer of an aminomethyl polystyrene (AM PS) resin. The shell layer thickness of the resin could be easily controlled under mild conditions. The efficiency of core–shell-type resin for solid-phase peptide synthesis (SPPS) was demonstrated by the synthesis of various peptides, and compared with commercially available non-core–shell-type resins, such as AM PS and poly(ethylene glycol)-based resins. The core–shell-type resin provided effective performance during the synthesis of hydrophobic peptide sequences, a disulfide-bridged cyclic peptide and a difficult PNA sequence. Furthermore, a highly aggregative peptide fragment, MoPrP 105–125, was synthesized more efficiently on the core–shell-type resin under microwave condition than AM PS and ChemMatrix resins.

Keywords: solid-phase peptide synthesis, core–shell-type resin, ionic liquid resin, Suzuki coupling reaction, heterogeneous catalyst, oxime palladacycle resin

Student Number: 2007-21226

Table of Contents

Chapter II. Polymer-Supported Electron-Rich Oxime Palladacycles as an Efficient Catalyst for C-C Coupling

Chapter III. Ionic Liquid Resin for Solid-Phase Peptide Synthesis

Chapter IV. Core–Shell-Type Resin for Solid-Phase Peptide Synthesis

List of Abbreviations

ACP	acyl carrier protein
AM PS	aminomethyl polystyrene
API	1-(3-aminopropyl)imidazole
β_2M	β_2-Microglobulin
Boc	*t*-butoxycarbonyl
Bts	benzothiazole-2-sulfonyl
*t*Bu	*tert*-butyl
CLEAR	cross-linked ethoxylate acrylate resin
CLSM	confocal laser scanning microscope
CM PS	chloromethyl polystyrene
CNC	2,4,6-trichloro-1,3,5-triazine
DIPEA	*N*,*N*-diisopropylethylamine
DMA	dimethylacetamide
DMF	*N*,*N*-dimethylformamide
DMSO	dimethylsulfoxide
DVB	divinylbenzene
EA	elementary analysis
EDX	energy dispersive X-ray spectrometer
EGDMA	ethylenglycol dimethylacrylate
EtOH	ethanol
FE-SEM	field emission scanning electron microscopy
FITC	fluorescein isothiocyanate

Fmoc	9-fluorenylmethoxycarbonyl
Fmoc-Rink-linker	*p*-[(R,S)-*α*-[1-(9H-fluoren-9-yl)-methoxyformamido]-2,4-dimethoxybenzyl]-phenoxyacetic acid
FT-IR	Fourier transform-infrared spectroscopy
GC-MS	gas chromatography-mass spectrometry
HBTU	2-(1H-benzotriazole-1-yl)-1,1,3,3-tetramethyl-uronium hexafluorophosphate
HOBt	1-hydroxybenzotriazole
HPLC	high-performance liquid chlromatography
ICP-AES	inductively coupled plasma-atomic emission spectrometry
IL	ionic liquid
iRGD	internalized RGD
JR 10-mer	Jung–Redemann 10-mer
MALDI-TOF	matrix-assisted laser desorption and ionization-time of flight
MeCN	acetonitrile
MeOH	methanol
MoPrp	mouse prion peptide
NHC	*N*-heterocyclic carbene
NMP	*N*-methylpyrrolidinone
NMR	nuclear magnetic resonance
OTf	trifluoromethanesulfonate
PEG	poly(ethylene glycol)
PNA	peptide nucleic acid
PS	polystyrene
PVP	poly(vinylpyridine)
SPOS	solid-phase organic synthesis

SPPS	solid-phase peptide synthesis
TBA	tributylamine
TBAB	tetrabutylammonium bromide
TEA	triethylamine
TEG	triethyleneglycol
TFA	2,2,2-trifluoroacetic acid
TFSI	bis((trifluoromethyl)sulfonyl)imide
THF	tetrahydrofuran
TIS	triisopropylsilane
TLC	thin layer chromatography
TMS	tetramethylsilane
TOF	turnover frequency
TON	turnover number
Trt	trityl
UV-vis	ultraviolet-visible spectrophotometer
XPS	X-ray photoelectron spectroscopy

List of Figures

List of Schemes

List of Tables

Table 12. Peptide Sequences of MoPrP(105–125) Peptide Fragments Analyzed by Edman Degradation

Chapter I

General Introduction

1. Solid-Phase Peptide Synthesis

As a therapeutic molecule, peptides have various advantages based on their high specificity for targets, low immunogenicity, no tissue accumulation, and minimal side effects.[1] For these reasons, peptide therapeutics has begun to receive much attention from many pharmaceutical companies in innovative drug development. In 2010, there were around 60 peptide drugs that had been approved by Food and Drug Administration (FDA), and 140 peptide drugs in clinical trials and over 500 peptide drugs in pre-clinical phases.

These peptides are mostly manufactured by recombinant and chemical synthetic methods. The recombinant method is not only a natural process, but also an effective process for longer sequences of more than 100 residues. It can also offer a price advantage at large production scales.[2] Despite the advantages of the recombinant method, it is still a complicated process and cannot produce unnatural and modified peptide sequences.[3] In contrast, the chemical method is a simpler process and easier to scale up and it can be more cost-effective from gram to multi-kilogram scale.[4] In chemical synthesis, there are two major synthetic methods; solution-phase and solid-phase synthesis. Solution-phase synthesis is widely used for production of short peptide chains, large-scale production, structure modification, peptide ligation, and conjugation.[5] However, it has technical problems in solubility, isolation, and purification in each step. In order to address the

difficulties in solution-phase synthesis, Bruce Merrifield first introduced solid-phase peptide synthesis, which proceeds on the attachment of amino acid to a polymer support, elongating peptide chain in stepwise manner, and cleavage of the final peptide from the solid support.[6] This method offers numerous advantages over conventional synthesis in terms of synthetic efficiency as well as convenient work-up and purification procedures. Because of using the polymer support, however, solid-phase peptide synthesis sometimes encounters coupling difficulty and certain limitation during the synthesis of aggregative peptide. As a result, diverse attempts have been tried to enhance the efficiency of SPPS, such as the development of a new synthetic strategy, new coupling reagents, new polymer supports, and the use of microwave reactors.[7]

Recently, solid-phase and solution-phase hybrid synthesis method have been focused as the key to manufacture large scale and long sequences peptide synthesis[8], through synthesizing protected peptide fragments by SPPS and combining them by solution-phase method. Using these methods, various peptide pharmaceuticals have been manufactured for clinical purpose (Table 1).[9,10]

Table 1. Approved Peptide Pharmaceuticals Manufactured by Various Methods[9,10]

peptide	length	manufacturing method[a]
adrenocorticotropic hormone (1–24)	24	C
bivalirudin	20	C
growth-hormone-releasing factor (1–29)	29	SP
integrelin	7	C
oxytocin	9	C
atosiban (oxytocin antagonist)	9	C
thymopentin (TP-5)	5	C
thymosin α-1	28	SP
thyrotropin-releasing hormone	3	C
cyclosporin	11	E
insulin	51	E, S, R
glucagon	29	E, SP, R
calcitonins (Human)	32	C
calcitonins (Salmon)	32	C, SP
leuprolide	9	C, SP
goserelin	10	C
cetrorelix	10	SP
somatostatin and analogues	14	C, SP
secretin	27	E

[a]Manufacturing methods – C: classical (solution-phase) synthesis; E: extraction from natural sources; R: recombinant; S: semisynthesis; SP: solid-phase synthesis.

2. Core–Shell-Type Resin

2.1. Core–Shell Structure

Core–shell-type structure of a polymer particle is the one, in which compositions or functional groups in core part are different from those of shell part, or composition are the same, but each property of them is different by degree of crosslinking. Since the physical properties of core–shell particles has been investigated by Hughes and Brown,[11] various interesting particles, which has core–shell structure, have been prepared and applied as impact modifiers, toughening agents, film aids, carriers, and solid supports. The general preparation methods of core–shell-type polymer are shown in Figure 1.[12]

Two-stage seeded emulsion polymerization (Figure 1a) is the common method developed to prepare latex polymers with core–shell structure.[11,13–15] The first stage to prepare core latex is carried out either separately or in situ, and then the second stage polymerization is performed on a seeded swelling batch or a semi-batch process. This process is usually used to produce highly cross-linked latex particles.

Core–shell-type particles can be also obtained by suspension polymerization with a hydrophobic monomer and an amphiphilic monomer, which acts as a comonomer and a stabilizer, as in the case of styrene monomer and poly(ethylene glycol) (PEG) modified monomer.[16–20] Under the proper condition (temperature, pH, and the

concentration of the monomer), a hydrophobic monomer is polymerized in the core part, and amphiphilic monomer, which is located at the interface between the water and the styrene drop, is copolymerized on the shell of the particles (Figure 1b).

Using block copolymers, core–shell structure can be produced by controlling the crosslinking part (Figure 1c). After preparing micelle structure using amphiphilic block copolymer, core–shell-type polymers are produced by cross-linking the segregated chains in the spherical microdomains of di- or triblock copolymer films or micelles.[21,22] As a result, core-crosslinking block copolymer particles with linear chains are attached to the core surface, and shell-crosslinking block copolymer particles were synthesized for analytical, biomedical, and environmental application.[23–25]

Polystyrene resin (PS) is composed of hydrophobic matix and can be swollen well in CH_2Cl_2, NMP, and DMF. When incompatible solvents to the PS resin such as EtOH, and ethylene glycol are used, the solvents can partially contact the shell part of resin and do not fully penetrate into the inner part of resin.[26–28] Therefore, the resin containing an amide or ester bond can be partially hydrolyzed by acid or base reagents dissolved in such incompatible solvents. By using this method, core–shell structure, which has different functional groups in the core and the shell part of resin, is generated on PS resin (Figure 1d).

Bi-phasic funtionalization method can construct topologically segregated bifunctional structure on a resin by utilizing the phase difference between resin and solvent (Figure 1e).[29–32] In order to build bi-phasic environment, water phase is

formed in the resin by acid treatment, and then the resin is exposed to organic solvent that contains derivatizing reagents. In this reaction, derivatizing reagents in organic solvent can contact only the outer layer of resin, and can change the functional group on the shell part. After modifying the shell of resin, the core of resin can be also changed to another functional group. By varying the ratio of organic solvents and adjusting the amount of reagents used, the thickness of the shell layer can be controlled.[30]

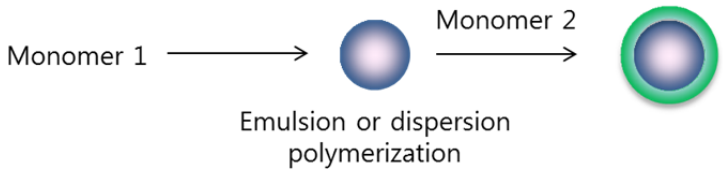

(a) Two-stage seeded emulsion polymerization

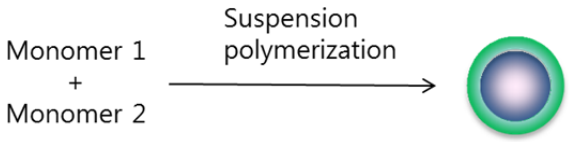

(b) Suspension polymerization with hydrophilic monomer 2

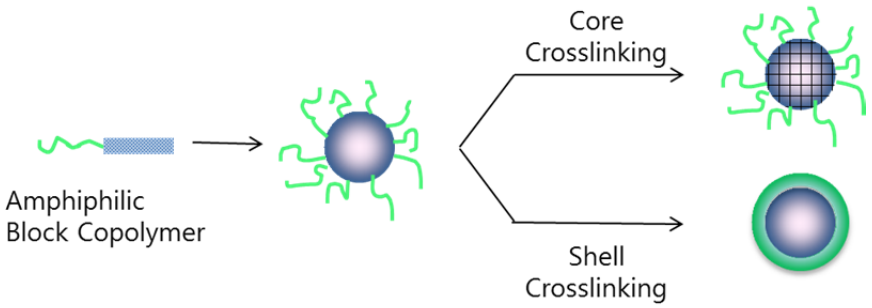

(c) Core-crosslinking or shell crosslinking polymerization

Figure 1. General procedure for preparation of core–shell-type resin. (continued)

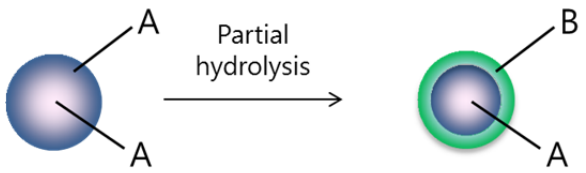

(c) Partial hydrolysis method

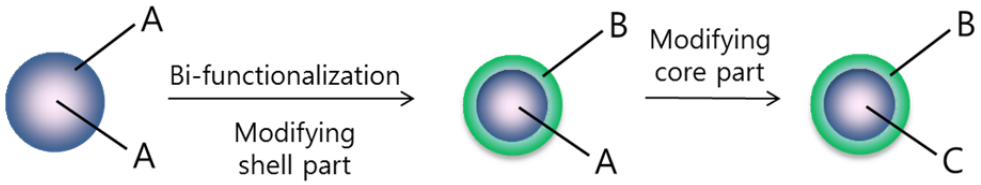

(c) Bi-phasic functionalization method

Figure 1. General procedure for preparation of core–shell-type resin.

2.2. Core–Shell-Type Resin for Peptide Synthesis

A resin, in which reactive functional groups are located on shell layer, has the advantage over non-core–shell-type resin in solid-phase organic reaction due to its distinctive structure. As it has high accessibility from incoming reagents, core–shell-type resin can overcome diffusion problems caused by polymer matrix, thereby, enabling efficient solid-phase reaction.[17,27] The common core–shell-type resin prepared by several methods are in Figure 2.

CutiCore® resin has amino groups with PEG at the shell layer of the resin prepared by suspension co-polymerization with styrene, divinylbenzene (DVB), and PEG macromonomer.[16,17] During suspension polymerization, styrene monomer and PEG macromonomer with DVB were copolymerized in monomer droplets (Figure 2a). In this reaction, PEG macromonomers, added as a comonomer and a stabilizer, were distributed on the surface of the reaction droplet due to their amphiphilic property. As a result, the functional groups with PEG were concentrated on the shell layer of resin. It gave better coupling efficiency than that of TentaGel resin in early stage of amino acid coupling in SPPS and exhibited rapid release of synthesized peptide in photolysis reaction.

HiCore® resin, which has similar structure to CutiCore® resin, was prepared by core-crosslinking and further grafting method (Figure 2b).[18] 2,4,6-Trichloro-1,3,5-triazine (cyanuric chloride, CNC) as a crosslinker was used to crosslink the core

part of aminomethyl polystyrene resin (AM PS). And then, a diamino-PEG derivative was added to replace the remaining chloride group of CNC on the shell layer. This core–shell-type resin also showed excellent results in the photocleavage reaction and more efficient initial loading kinetics than that of TentaGel and PS resins.

Another approach for preparation of core–shell-type resin for SPPS is partial hydrolysis method to prepare AMSURE^{TM} resin and core–shell-type MBHA resin (Figure 2c–d).[26–28] Before hydrolysis process, amide group containing resins were synthesized by attaching acetamidomethyl group or bis(formamide) group to PS resin. To construct core–shell structure, the amide groups on the resins were partially hydrolyzed under acidic condition in polar solvent, such as ethylene glycol or ethanol, which is not compatible to PS resin. Since hydrophilic reagents were not easily accessible to the core of hydrophobic PS resin during hydrolysis, the amide groups were converted into amino groups on the shell layer of the resins. Due to this core–shell structure which has high accessibility, the resins provided efficient performance during the synthesis of difficult peptide sequences.

To enhance the flexibility of polymer chains, soft shell resins were synthesized by two-step polymerization (Figure 2e).[33] Core–shell structure on resin was formed by the different degree of crosslinking between the core part and the shell part of the resin. After preparation of a crosslinked PS core with DVB, styrene was added and polymerized once again with little or without DVB to make a flexible shell layer of the resin. Combining the flexible property and core–shell structure, soft shell resin

enhanced the synthetic efficiency in SPPS.

Sulfonated core–shell-type resin was also prepared by partial sulfonation.[34] Sulfonated core–shell structure was formed using sulfuric acid in 1,2-dichloroethane in the same way as partial hydrolysis system. High local concentration of sulfonate groups on the shell layer of resin was attributed to higher catalytic activity than that of commercial sulfonated resin in alkylation of benzene with propene. Furthermore, amino groups were introduced exclusively on the surface of porous PS resin by plasma-chemical functionalization using allylamine or diaminopropane as the functionalizing agent.[35] Although loading level was relatively low, it allowed faster reaction than conventional resin in scavenging of benzoyl chloride.

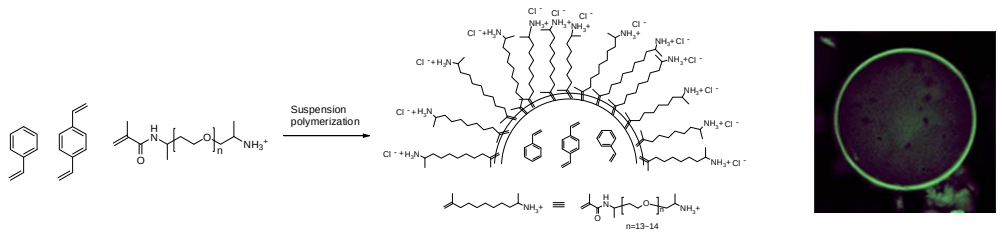

(a) CutiCore®

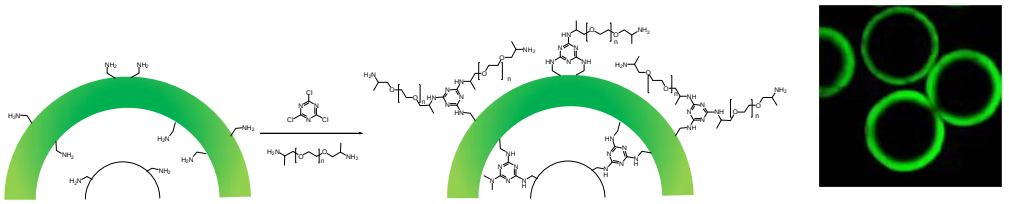

(b) HiCore®

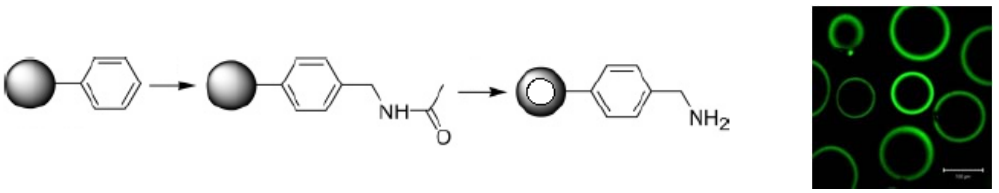

(c) AMSURE™

Figure 2. Various core–shell-type resins. (continued)

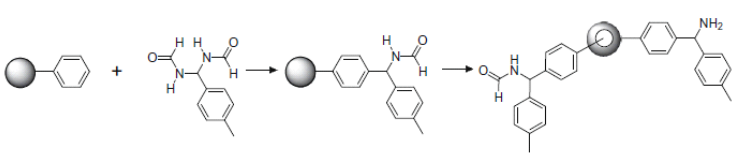

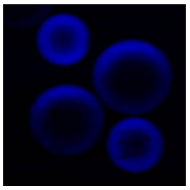

(d) Core–shell-type MBHA resin

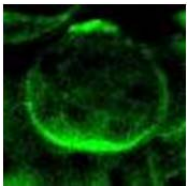

(e) Soft shell resin

Figure 2. Various core–shell-type resins.

3. Ionic Liquid Resin

3.1. Ionic Liquid

Ionic liquids (ILs) are salts that consist of cations and anions and remain liquid state at room temperature or below 100 °C.[36] Due to their versatile chemical and physical properties such as extremely low vapor pressure, high thermal stability, high conductivity, non-flammability, excellent miscibility, and tunable polarity, ILs have drawn increasing attention in their use as reaction media, electrolytes, catalysts, and soluble supports.[37–47]

The cations and anions generally used for ILs are listed in Figure 3. Most cations have positively charged nitrogen, phosphorus, and sulfur atom in low symmetric structure. From these atoms, heterocyclic and non-heterocyclic cations such as imidazolium, pyridinium, pyrrolidinium, phosphonium, ammonium, and sulfonium are synthesized for use as ionic liquids. Anions are weakly basic inorganic and organic compounds, which have negative charge. The most commonly employed IL anions are polyatomic inorganic anions such as $TFSI^-$ (bis((trifluoromethyl)sulfonyl) imide), OTf^- (trifluoromethanesulfonate), $N(CN_2)^-$, PF_6^-, BF_4^-, Hal^-.[48] Through the combination of cations and anions, various kinds of ILs are available.

Since the discovery of ILs such as ethanolammonium nitrate and ethylammonium

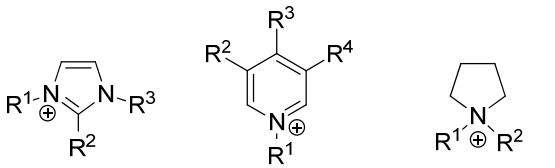

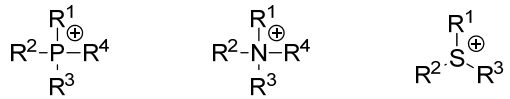

(a) Cations of ILs

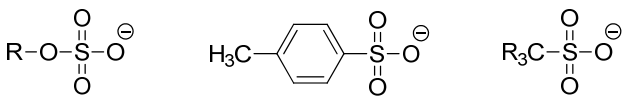

(b) Anions of ILs

Figure 3. Generally used cations and anions for ionic liquids.

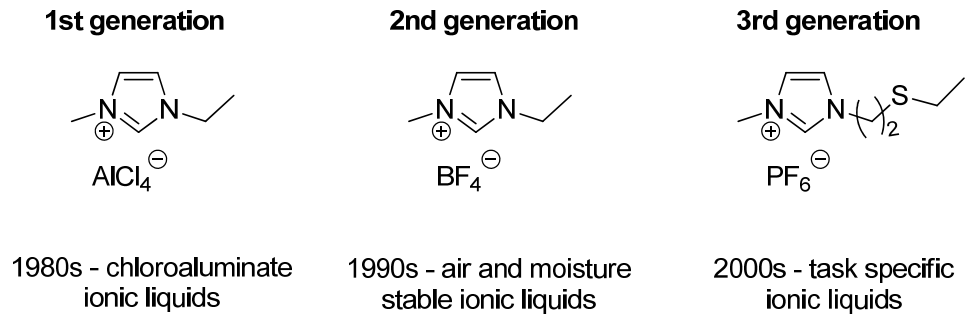

Figure 4. Improvement of the properties of ILs.

nitrate,[49,50] diverse types of IL have been synthesized and applied in various fields (Figure 4).[36] 1-Alkyl-3-methylimidazolium salts, widely used in ILs applications, were first introduced with tetrachloroaluminate anion (first generation), which afforded promising activity in electrochemistry.[51] To supplement air and moisture sensitivity of ILs, air and moisture stable ILs (second generation) were developed by replacing tetrachloroaluminate anion to tetrafluoroborate and other anions.[52] These ILs are still used in many applications as solvents and reaction media. As the next generation of ILs, task-specific ILs (third generation) were developed to add more functionalities designed to improve activity or provide particular properties.[53,54] The functionalities are incorporated on ILs by grafting precursors onto one of the ion structures. Because many ILs for specific reaction can be synthesized by loading diverse functional groups, the area of IL applications is continuously expanding.

3.2. Characteristics Properties of Ionic Liquid

The physical and chemical properties of ILs are diverse over a wide range by the suitable selection of both cations and anions. For examples, acidity, hydrophobicity, conductivity, and viscosity of ILs can be easily modified by changing only anion. Due to tunable properties to optimize reaction environment with a specific purpose, ILs have been refer to as "designer solvents".[55] Distinctive and changeable features of ILs by changing their structure and ion species are summarized (Table 2).[56–61]

Melting point

Being different from inorganic salts (NaCl: 803 °C, KCl: 772 °C), ILs have relatively low melting point from below room temperature to above 100 °C. The following features are attributed to low melting point by disrupting packing efficiency and hydrogen bonding: low symmetry, weak intermolecular interaction and a good distribution of charge in the cation.[62–64] In most cases, an increasing size of the anion leads to a decreasing melting point of ILs.[65]

Vapor pressure and thermal stability

A negligible vapor pressure and high decomposition temperature (120–360 °C)

arise from the strong ionic interaction between ions within ILs. They allow ILs to have non-volatile, highly thermal stable and non-flammable properties, which are advantageous from process engineer's viewpoint. In terms of thermal stability, ILs with $TFSI^-$ or OTf^- anion are generally used in the chemical reaction, which requires harsh condition since hydrolysis of PF_6^- or BF_4^- anions produces the formation of HF.[66]

Density

The density of an ionic material is usually determined by the size and shape of ions and the extent of interaction between ions. In most ILs, the density basically decreases as the bulkiness of cation increases and as the alkyl chain length increases. Heterocyclic amine cation containing ILs have higher density than those of the alkylammonium cation due to their structural features.[58] Changing the anion also results in more obvious effects in several examples. The order of the density of anion species with 1-buthyl-3-methyl imidazolium cation are shown as $TFSI^- > PF_6^- > OTf^- > BF_4^- > Cl^-$ (Table 2). Substitution of functional groups on a cation and an anion can have influence on the density of ILs. A hydroxyl group introduction onto the alkyl chain of the cation or the anion significantly increases the density because of decreasing the ion-ion separations by increased hydrogen bonding.[67] In contrast to viscosity, increasing temperature have little effect on the density of ILs.

Viscosity

The viscosity essentially depends on ion-to-ion interactions within ILs such as hydrogen bonding and van der Waals interactions.[68] The viscosity of ILs generally increase as the size of cation increases with alkyl chain length, which results in greater van der Waals interaction. In anion cases, ILs with strongly coordinated anions (Cl^- and NO_3^-) have higher viscosity than those with weakly coordinated anions (BF_4^-, PF_6^-, OTf^-, and $TFSI^-$).[69] Strongly coordinated anions can contribute to increase of ion-to-ion interaction within ILs. As expected, the viscosity of ILs is sharply lowered by slightly increasing temperature or by adding some co-solvents.[70,71]

Ionic conductivity

The ionic conductivity is controlled by the ions mobility. This factor depends on the viscosity and the number of charge carriers, which is controlled by molecular weight, density, and sizes of ions.[72–74] As a result, ILs with low viscosities and good distributions of charge have higher conductivities. Typical ILs conductivities are in the range from 1.0 mS/cm to 10.0 mS/cm. Therefore, ILs are good candidates for use as electrolytes or in other applications where a high conductivity combined with wide electrochemical window, non-volatile, electrochemical stability is required.

Polarity

ILs are generally regarded as highly polar substances due to their ionic nature. Their polarities are determined by molecular structure and interaction based on coulombic interactions, dipole interactions, hydrogen bonding, and van der Waals force.[75,76] Hence, different combinations of cations and anions generate various ILs with different polarities. Dielectric constant (ε), one of the criteria that estimates the polarity of pure liquid, provides the propensity of the polarity of ILs (Table 2). In general, solvents with $\varepsilon < 9$ are considered to be nonpolar, those with $9 < \varepsilon < 15$ are reasonably polar, values in the range $15 < \varepsilon < 30$ are considered as polar solvent, and highly polar solvents have the values in excess of 50.[61] Most imidazolium ILs are characterized as moderate polar liquids ($9 < \varepsilon < 15$). The order of the dielectric constants of ILs with anions decreases as $Cl^- > OTf^- > BF_4^- > PF_6^- \approx TFSI^-$, which is the order of the decreasing basicity of the ions. The dielectric constant decreases as the length of the alkyl chain on the cations increases. These effects are similar to the behaviors of common solvents. The polarities of ILs are easily changed by changing anions or modifying alkyl chain length on cations.

Environmental aspect

Recently, ILs have turned out to be promising solvents for “clean processes” and “green chemistry”.[55,77] On account of their inherent properties, ILs can provide efficient processes in chemical reactions, particularly with regard to solvent and

catalyst usage. As solvents, ILs, which have negligible vapor pressure, can lead to no loss of solvent through evaporation and can contribute to safety by avoiding production of a volatile organic material.[78] In catalytic reactions, catalyst consumption can be reduced with the use of ILs. The distinctive solubility feature of ILs can set up bi-phasic reaction condition to allow catalyst to be isolated effectively during reactions.[61,79]

Table 2. Physico-Chemical Properties of Ionic Liquids at 20°C[56–61]

solvents or ILs	molecular weight	density (g/cm^3)	viscosity (cP)	melting point (°C)	dielectric point (ε)	polarity (Reichardt)
C4mim[Cl]	175	1.086	3950	41	15.0	–
C8mim[Cl]	231	1.009	337	-82	7.0	55
C2mim[BF_4]	198	1.294	66.5	15	14.8	–
C4mim[BF_4]	226	1.198	219	-81	12.9	68
C6mim[BF_4]	254	1.148	314	-82	11.3	70
C8mim[BF_4]	282	1.099	135	-80	7.5	67
C2mim[TfO]	263	1.387	45	-9	15.8	–
C4mim[TfO]	288	1.292	90	16	13.5	67
C2mim[PF_6]	256	–	–	60	14.7	–
C4mim[PF_6]	284	1.362	371	10	11.4	67
C6mim[PF_6]	312	1.293	680	-61	11.1	66
C8mim[PF_6]	340	1.235	866	-75	9.7	60
C2mim[Tf_2N]	391	1.518	34	-15	11.5	68
C4mim[Tf_2N]	419	1.435	60	-4	9.4	64
C6mim[Tf_2N]	447	1.377	87	-7	7.0	65
C8mim[Tf_2N]	475	1.337	119	–	6.5	63

The ILs are denoted as [C(n)mim][X] (1-alkyl-3-methylimdazolium, X^- = Cl^-, BF_4^-, TfO^-, PF_6^-, Tf_2N^- where n indicates the number of carbon atoms in 1-alkyl chain.

3.3. Supported Ionic Liquid

Due to their versatile features of ILs, ILs have been utilized in catalytic reactions and as soluble supports.[47,61] ILs with acidic anions have been used as catalysts and also solvents in esterification and dehydration reaction.[80–83] As coordinating ligand, ILs have been employed in hydrogenation, hydroformylation, and C-C coupling reactions with various transition metals.[84,85] Peptides or small molecules have been synthesized on ILs as soluble supports for easy separation of the product.[47] However, homogeneous system have some problems in separation of the catalyst from the products of the reaction. Such difficulty leads to waste of expensive catalysts and to the danger of exposing highly reactive chemicals into the environment. Therefore, heterogenized ILs have been recently emerged as a new solid support.[86] This supported-IL facilitates easy separation and purification of catalyst or product from reaction mixture.

There are several approaches to immobilize ILs on solid supports (Figure 5). Via anion immobilization, a solid support is impregnated with a IL which contains catalytic activity. The supported ILs composed of aluminum chloride derivatives are examined for Friedel-Crafts reactions.[87,88] Another approach is to immobilize the cation of IL on solid support with and without the metal complex. The IL attached to an organic anchoring group can be covalently immobilized on solid support. Furthermore, precursor of IL such as an imidazole group is directly immobilized on

halogenated surface for the formation of a IL.[89,90] The resulting catalysts, which were investigated for the alkylation of benzene with olefins, exhibited excellent activities and selectivities.[89] Supported-ILs can also chelate various transition metals to make metal complex on solid support. These metal catalysts provided reasonable catalytic activity and reusability for hydrogenation, hydroformylation, olefin metathesis, and several C-C coupling reactions.[91–96] For encapsulation of ILs catalyst, ILs grafted with alkyl chain or polymer precursor such as vinyl, methyl methacrylate, and silanol groups are polymerized with another monomer or themselves to obtain ILs-incorporated nano/microparticles.[97–102] Depending on the preparation methods, a variety of structures were developed to improve catalytic activity.[100,102]

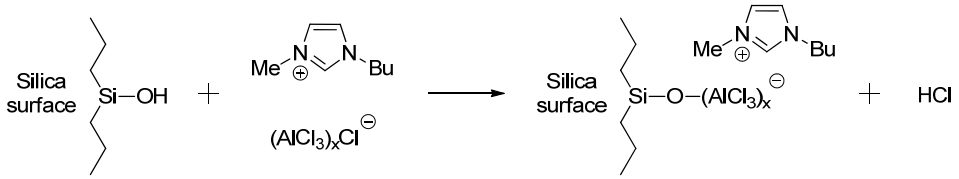

(a) Immobilization method via the anion

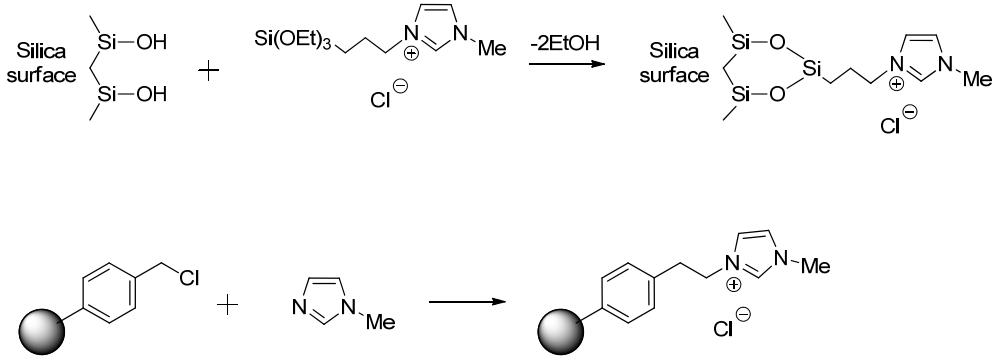

(b) Immobilization method via the cation

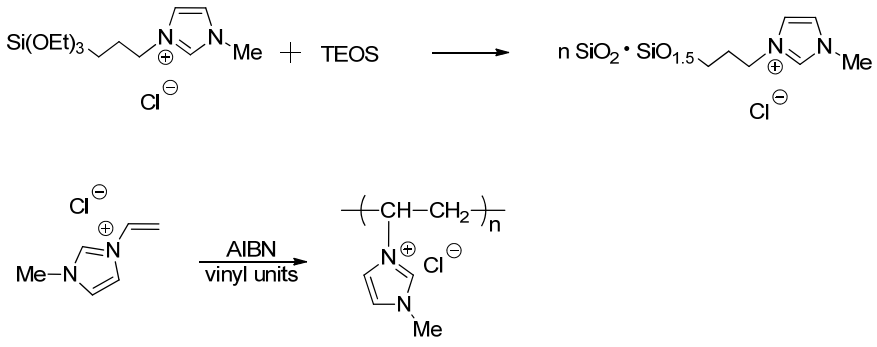

(c) Encapsulation methods

Figure 5. Various immobilization methods of ILs.

4. Oxime Palladacycle Resin

4.1. Oxime Palladacycle

Palladacycles,[103] defined as a palladium complex containing one palladium-carbon bond intramolecularly stabilized by one or two neutral donor atoms, have been exhibited to be very efficient precatalysts for palladium-mediated coupling reactions. Since cyclopalladated azobenzene complexes were first synthesized by Cope and Siekman in 1965 (Figure 6, **1**),[104,105] palladacycles have become more interested in coupling reactions due to their availability, thermal stability, and high catalytic activity.[103] The research on palladacycles as catalysts began in earnest by Herrmann and Beller in 1995 (Figure 6, **2**). They developed phosphopalladacycles for the Pd-catalyzed Heck and Suzuki reactions of unreactive aryl bromides and activated aryl chlorides with high turnover numbers (TONs).[106,107] The compound, which has

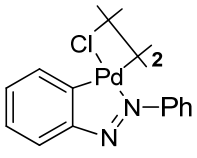

1

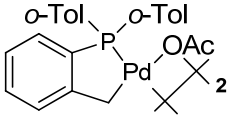

2

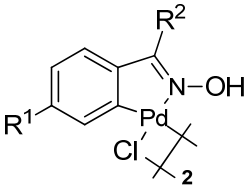

3a, R^1 = Cl; R^2 = 4-ClC_6H_4
3b, R^1 = OH; R^2 = Me
3c, R^1 = H; R^2 = Me

Figure 6. Typical palladacycles.

stable palladium with high thermal stability, can be prepared at low cost. Recently, Nájera and co-workers reported highly active oxime palladacycles which is robust and easily prepared catalyst for a wide range of C-C coupling reactions (Figure 6, **3**). These oxime-derived palladacycles are remarkably thermal stable and not sensitive to oxygen and moisture, as well as their facile and economical synthetic route.[108]

Oxime palladacyles are easily synthesized via the aromatic metallation of the oximes with palladium source.[109] The catalysts (**3a** and **3b**) have been investigated as precatalysts in aprotic polar solvent such as DMF, DMA, and NMP for Heck, Suzuki, Stille, Ullmann, and Sonogashira coupling reactions and also for cycloannulation reactions with internal alkynes.[110–112] Among them, oxime palladacycle **3a** exhibited outstanding catalytic activity (TON up to 10^{10}) in Heck reaction with n-butyl acrylate and phenyl iodide.[113] Oxime palladacycle **3b** was designed to operate under aqueous media condition employing conventional thermal or microwave heating. The catalyst afforded high catalytic activity for Heck, Suzuki, and Hiyama reactions under neat water in the presence of TBAB.[110–112] Furthermore, an interesting approach for oxime palladacycle catalyst is to combine oxime palladacycles with bulky and electron-rich ligands such as phosphine and *N*-heterocyclic carbene (NHC) (Figure 7, **5**–**7**).[114,115] The hybrid palladium complexes were prepared by the reaction of corresponding chloro-bridged cyclopalladated compounds with monodentate phosphine and NHC ligands. The monomeric complexes enhanced thermal stability and reactivity of the palladacycles compared to those of the dimeric ligands.[115]

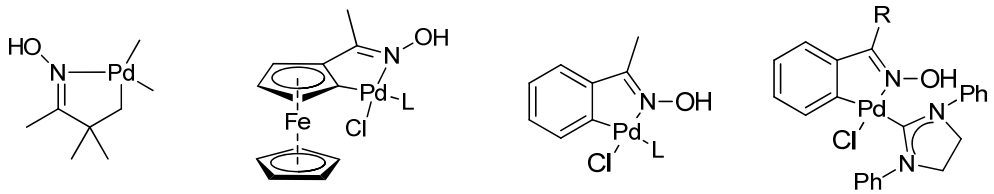

4

5a, L = PPh_3
5b, L = $P(OEt)_3$

6a, L = PPh_3
6b, L = $P(OEt)_3$

7a, R = Me
7b, R = Ph

Figure 7. Other oxime-palladacycles.

4.2. Supported Oxime-Derived Palladacycle

As oxime palladacycles showed highly catalytic activity in various C-C coupling reactions, interests in heterogenized oxime palladacycle grow for easy separation, reuse of the catalyst, and green process. To combine oxime palladacycles with heterogeneous system, various organic and inorganic supports such as ionic liquid, SiO_2, MCM-41, PS, poly(vinylpyridine) (PVP), and ethyleneglycol-grafted dimethylacrylate polymer (EGDMA) have been utilized (Figure 8).[111,112]

Corma and co-workers modified oxime palladacycle (**3b**) and anchored it on various supports. Using silicate precursor, oxime palladacycle was covalently anchored on SiO_2 and MCM-41 (Figure 8a). Immobilized oxime palladacycle maintained its inherent catalytic activity in Suzuki coupling reaction with activated aryl chlorides in water system and was reused in seven times.[116,117] PS- and EGDMA-supported oxime palladacycles were obtained by radical polymerization of catalyst **3b** having terminal C=C double bond with PS-DVB and EGDMA, respectively (Figure 8b, 8c). These polymer-supported catalysts exhibited appropriate catalytic activity in Suzuki coupling reaction, but not as much as that from silica-supported catalysts in water system.[118] Moreover, C4mim[PF_6] IL was used as soluble support to immobilize catalyst **3b** for easy separation (Figure 8d).[119,120] Allowing easy isolation from reaction mixture by bi-phasic system, however, IL-supported catalyst had a limitation under basic condition due to the

formation of a complex between the carbene of IL and Pd. To address this problem, IL-supported catalyst was adsorbed on Al/MCM-41 by ionic interaction, which caused increasing the activity and reusability of Pd catalyst. But supported oxime palladacycle was not entirely stable under the reaction condition and still had palladium leaching problem.[119]

A new polymer supported oxime palladacycle was prepared from Kaiser oxime resin by Nájera's group (Figure 8e). The palladated Kaiser oxime resin afforded very efficient coupling activity in Suzuki and Heck reaction under organic and aqueous media.[121–123] Although coupling efficiency was slightly lower than that of dimeric palladacycles, reusability test showed high stability and activity of the catalyst with low levels of Pd leaching during at least eight times of repeated use.[121]

In different approaches to immobilize oxime palladacycle, coordination method using PVP resin and self-supported method via star-shaped ligands and Pd-chloro bridges were used (Figure 8f, 8g).[124,125] The non-covalently attached catalyst on PVP showed promising result in a batch as well as a continuous-flow process with good catalytic activity. The self-supported catalyst was stable, reusable and effective in Suzuki coupling reaction. However, these immobilization methods did not totally solve the basic problem of Pd leaching in coupling reaction condition.

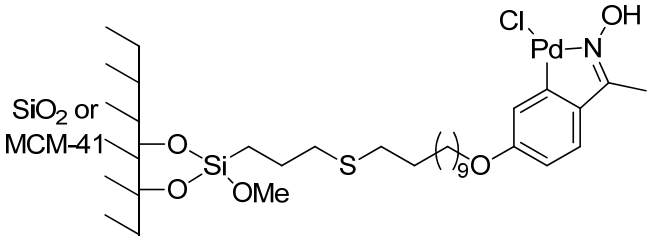

(a) silica-supported oxime palladacycle

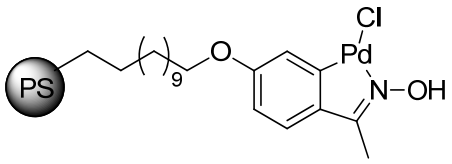

(b) PS-supported oxime palladacycle

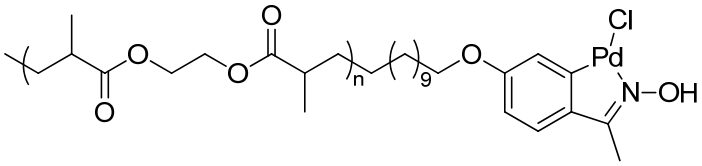

(c) EGDMA-supported oxime palladacycle

Figure 8. Supported oxime palladacycles. (continued)

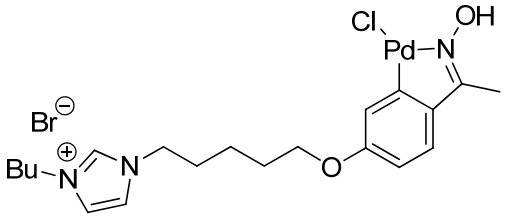

(d) IL-supported oxime palladacycle

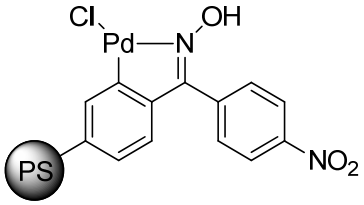

(e) Palladated Kaiser oxime resin

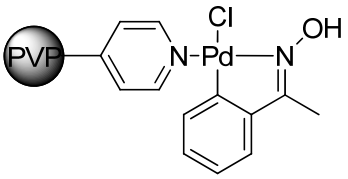

(f) PVP-supported oxime palladacycle

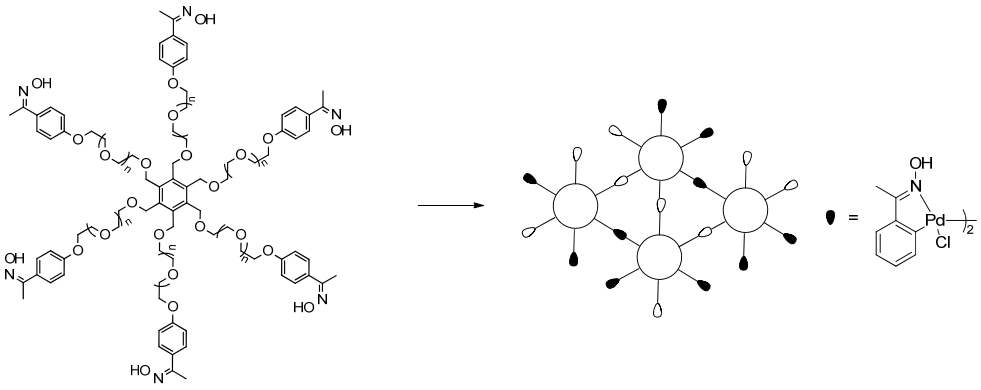

(g) Self-supported star-shaped oxime-palladacycles

Figure 8. Supported oxime palladacycles.

5. General Experimental Method

Materials

Unless otherwise noted, all solvents and reagents were obtained from commercial suppliers and used without further purification. CM PS, AM PS, and Kaiser oxime resin (1% DVB-PS, 100-200 mesh) was obtained from BeadTech, Inc. (Korea). CLEAR Resin was purchased from Peptide International, Inc. (Louisville, KY). TentaGel HL NH_2 was purchased from Rapp Polymere (Germany). H-Rink Amide-ChemMatrix was obtained from PCAS BioMatrix, Inc. (Canada). Bts (Benzothiazole-2-sulfonyl)-PNA monomer reagents were donated by Panagene, Inc. (Korea).

Instruments

^{1}H NMR data were recorded at Brucker 400 MHz spectrometer, and chemical shifts are based on TMS peak in $CDCl_3$ and DMSO-d_6. The resins were characterized by FT-IR (Bomem, FTLA2000) and elemental analysis (EA, Leco, CHNS-932). Confocal laser scanning microscope (CLSM, Carl Zeiss-LSM510) was used to verify core–shell-type structure. The morphologies of the resin were investigated by field emission scanning electron microscopy (FE-SEM, Jeol Inc. JSM-6700F). Palladium immobilized on the resin was detected by energy dispersive

X-ray spectrometer (EDX, Jeol Inc. JSM-6700F) and quantified by inductively coupled plasma-atomic emission spectroscopy (ICP-AES, SHIMADZU, ICPS-1000 Ⅳ). Palladium 3d binding energy was investigated by X-ray photoelectron spectroscopy (XPS, ThermoVG, SIGMA PROBE). The peptide fragments were analyzed on Younglin HPLC (Korea) using a SPIRIT PEPTIDE 120 C18 column (5 μm, 250 mm × 4.6 mm) (Louisville, KY) and Waters symmetry C18 (5 μm, 150 mm × 3.9 mm) (Milford, MA). Mass spectra were acquired on MALDI-TOF, Voyager-DETM STR Biospectrometry Workstation (Applied Biosystems, Inc., USA). Prion peptide was synthesized on a microwave-assisted peptide synthesizer (CEM).

Ninhydrin Color Test (Kaiser Test)[126]

To check whether amino groups exist or not on a resin, the stock solutions were prepared: potassium cyanide solution (2 mL of a 1 mM solution of KCN diluted to 100 mL with pyridine), ninhydrin solution (500 mg of ninhydrin in 10 mL of EtOH), and phenol solution (80 g of phenol in 20 mL of EtOH). One or two drops of each stock solution was added to 1–2 mg of resin sample in a test tube. The mixture was heated at 100 ℃ for 5 min. When primary amino groups exist on the resin, the color of the resin was changed to dark blue. If not, the color of the resin remains yellow.

Fmoc Titration[127]

To determine the amount of Fmoc group on a resin, 30 mg of resin sample was suspended in 3 mL of 20% piperidine in DMF. The mixture was shaken in shacking incubator at 25 ºC for 50 min. Aliquot (100 μL) of the supernatant solution was withdrawn and diluted to 10 mL with DMF. The resulting fulvene-piperidine adduct was quantified by UV absorbance at 290 nm. The loading level of the resin was given by the following equation.

$$\text{Loading level (mmol/g)} = (55.206 \times \text{Abs} - 1.0223) / 30$$

HPLC conditions

Condition A

For HPLC analysis, a flow rate of 1.0 mL/min and a 30 min-gradient of 0–60% of solvent B followed by a 10 min-constant flow of 100% solvent B (solvent A, 0.1% TFA in water; solvent B, 0.1% TFA in acetonitrile) was used with analytical column. Absorbance was measured at 230 nm and 260 nm.

Condition B

For HPLC analysis, a flow rate of 1.0 mL/min and a 30 min-gradient of 10–60% of solvent B followed by a 10 min-constant flow of 100% solvent B (solvent A, 0.1% TFA in water; solvent B, 0.1% TFA in acetonitrile) was used with analytical column. Absorbance was measured at 230 nm and 260 nm.

Chapter II

Polymer-Supported Electron-Rich Oxime Palladacycles as an Efficient Catalyst for C-C Coupling

1. Introduction

Recently, palladacycles[103] have been developed as an efficient catalyst to advance the stability of palladium complex and to increase catalytic activity for C-C coupling reaction.[128] Since phosphapalladacycle was highlighted by Herrmann for Heck and Suzuki reaction,[106,107,129] various kinds of phosphorous-,[130,131] nitrogen-,[132,133] sulfur-,[134] and oxygen-derived palladacycles[135] were emerged as prospective catalysts presenting high turnover numbers (TON) in various C-C coupling reactions. Nájera and co-workers reported that oxime palladacycles are highly active palladium catalyst for Heck, Suzuki, Stille, Sonogashira, Ullmann, and cycloannulation reactions.[110–112] These oxime palladacycles possess air, moisture and thermal stability and excellent TON in organic and aqueous solvents.

Despite a lot of successful demonstrations of oxime palladacycles in various C-C coupling reactions, homogeneous catalytic system gives rise to some problems related to the separation of catalyst and recycling for successive reaction. These limitations also lead to environmental issues when heavy metals are released during reaction. Therefore, it is important to transform a homogeneous catalytic system into a heterogeneous catalytic system which can lead to efficient recovery and reuse of the catalyst for green process.[96,136,137] Corma and co-workers immobilized covalently oxime palladacycle on high surface area solid supports as heterogeneous catalysts for Suzuki reaction.[116,118] On silica supports, oxime palladacycle with silica

precursor was covalently anchored maintaining its catalytic activity. PS- and EGDMA- supported oxime palladacycles were also prepared by radical polymerization of oxime palladacycle containing the terminal C=C double bond with PS-DVB and EGDMA monomers, respectively. Very recently, Nájera and co-workers prepared polymer supported oxime palladacycle from Kaiser oxime resin for Heck reaction.[121–123] The palladated Kaiser oxime resin was obtained by treating Kaiser oxime resin with palladium precursor (Li_2PdCl_4). This polymer supported catalyst could be reused during repeated reaction with low leaching of Pd.

In order to enhance the catalytic activity of Pd complex, the ligands have been modified or new ligand systems have been developed.[138,139] The performance of ligand as an efficient Pd catalyst are controlled by the bulkiness and electron richness. The bulkiness of ligand is known to accelerate the reductive elimination of product, while electron richness enhance the oxidative addition ability of Pd, which is a key step in catalytic cycle.[140,141] These two factors promote catalytic performance and stability of Pd in coupling reactions. Thus, various bulky aryl substituted NHCs and monodentate phosphine ligands possessing a bulky binaphthyl or dialkylbiaryl skeleton have been developed.[142–145]

Electron richness of oxime palladacycle can be tuned by varying substituents on acetophenone or benzophenone precursors. Although the catalytic effects of substituents on para position of acetophenone oxime or benzophenone oxime were reported,[108] an in-depth study of oxime palladacycle for C-C coupling reactions did

not progress in terms of electron richness. Thus, we synthesized series of electron-rich oxime palladacycles and immobilized them on PS resin. Unlike palladated Kaiser oxime resin, methoxy substituted oxime groups were used for electron-rich palladated oxime resin. The degree of electron richness of oxime ligand was controlled by the number of methoxy group. The catalytic activity of the palladated oxime resins was evaluated in Suzuki coupling reaction of aryl halide (Cl, Br, I) with arylboronic acid. Lastly, the reusability test of the catalysts was carried out.

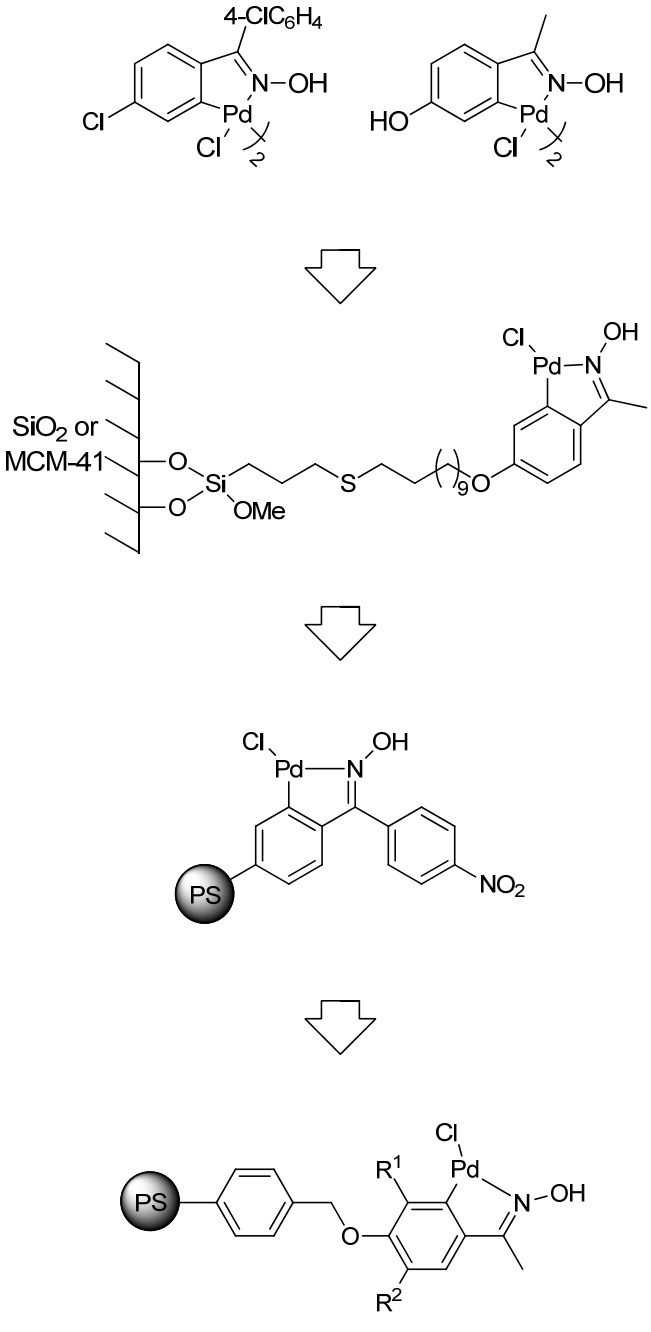

Figure 9. Development of oxime palladacycle catalysts.

2. Experimental Section

2.1. Preparation of Palladated Oxime Resins

2.1.1. Immobilization of 4′-Hydroxyacetophenone Derivatives on CM PS

CM PS resin (3 g, 2.19 mmol/g) was pre-swollen in DMF (100 mL) and 4′-hydroxyacetophenone (1.79 g, 13.14 mmol) and sodium methoxide (0.71 g, 13.14 mmol) were added to the resin. The mixture was stirred by overhead stirrer at 70 °C for 12 h. After cooling to room temperature, the resin **1a** was washed with H_2O, 1*N* HCl, DMF, CH_2Cl_2, and MeOH (×3) and dried in vacuo. **1b** resin and **1c** resin were also prepared using 4′-hydroxy-3′-methoxyacetophenone (2.18 g, 13.14 mmol) and 3′,5′-dimethoxy-4′-hydroxyacetophenone (2.58 g, 13.14 mmol) by the same procedure as **1a**.

2.1.2. Preparation of Oxime Resins

The excess amount of hydroxylamine hydrochloride (6.95 g, 100 mmol) and pyridine (8.09 mL, 100 mmol) were added to the resins **1a**−1**c** which were pre-swollen in EtOH. The mixture was heated at reflux with stirring for 24 h. After

cooling to room temperature, the resins were washed with EtOH, DMF, CH_2Cl_2, and MeOH (×3) and dried in vacuo. The loading level of oxime was determined by nitrogen analysis (**2a**: 1.50 mmol/g, **2b**: 1.50 mmol/g, and **2c**: 0.96 mmol/g).

2.1.3. Preparation of Palladated Oxime Resins

To a suspension of oxime resin **2a** (1 g, each) in THF, Li_2PdCl_4 (105 mg, 0.40 mmol) dissolved in THF was added. The mixture was stirred at room temperature for 6 h. After the reaction, the resin was washed with THF in a Soxhlet system and dried in vacuo. The palladium content on palladated oxime resin **3a** was determined by ICP-AES. For ICP-AES analysis, the resin was treated with HNO_3 at 100 °C for 4 h. After filtration and washing the resin with distilled water, the filtrate was diluted to 25 mL with distilled water and analyzed by ICP-AES. To adjust for similar palladium loading level, **2b** and **2c** resins were treated with Li_2PdCl_4 (52 mg, 0.20 mmol) and Kaiser oxime resin was treated with Li_2PdCl_4 (105 mg, 0.40 mmol). Other palladated oxime resins were prepared by the same procedure as **3a** (palladium loading level, **3a**: 0.11 mmol/g, **3b**: 0.14 mmol/g, **3c**: 0.13 mmol/g, and **3d**: 0.05 mmol/g).

2.2. Suzuki Coupling Reaction Catalyzed by Palladated Oxime Resins

2.2.1. Optimization of Suzuki Coupling Reaction

Suzuki coupling reaction of 4-bromoanisole (1 mmol) with phenylboronic acid (1.2 mmol) and Cs_2CO_3 (1.5 mmol) was carried out using palladated oxime resin (1 mol% Pd, **3a**: 91 mg) in various solvent systems to investigate the best condition. Following solvent systems (5 mL) were examined: H_2O, toluene, DMF, H_2O/THF (4:1), H_2O/dioxane (1:1), H_2O/DMF (1:1), H_2O/DMF (2:1), H_2O/DMF (2:3), H_2O/DMF (3:2), H_2O/DMF (3:5), and H_2O/DMF (5:3). The mixture was stirred at RT for 2 h. For base screening, Na_2CO_3, K_2CO_3, Cs_2CO_3, K_3PO_4•H_2O, CH_3COONa, KOH, and Na_3PO_4•H_2O were used in H_2O/DMF (1:1) system. The reaction was performed at 80 °C for 2 h. After filtration and washing the resins with distilled water (3 mL × 5) and diethyl ether (3 mL × 5), the filtrate was poured into diethyl ether. The organic layer was washed with water and dried over $MgSO_4$ and solvent was evaporated under reduced pressure. The crude product was analyzed by gas chromatography/mass spectroscopy (GC-MS).

2.2.2. General Experimental Procedure for Suzuki Coupling Reaction of Aryl Halides with Phenylboronic Acid

Arylhalide (1 mmol), phenylboronic acid (1.2 mmol, 1.2 equiv), and base (1.5 mmol, 1.5 equiv) dissolved in distilled water and DMF (1/1, v/v, 5 mL) were added to palladated oxime resins **3a**−**3d** (1 mol% Pd, **3a**: 91 mg, **3b**: 71 mg, **3c**: 77 mg, and **3d**: 200 mg) suspended in distilled water and DMF (1/1, v/v, 1 mL). The mixture was stirred at 50 °C for 2 h. After filtration and washing the resins with distilled water (3 mL × 5) and diethyl ether (3 mL × 5), the filtrate was poured into diethyl ether. The organic layer was washed with water and dried over $MgSO_4$ and the solvent was evaporated under reduced pressure. The crude product was purified by column chromatography and the final product was identified by gas chromatography /mass spectroscopy (GC-MS) and NMR. The isolation yield was calculated based on the mass of product.

2.2.3. Reusability Test of Palladated Oxime Resins

4-Bromoanisole (125 μL, 1 mmol), phenylboronic acid (146 mg, 1.2 mmol), and K_2CO_3 (207 mg, 1.5 mmol) dissolved in distilled water and DMF (1/1, v/v, 5 mL) were added to palladated oxime resins **3a**−**3d** (1 mol% Pd, **3a**: 91 mg, **3b**: 71 mg, **3c**:

77 mg, and **3d**: 200 mg) suspended in distilled water and DMF (1/1, v/v, 1 mL). The mixture was stirred at 50 °C for 2 h. After filtration and washing the resins with distilled water (3 mL × 5) and diethyl ether (3 mL × 5), the filtrate was poured into diethyl ether. The organic layer was washed with water and dried over $MgSO_4$ and the solvent was evaporated under reduced pressure. The crude product was purified by column chromatography (Hexane:$CHCl_3$ = 3:1) and final product was identified by GC-MS and NMR. The isolation yield was calculated based on the mass of product. The filtered resins were reused 5 times for the same reaction.

3. Results and Discussion

3.1. Preparation and Characterization of Palladated Oxime Resins

3.1.1. Preparation of Oxime Resins

In order to prepare electron-rich oxime palladacycle on polymer support, methoxy substituted hydroxyacetophene groups as oxime precursors were chosen. As shown in Scheme 1, hydroxyacetophenone derivatives were immobilized on CM PS in the presence of $NaOCH_3$. The ketone group was converted to oxime group by reacting with excess hydroxylamine and pyridine. In this step, oxime group was generated as (E)-isomer which is thermodynamically more stable than the corresponding (Z)-isomer.[146] Loading levels of oxime group, determined by nitrogen analysis, were 1.50 mmol/g (**3a)**, 1.50 mmol/g (**3b)**, and 0.96 mmol/g (**3c**), respectively. The chemical conversions from CM PS to oxime resin were verified by FT- IR analysis (**1a–1c**: ketone band, **2a–2c**: hydroxyl band and oxime band, Figure 10).

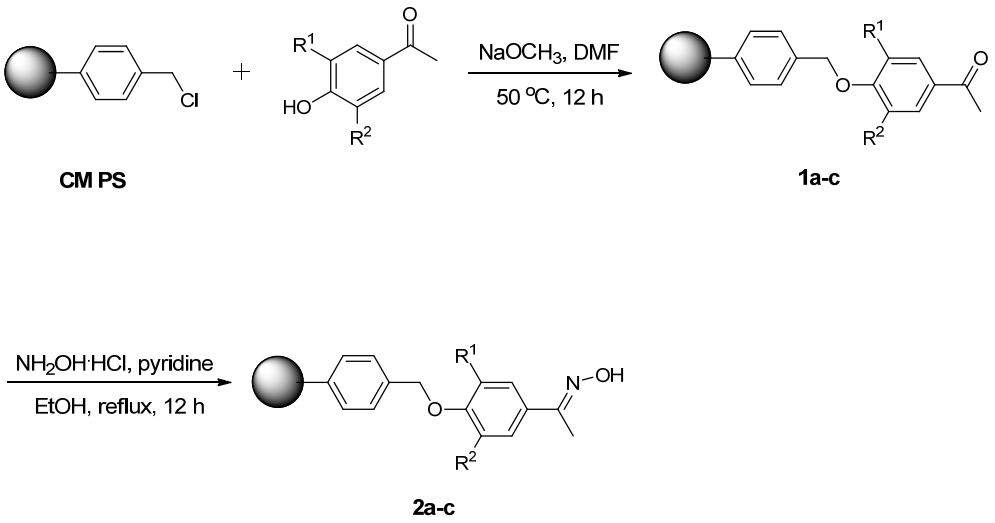

Scheme 1. Preparation of Oxime Resins

(a)

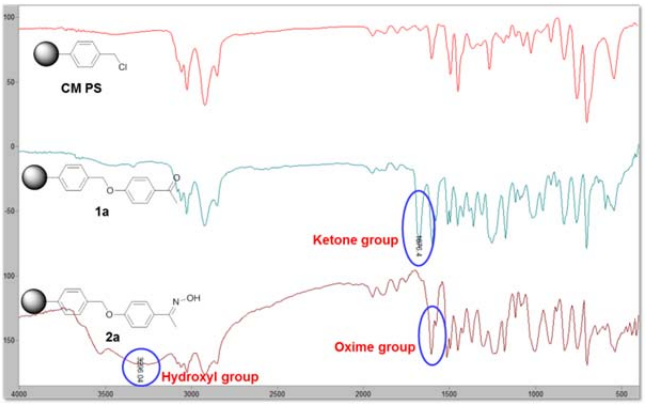

(b)

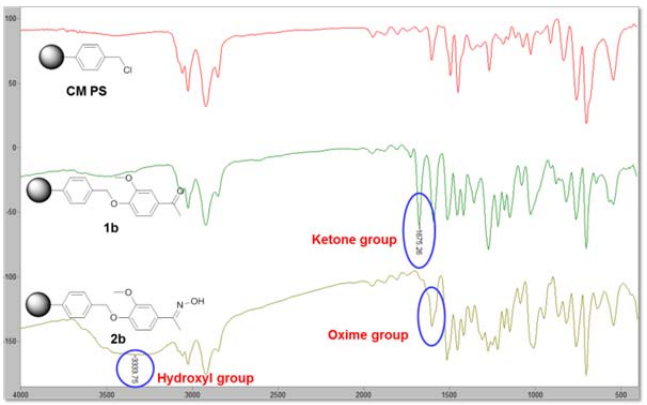

(c)

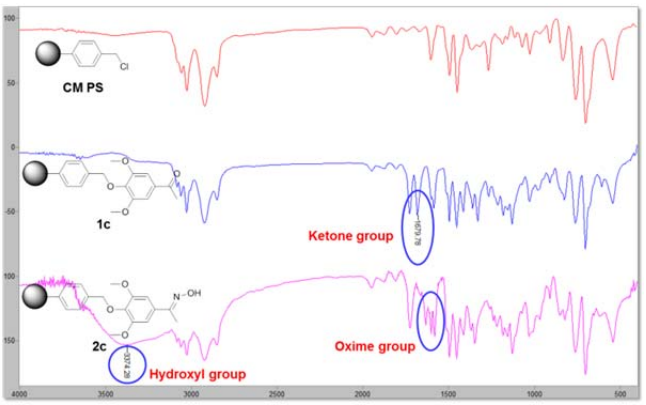

Figure 10. FT-IR spcetra of oxime resins: (a) **1a–2a**, (b) **1b–2b**, and (c) **1c–2c**.

3.1.2. Preparation of Palladated Oxime Resins

As shown Scheme 2, the oxime resins and Kaiser oxime resin,[147] as a control, were treated with palladium precursor (Li_2PdCl_4) in THF and were shaken at RT for 6 h. In the formation of Pd complex, resin 2c showed the best absorption rate of palladium. It means that two methoxy group attached oxime ligand could catch and stabilize palladium source more efficiently than the others due to good σ-donor of electron-rich ligand.

The resulting palladated oxime resins (**3a–3d**) were analyzed by FE-SEM to identify any external morphology changes during the reaction. The FE-SEM images exhibited clear surface morphology of the resins without any physical damages during the reactions (Figure 11). The existence of Pd on the resin was verified by EDX analysis. From the detection of Cl and Pd atoms in EDX spectra (Figure 12a), we indirectly concluded that the oxime ligands formed a palladium complex via the chloro bridge form.[108] To support this results, the oxidation state of Pd on the resins were determined by XPS, and Pd peak (Pd 3d5) was found in 337.77 eV which corresponds to Pd(II) (Figure 12b).[148] Therefore, it is demonstrated that Pd atom was immobilized on the oxime palladacycle resin as a chloro bridge complex in +2 state. The amount of immobilized Pd on the palladated oxime resins were quantified by ICP-AES. The loading levels of Pd on each resin were 0.11 mmol/g (**3a**), 0.14 mmol/g (**3b**), 0.13 mmol/g (**3c**), and 0.05 mmol/g (**3d**).

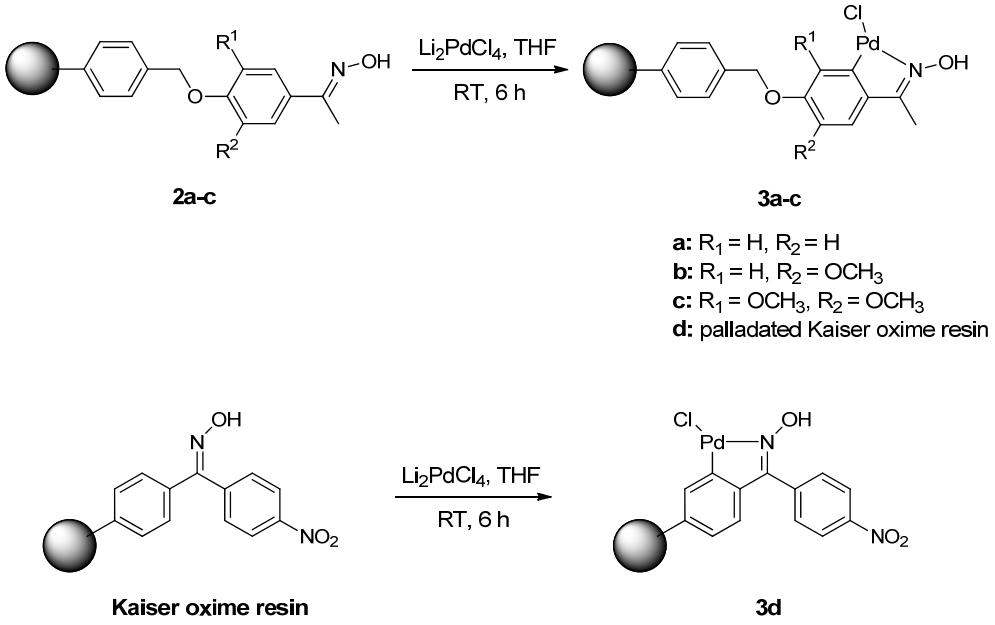

Scheme 2. Preparation of Palladated Oxime Resins

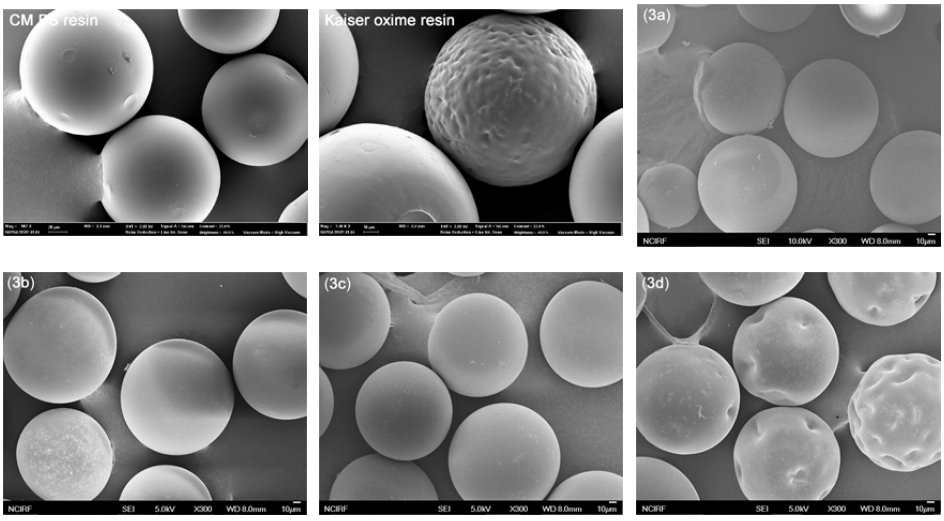

Figure 11. SEM images of CM PS resin, Kaiser oxime resin, and palladated oxime resins (**3a–3d**).

(a) (b)

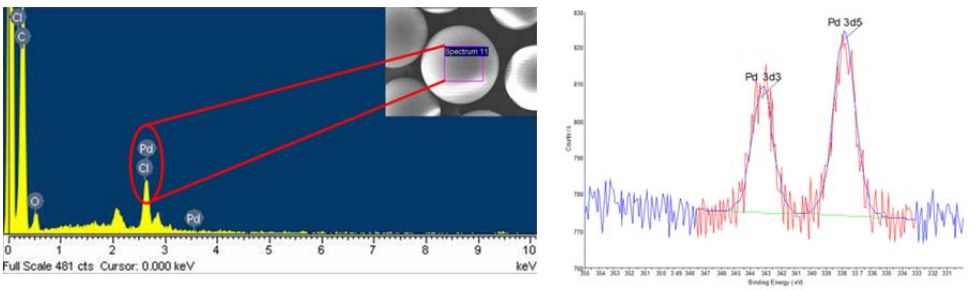

Figure 12. Identification of palladium on palladated oxime resin (**3c**) by (a) EDX data and (b) XPS spcetra.

3.2. Suzuki Coupling Reaction Catalyzed by Palladated Oxime Resins

3.2.1. Effects of Solvents and Bases on Suzuki Coupling Reaction

Before testing Suzuki coupling reaction, a model reaction of 4-bromoanisole with phenylboronic acid was carried out to optimize the reaction condition using **3a** Pd catalysts. Firstly, various solvent systems were examined for the Suzuki coupling reaction using Pd catalysts with Cs_2CO_3 (Scheme 3). H_2O/DMF (1:1) system gave the higher yield of 4-methoxybiphenyl than other solvent systems (Table 3). From the results of the solvent system (entry 6–11 in Table 3), we found that a delicate balance of solvent system is one of the important factors for Suzuki coupling reaction when inorganic base is used, because heterogeneous reaction requires both the compatibility of solid support or the solubility of organic and inorganic reagents.

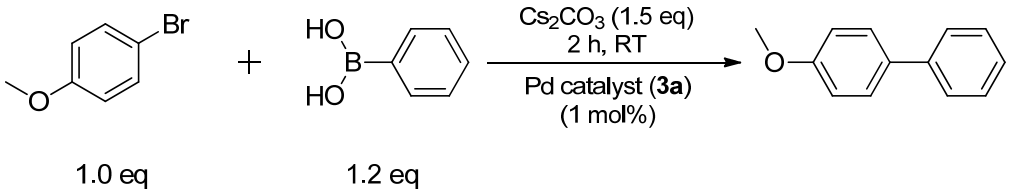

Scheme 3. Suzuki Coupling Reaction of 4-Bromoanisole with Phenylboronic Acid in Various Solvent Systems

Table 3. The Effect of Solvent Systmes in Suzuki Coupling Reaction of 4-Bromoanisole with Phenylboronic Acid[a]

Entry	Solvent	Yield (%)[b]
		3a
1	H_2O	-
2	Toluene	3
3	DMF	21
4	H_2O/THF (4:1)	-
5	H_2O/dioxane (1:1)	2
6	H_2O/DMF (1:1)	53
7	H_2O/DMF (2:1)	19
8	H_2O/DMF (2:3)	40
9	H_2O/DMF (3:2)	32
10	H_2O/DMF (3:5)	26
11	H_2O/DMF (5:3)	36

[a]Conditions: 4-Bromoanisole (1 mmol), phenylboronic acid (1.2 mmol), palladated oxime resins (**3a** and **3b**, 1 mol%), Cs_2CO_3 (1.5 mmol), in diverse solvent systems (v/v, 5 mL), at RT, for 2 h. [b]GC yields.

For bases screening, Suzuki coupling reactions were carried out in H_2O/DMF (1:1) using **3a** and **3b** Pd catalysts (Scheme 4). As shown Table 4, inorganic bases generally exhibited good performance in coupling reaction of 4-bromoanisole with phenylboronic acid except for CH_3COONa. Organic bases such as TEA, TBA, and pyridine were not suitable for these reaction systems. Therefore, H_2O/DMF (1:1) as a solvent and K_2CO_3, K_3PO_4, or Cs_2CO_3 as a base were used in the following Suzuki coupling reaction.

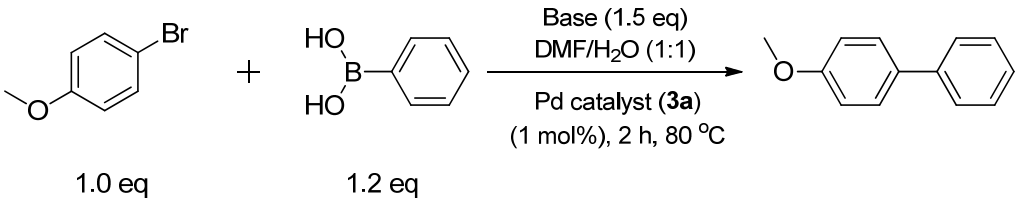

Scheme 4. Suzuki Coupling Reaction of 4-Bromoanisole with Phenylboronic Acid in the presence of Various Bases

Table 4. Effect of Various Bases in Suzuki Coupling Reaction of 4-Bromoanisole with Phenylboronic Acid[a]

Entry	Base	Yield (%)[b]
		3a
1	Na_2CO_3	91
2	K_2CO_3	96
3	Cs_2CO_3	96
4	$K_3PO_4 \cdot H_2O$	95
5	CH_3COONa	4
6	KOH	92
7	$Na_3PO_4 \cdot H_2O$	95

[a]Conditions: 4-Bromoanisole (1 mmol), phenylboronic acid (1.2 mmol), palladated oxime resins (**3a** and **3b**, 1 mol%), various bases (1.5 mmol), in H_2O/DMF (1:1, v/v, 5 mL), at 80 °C, for 2 h. [b]GC yields.

3.2.2. Suzuki Coupling Reaction of Various Aryl Halides with Phenylboronic Acid

Suzuki coupling reaction of aryl halides with phenylboronic acid was performed under mild condition to see the differences in the catalytic performance among the palladated oxime resins (Scheme 5). The electron richness of palladated oxime resins increases in the order **3a** < **3b** < **3c**, as the number of methoxy group on oxime ligand increases. As shown in Table 5, palladated oxime resins (**3a**–**3c**) afforded better catalytic performance than palladated Kaiser oxime resin (**3d**) and the most electron-rich palladated oxime resin (**3c**) showed excellent catalytic activity in Suzuki coupling reaction. Deactivated aryl bromides as well as aryl chlorides were converted to the corresponding biaryl compounds in excellent yield using **3c** catalyst (entry 1–2, 4–7 in Table 6). Furthermore, **3c** catalyst (0.005 mol%) gave high TON up to 20,000 for the coupling reaction of 4-iodoacetophenone with phenylboronic acid. From these results, we could confirm that electron richness of

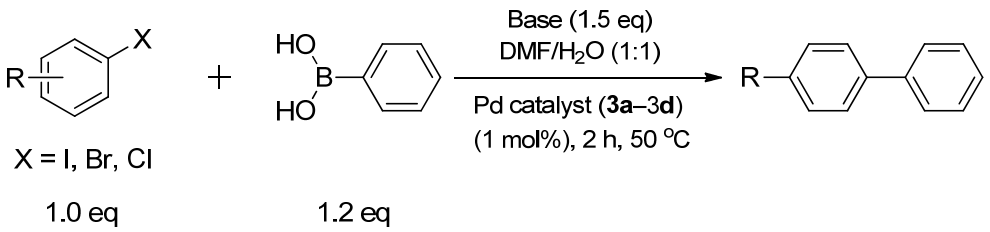

Scheme 5. Suzuki Coupling Reaction of Aryl Halides with Phenylboronic Acid

ligand is an important factor to enhance the catalytic activity of palladacycle catalyst in Suzuki coupling reaction.

Substituted heterocyclic compounds are important in the fields of pharmaceutical industry for developing new drugs.[149–152] Due to their useful features, we tried to carry out Suzuki reaction of various heterocyclic halides with phenylboronic acid using **3c** catalyst. 2-Bromopyridine and 2-bromothiophene were converted well to the corresponding biaryl compounds under mild condition (entry 9, 11 in Table 6). Although Suzuki reaction of heterocyclic chlorides gave not so good yield (entry 10 in Table 6), optimization of the reaction condition using **3c** catalyst will further improve the coupling performance. Therefore, we can conclude that two methoxy substituted oxime palladacycle resin afforded highly efficient catalytic activity in Suzuki coupling reaction due to its electron-rich oxime ligand.

Table 5. Suzuki Coupling Reaction of Various Aryl Halides with Phenylboronic Acid in the Presence of Oxime Palladacycle Resins (**3a**, **3b**, **3c**, and **3d**)[a]

Entry	Substrate	Base	Yield (%)[b]			
			3a	**3b**	**3c**	**3d**
1	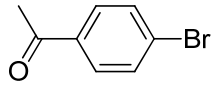	Cs_2CO_3	84	92	99	1
		K_2CO_3	40[c]	63[c]	99[c]	-
2	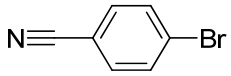	K_2CO_3	32[c]	50[c]	99[c]	-
3	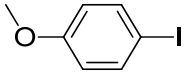	K_2CO_3	85	88	99	-
4	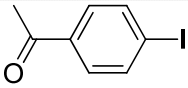	K_2CO_3	99	99	99	56

[a]Conditions: Aryl halides (1 mmol), phenylboronic acid (1.2 mmol), palladated oxime resins (**3a**, **3b**, **3c**, and **3d**, 1 mol%), bases (1.5 mmol), in H_2O/DMF (1:1, v/v, 5 mL), at 50 ^oC, for 2 h. [b]GC yield. [c]Reaction time: 0.5 h

Table 6. Suzuki Coupling Reaction of Various Aryl Halides and Heterocyclic Halides with Phenylboronic Acid in the Presence of Oxime Palladacycle Resin (**3c**)[a]

Entry	Substrate	Base	Temp (°C)	Yield (%)[b]
				3c
1	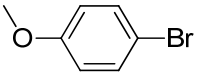	K_2CO_3	50	90
2	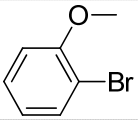	K_2CO_3	50	92
3	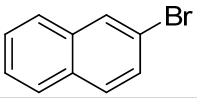	Cs_2CO_3	50	99
4	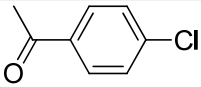	Cs_2CO_3	100	92
5	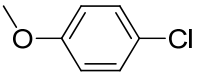	Cs_2CO_3	100	55
6	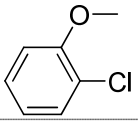	Cs_2CO_3	100	40
7	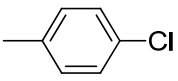	Cs_2CO_3	100	70
8	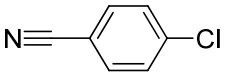	Cs_2CO_3	100	79
9	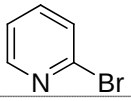	Cs_2CO_3	50	60
10	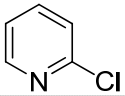	Cs_2CO_3	100	55
11	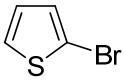	Cs_2CO_3	50	63

[a]Conditions: Aryl halides (1 mmol), phenylboronic acid (1.2 mmol), palladated oxime resins (**3c**, 1 mol%), bases (1.5 mmol), in H_2O/DMF (1:1, v/v, 5 mL), for 2 h. [b]GC yield.

3.2.3. Reusability Test of Palladated Oxime Resins for Suzuki Coupling Reaction

One of the advantages of heterogeneous catalyst is that the catalyst can be easily isolated and reused. To evaluate the reusability of electron-rich oxime palladacycle resins, recycling test was carried out by using recovered the catalysts in Suzuki coupling reaction of 4-bromoanisole with phenylboronic acid (Scheme 6). As the recycling number increased, the catalytic activity of **3a** and **3b** catalysts dramatically decreased even from the second cycle (Table 7). In contrast, **3c** catalyst consistently gave 4-bromobiphenyl in high yield until fifth cycle, maintaining good catalytic activity. After each cycle of the reaction, **3c** catalyst was analyzed by ICP-AES to measure the amount of Pd loading on the catalyst. The ICP-AES results showed that Pd leaching was not significant during the reactions maintaining Pd loading of 0.10–0.13 mmol/g in every cycle. To support this, Suzuki couipling reaction of 4-bromoanisole with phenylboronic acid was performed for 30 min in the presence of **3c** catalyst. After filtering the catalyst, the filtrate solution was allowed to react for another 1 h under the same reaction condition. We could not observe any further reaction from the solution. Based on these results, we can conclude that two methoxy substituted oxime palladacycle resin is a stable and potent catalyst in successive Suzuki coupling reactions without significant Pd leaching up to fifth cycle.

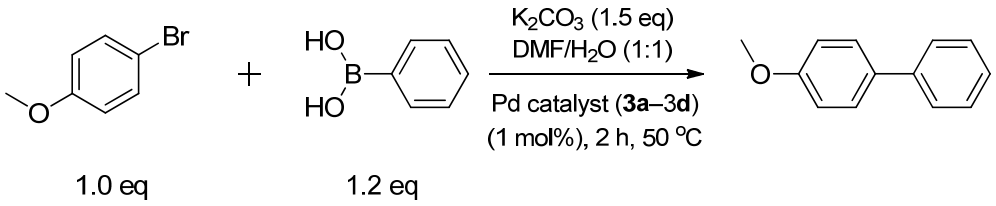

Scheme 6. Suzuki Coupling Reaction for Reusability Test with Palladated Oxime Resins

Table 7. Reusability of the Palladated Oxime Resins in Suzuki Coupling Reaction of 4-Bromoanisole with Phenylboronic Acid in the Presence of Oxime Palladacycle Resins (**3a**, **3b**, and **3c**) [a]

Catalyst	Yield (%)[b]				
	1st cycle	2nd cycle	3rd cycle	4th cycle	5th cycle
3a	60	6	-	-	-
3b	65	8	-	-	-
3c	90	92	91	88	84

[a]Conditions: 4-Bromoanisole (1 mmol), phenylboronic acid (1.2 mmol), palladated oxime resins (**3a, 3b,** and **3c**, 1 mol%), K_2CO_3 (1.5 mmol), in H_2O/DMF solvent (1:1, v/v, 5 mL), at 50 °C, for 2 h. [b]Isolated yields by column chromatography.

4. Conclusion

In summary, various electron-rich oxime palladacycle resins were prepared as heterogeneous catalysts for Suzuki coupling reaction. The electron-richness of oxime ligand was controlled by the number of electron donating group (methoxy group) on the benzene ring. Unlike Kaiser oxime resin, electron-rich oxime resins afforded efficient and stable environment to form a Pd complex. Different catalytic activities in Suzuki coupling reaction of aryl halides with arylboronic acid were observed depending on the electronic effect of oxime ligand. The most electron-rich oxime resin (**3c**) contributed to the enhanced catalytic efficiency in high yield and displayed high TON in Suzuki coupling reaction. In addition, **3c** catalyst could be reused up to 5 cycles maintaining a good catalytic activity without sever Pd leaching.

Chapter III

Ionic Liquid Resin for Solid-Phase Peptide Synthesis

1. Introduction

Polystyrene (PS) resin is one of the most commonly used polymer supports in solid-phase peptide synthesis (SPPS).[6] It has high mechanical and chemical stability, as well as good swelling properties in various solvents. However, PS resin presents some problems because of the hydrophobic matrix, which causes difficulties in diffusion of reagents and aggregation of growing peptides suspended on resin.[153,154] For these reasons, polymer backbones composed of polyamide or polyethylene glycol (PEG) were introduced to provide a hydrophilic environment on polymer supports.[153,155] Furthermore, ethylene glycol units have been used as crosslinkers to increase the flexibility of the polymer matrix.[154,156] Since hydrophilic polymer supports are fully solvated by polar solvents and compatible with peptides on resin, they can afford high yield and purity of peptide in SPPS. Previously, we developed core–shell-type resins to circumvent the problems caused by the hydrophobic matrix.[16–18,26,28,33] Core–shell-type resins can minimize the influence of hydrophobic environments on the resin due to their distinctive structures. Despite many efforts, the controversy over the interaction of polymer matrix, peptide chain and solvent is continuing with heated discussions.

Recently, as part of an effort to synthesize peptides more efficiently, ionic liquid (IL) was introduced as a solvent[157] and a soluble support.[47,158,159] In peptide synthesis, coupling reagents and amino acid derivatives can be effectively dissolved

in IL and stabilized for selective reactions.[157,161] In addition, an attractive feature of ILs is that its polarity and solubility can be easily modulated by changing the anion species. This unique characteristic facilitates the generation of controllable environments when ILs are used as a soluble support or reaction media. Furthermore, IL can affect the folding property of peptides due to its H-bonding ability. Because the peptides which have α-helix or β-hairpin structure are destabilized in the IL media,[162] IL is expected to prevent the peptide from aggregating during peptide synthesis. Therefore, introducing versatile IL groups to PS resin may address the weaknesses of the PS resin and enhance the efficiency in peptide coupling reactions.

Immobilization of imidazole groups on a solid support is one way of introducing an IL environment on the PS resin. ILs have been immobilized on solid supports, such as silica particles[93,163] and PS resin,[164,165] to develop heterogeneous catalysts. However, to the best of our knowledge, there has been no report on the application of IL conjugation to polymer support for efficient SPPS. Thus, we have prepared imidazolium IL coupled resins, which are designed to allow variable IL environments with improved performance in SPPS.

2. Experimental Section

2.1. Preparation of Ionic Liquid Resin

2.1.1. Synthesis of Boc Protected 1-(3-Aminopropyl)imidazole (Boc-API)

1-(3-Aminopropyl)imidazole (API, 2.4 mL, 20 mmol) was dissolved in THF (50 mL). To prepare bi-phasic aqueous condition, a $NaHCO_3$ (4.2 g, 50 mmol) aqueous solution (50 mL) was added to API solution in an ice bath. A solution of the Boc anhydride (5.6 g, 26 mmol) in 25 mL of THF was added dropwise under vigorous magnetic stirring. After stirring the mixture for 3 h at room temperature, the solvent was evaporated in vacuo. The residue was dissolved in ethyl acetate, and washed with water. The organic phase was dried over $MgSO_4$ and concentrated (yield : 79%). 1H NMR (300 MHz, $CDCl_3$, 25 ºC, TMS): δ (ppm) = 7.5 (s, 1H), 7.0 (s, 1H), 6.9 (s, 1H), 4.8 (s, 1H), 4.0 (t, 2H), 3.1 (q, 2H), 1.9 (quin, 2H), 1.4 (s, 9H).

2.1.2. Immobilization of Boc-API on CM PS

Boc-API (3.3 g, 14.65 mmol) was dissolved in 50 mL of NMP. CM PS resin (5 g, 2.2 mmol/g) swollen in 50 mL of NMP and reacted with Boc-API solution

overnight at 80 ºC. After reaction, the resin was filtered and washed with DMF, CH_2Cl_2 and MeOH (3 × 50 mL, each). Boc groups were removed by treating the resin with TFA/CH_2Cl_2 (50/50, v/v) solution for 1 h. The resulting resin was filtered and washed with CH_2Cl_2 and MeOH. The loading level was determined as 1.2 mmol/g by elemental analysis and Fmoc titration after coupling Fmoc-OSu.

2.1.3. Anion Exchange on IL Resin

Anions of IL resin were exchanged by concentration difference. Sodium and lithium salt (BF_4^-, OTf^-, PF_6^-, and $TFSI^-$, each 6 mmol) aqueous solution was prepared by dissolving each salt in H_2O/DMF (50/50, v/v) and was added to 1 g of IL resin. After shaking for 24 h at room temperature, the resins were filtered and washed with DMF, CH_2Cl_2 and MeOH (3 × 10 mL, each). The existence of each anion in the IL resin was verified by EDX.

2.1.4. Coupling Kinetics of the First Amino Acid

Fmoc-His(Trt)-OH was coupled on each IL resin (1.0 mmol/g) and AM PS resin (1.2 mmol/g). Pre-activated solution prepared from Fmoc-His(Trt)-OH (1 equiv.),

HBTU (1 equiv.), HOBt (1 equiv.) and DIPEA (2 equiv.) in NMP was added to each resin, respectively. Coupling reactions were performed for 5 min, 15 min, 30 min, 60 min, and 90 min, and the coupling reactions were monitored by Fmoc titration. Fmoc-Phe-OH was also introduced by the same method, and the coupling yields were measured by Fmoc titration.

2.2. Peptide Synthesis

2.2.1. Leu-enkephalin (H-YGGFL-NH_2)

Leu-enkephalin was synthesized on Fmoc-Rink-IL resins (50 mg, 0.48 mmol/g), which contained each anion (Cl^-, BF_4^-, OTf^-, PF_6^- and $TFSI^-$), and Fmoc-Rink-AM PS resin (50 mg, 0.55mmol/g). Fmoc-Rink-IL resins were prepared from the IL resins by coupling with Fmoc-Rink amide linker, HBTU, HOBt and DIPEA (2 equiv.) in NMP (2 mL) for 2 h at room temperature. The remnant amino groups were capped by adding excess acetic anhydride and DIPEA for 2h. The Fmoc group was removed using 20% piperidine/NMP (2 mL, 5min + 10 min). Following that, the anions of IL were exchanged by the same method as above. Pre-activated Fmoc-amino acid solution in NMP was added to the resin. All amino acid coupling reactions were carried out for 1 h at 25 ºC. The peptide was recovered by treating the resin with TFA/TIS/H_2O (95:2.5:2.5) solution for 1 h. For HPLC analysis, condition A was used with a SPIRIT PEPTIDE 120 C18 column. The product was analyzed with MALDI-TOF (calculated as 555.65 for $C_{28}H_{39}N_6O_6$ (H-YGGFL-NH_2) [M+H]+, found 555.2).

2.2.2. JR 10-mer (H-WFTTLISTIM-NH_2)

JR 10-mer was synthesized by the same procedure as used for Leu-enkephalin. The peptide was cleaved from the resin by TFA/thioanisole/1,2-ethanedithiol/anisole (90:5:3:2) solution for 1 h and was recovered as white solids by ether precipitation. HPLC condition was the same as in the case of Leu-enkephalin. The JR 10-mer peptide was identified by MALDI-TOF (calculated exact mass = 1210.6 for $C_{58}H_{90}N_{12}O_{14}S$ (JR 10-mer), $[M + Na]^+$, found 1234.0).

2.2.3. β_2M(59–71) (Ac-LDWSFYLLYYTE-NH_2)

β_2M(59–71) was synthesized by the same procedure as Leu-enkephalin and cleaved with TFA/TIS/H_2O (95:2.5:2.5) solution for 1 h and was recovered as white solids by ether precipitation. β_2M(59–71) peptide was analyzed by HPLC (condition A with a SPIRIT PEPTIDE 120 C18 column) and MALDI-TOF (calculated as 1667.79 for $C_{83}H_{109}N_{15}O_{22}$ (β_2M(59–71))[M+H]+, found 1668.84).

3. Results and Discussion

3.1. Preparation and Characterization of IL Resin

3.1.1. Preparation of IL Resins

The loading method of the imidazolium group on a polymer support is well known in the field of heterogeneous metals or Lewis acid catalysts.[93,163–165] However, imidazolium IL resin for solid-phase peptide synthesis requires an extra amine/hydroxy group, from which linkers or amino acids are elongated. Thus, 1-(3-aminopropyl)imidazole (API) was chosen as an imidazolium precursor and a linker for SPPS. Before introducing the imidazolium group on CM PS resin, the free amino group was protected by Boc group to obtain Boc-API (**1**) in 79% yield (Scheme 7). Then, CM PS resin was treated with an excess amount of compound **1**. The existence of imidazolium in the IL resin (**2**) was verified by FT-IR (carbamate band: 1699 cm^{-1}, quaternary imidazolium band: 1162 cm^{-1}, Figure 13). The loading level of the imidazolium group on IL resin (**3a**) was determined to be 1.2 mmol/g by measuring nitrogen contents and Fmoc titration after coupling Fmoc-OSu.

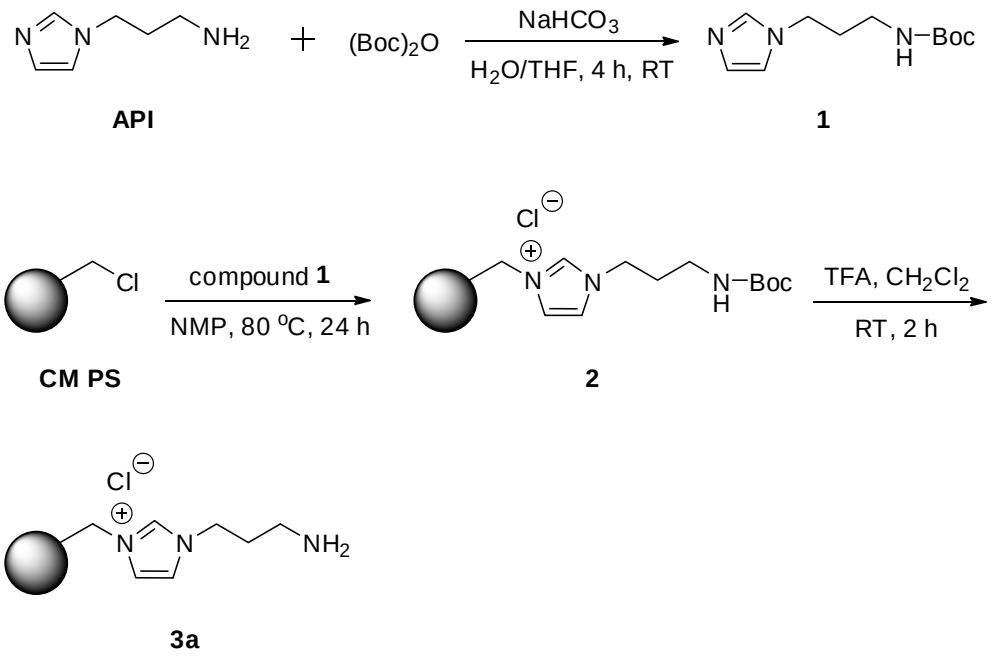

Scheme 7. Preparation of IL Resin

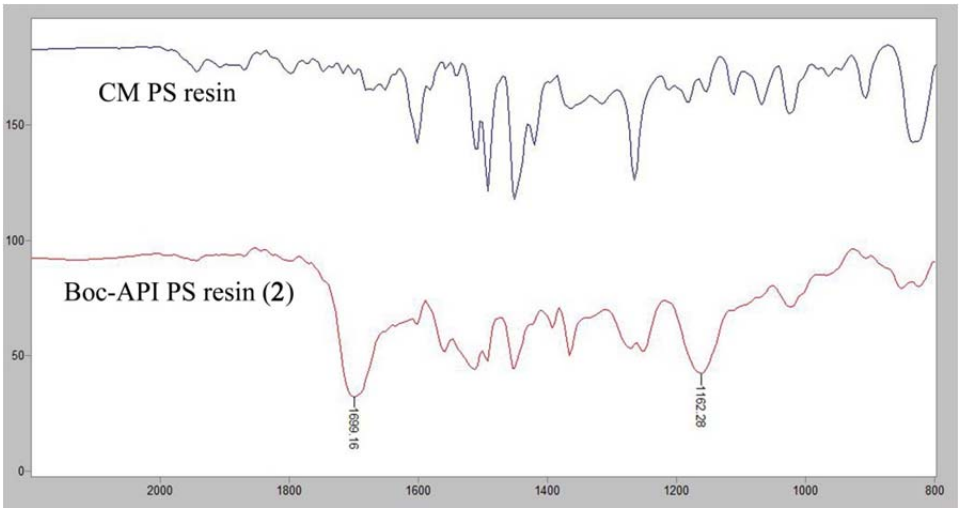

Figure 13. FT-IR spectra of (a) CM PS resin, and (b) Boc-API PS resin (**2**).

3.1.2. Preparation of IL Resin with Different Anions by Anion Exchange

To obtain IL resins with different anions (BF_4^-, OTf^-, PF_6^- and $TFSI^-$), the IL resin (**3a**) was treated with an excess amount of $NaBF_4$, NaOTf, $NaPF_6$, or LiTFSI in DMF/H_2O (1/1, v/v) (Scheme 8). The anions of imidazolium on the resin were easily identified by energy dispersive X-ray spectroscopy (EDX) (Figure 14). Traces of chloride ions were observed in **3b–e** resins, but the majority of original anions were mostly changed in each resin.

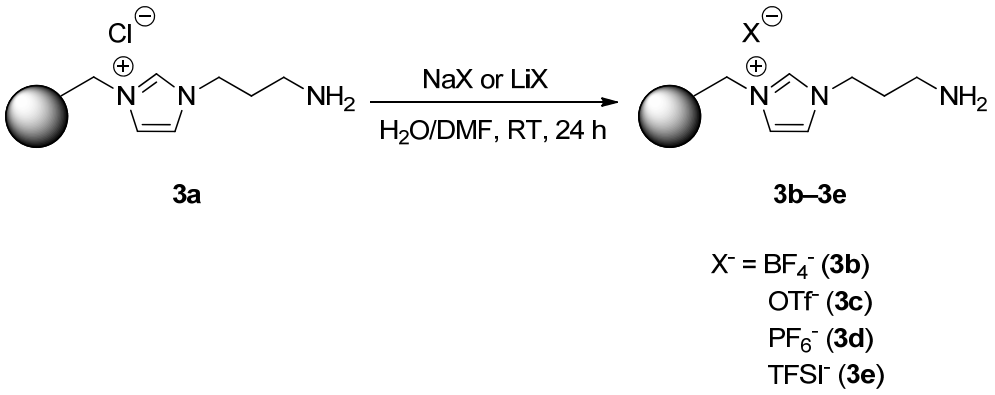

Scheme 8. Preparation of IL Resins with Different Anions

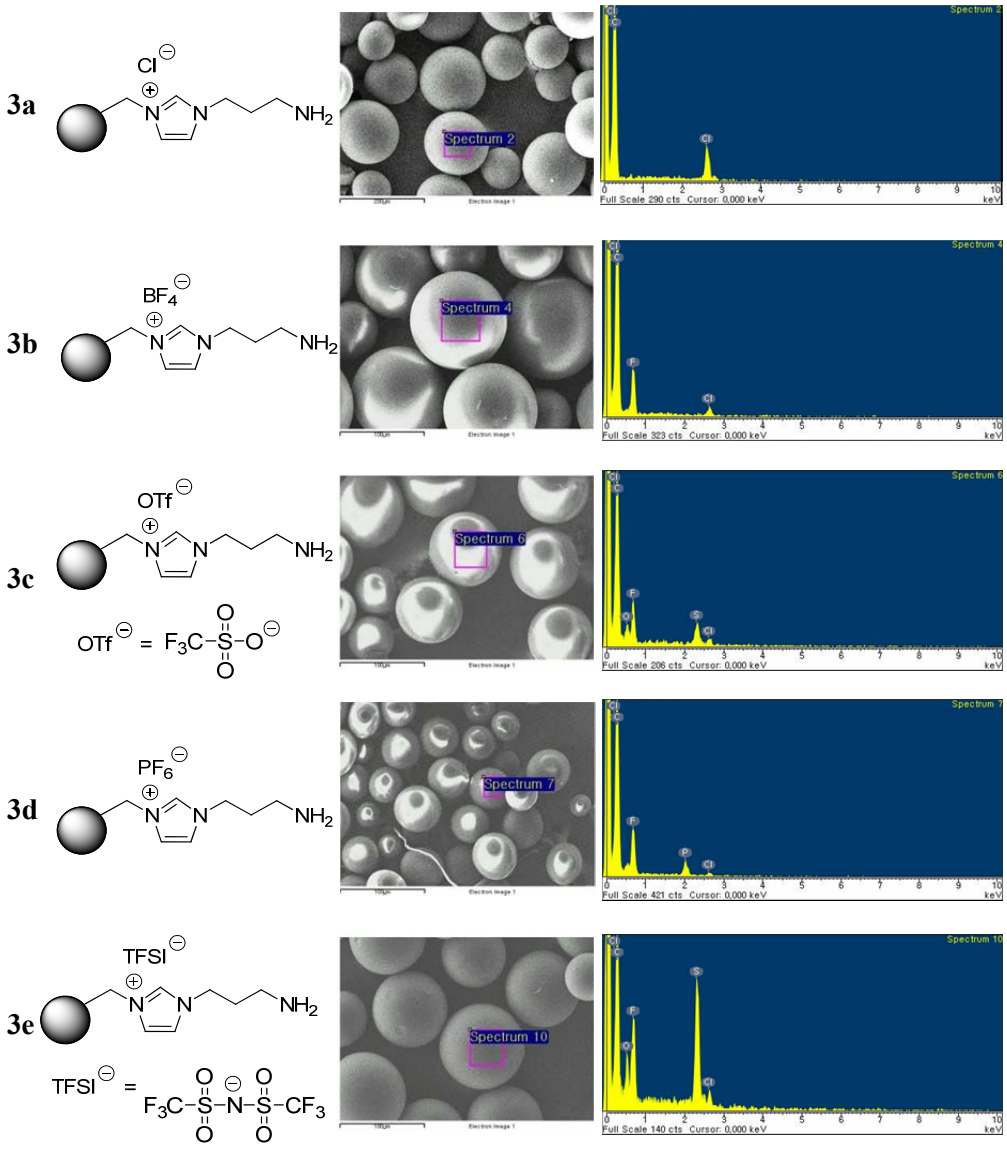

Figure 14. SEM images and EDX data of IL resins (**3a–3e**).

3.1.3. Swelling Properties

The swelling property of resins is the primary criterion for estimating solvent compatibility, which affects diffusion of the reagents into the resin and ultimately synthetic efficiency in SPPS. When the swelling properties of IL resins (**3a–e**) were compared in various solvents, there were considerable differences in each solvent depending on the anions (Table 8). In general, IL resins with hydrophilic anions had a tendency to swell more in polar solvents than in less polar solvents such as DCM, THF and hexane. It has been known that a polymer-supported ionic liquid system swells considerably well in polar aprotic solvents such as DMF and DMSO and its swelling property can be controlled by anion.[90] In our cases, IL resins (**3b–e**) also swelled well in polar aprotic solvents (NMP and DMF), and especially **3e** resin displayed the highest swelling property in NMP. Because $TFSI^-$ anion is the most hydrophobic among other anions (Cl^-, BF_4^-, OTf^- and PF_6^-), the ionic liquid with $TFSI^-$ anion might generate amphiphilic environment in polymer matrix which presumably gave the highest compatibility with NMP or DMF.

Table 8. Swelling Volume of IL Resin and AM PS Resin in Various Solvents

resin	swelling volume (mL/g)					
	dry	NMP	DMF	MeOH	H_2O	MeCN
3a (Cl^-)	1.9	4.4	4.2	6.1	3.3	1.7
3b (BF_4^-)	1.5	7.5	8.3	3.2	2.6	3.1
3c (OTf^-)	1.9	7.8	7.8	6.1	3.2	2.9
3d (PF_6^-)	1.8	8.8	8.9	3.6	2.2	2.9
3e ($TFSI^-$)	1.8	10.1	10.0	6.7	2.8	6.7
AM PS resin	1.6	8.5	7.7	2.7	2.7	2.0

3.1.4. Coupling Kinetics

To evaluate IL environment effects on peptide synthesis, the coupling reaction kinetics of the first amino acid, mostly affected by polymer matrix, on the resins was measured in NMP.[17] Fmoc-His(Trt)-OH and Fmoc-Phe-OH, which are known to have poor and good loading yield respectively,[28] were selected as model amino acids. During the time course of the reaction, small portions of the resin were withdrawn from the reaction mixture and the coupling kinetics was examined by Fmoc titration. As shown in the line graph (Figure 15a), coupling kinetics of Fmoc-His(Trt)-OH exhibited similar trends on IL resins and on AM PS resin except for **3a** resin. Because of the difficulty in coupling Fmoc-His(Trt)-OH on most of the polymer supports, the environmental change of IL resins gave little influence on coupling kinetics. In the case of **3a** resin, the low swelling property might contribute to low coupling kinetics. However, in the case of Fmoc-Phe-OH coupling (Figure 15b), the yield and coupling kinetics on IL resins were proportional to the swelling property. In particular, **3d** and **3e** resins afforded much better coupling efficiency than the AM PS resin. Therefore, IL resins with $TFSI^-$ or PF_6^- anion and NMP as a solvent give the optimal condition for coupling of the first amino acid in SPPS. Based on these results, we confirmed that the initial coupling kinetics was mostly affected by the swelling properties originated from IL environments.

(a)

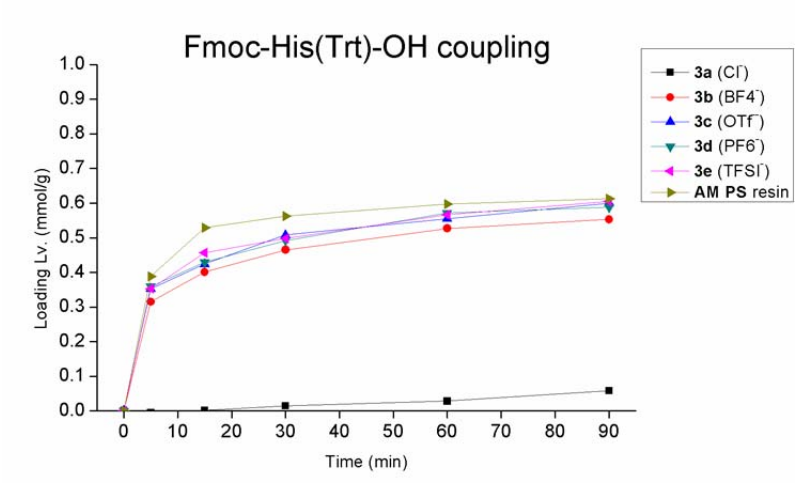

(b)

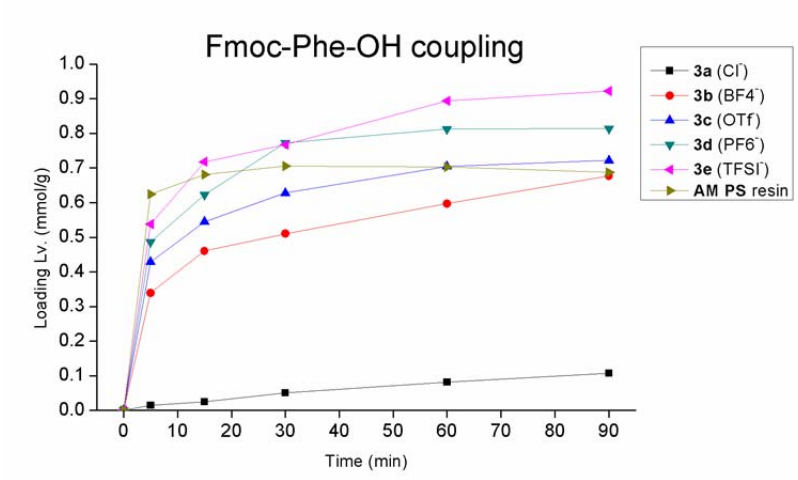

Figure 15. Coupling kinetics of (a) Fmoc-His(Trt)-OH and (b) Fmoc-Phe-OH on IL resins.

3.2. Synthesis of Peptides on IL resins

3.2.1. Synthesis of Leu-enkephalin

We applied imidazolium IL resins to SPPS to evaluate their synthetic performance. As a model pentapeptide, Leu-enkephalin (H-YGGFL-NH_2)[166] was synthesized using Fmoc/t-Bu chemistry after anchoring Fmoc Rink amide linker on the IL resins and AM PS resin, respectively. Then, the peptide was cleaved and analyzed by HPLC (Figure 16) and MALDI-TOF mass. Leu-enkephalin was recovered quantitatively in high purity (93% ~ 95% purity, Table 9) on IL resins (**3b–3e**). We found that **3a** resin showed relatively low yield (82%) and low purity (87%) due to the intrinsic property of IL[Cl^-]. However, IL resins generally exhibited better synthetic performance than AM PS resin (Table 9) and ionic liquid was used as a soluble support (overall yield: 50%, purity: 90%).[167] As results of synthesis of Leu-enkephalin, we can conclude that synthesis of peptide on IL resins is more efficient than on AM PS resin or in ionic liquid, although the synthetic performance of IL resins can not be precisely compared with other peptides in general.

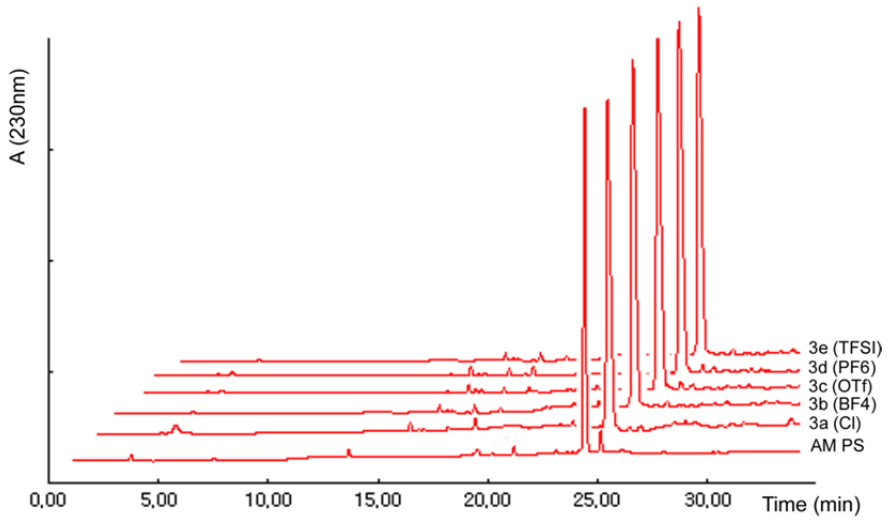

Figure 16. HPLC analysis of crude Leu-enkephalin from IL resins (**3a–3e**).

3.2.2. Synthesis of β_2M(59–71)

β2-Microglobulin is involved in human amyloid disease, and exists as a folded form that contains stable β-sheet secondary structure of B, C, D, E, and F strands.[168] Among them, the sequences of E strand in residues 59–71 can form amyloid-like fibril in vitro.[169] This highly aggregative peptide was synthesized on IL resins and AM PS resin to investigate IL environment effect in SPPS. According to the results of peptide synthesis from IL resins and AM PS resin (Table 9), IL resins with PF_6^- and $TFSI^-$ anions (**3d, 3e**), which showed good swelling property and coupling kinetics in the first coupling, yielded the desired peptide in higher purities than those of other IL resins and AM PS. As shown in HPLC patterns from the IL resins (**3d, 3e**) and AM PS resin (Figure 17), deletion sequences were alleviated in IL resins, while AM PS resin generated many side products in HPLC around the desired product. Although outstanding differences between the resins were not seen, the IL resins with PF_6^- and $TFSI^-$ anions provided better environment for the synthesis of aggregative peptide than the conventional PS resin.

(a)

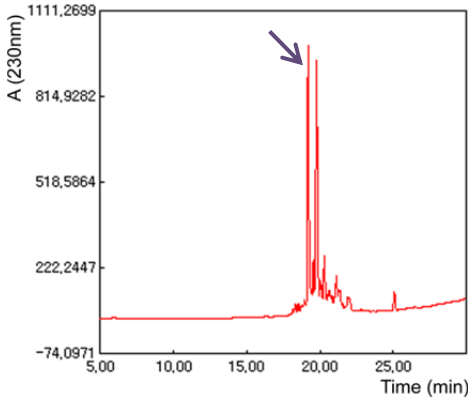

(b)

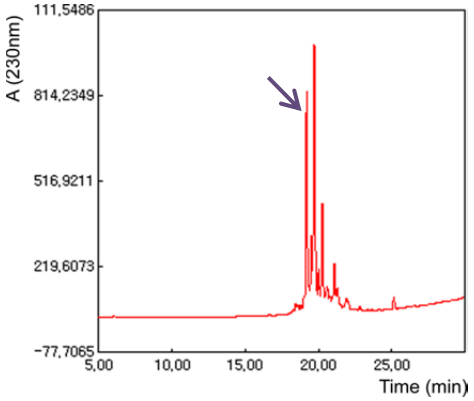

(c)

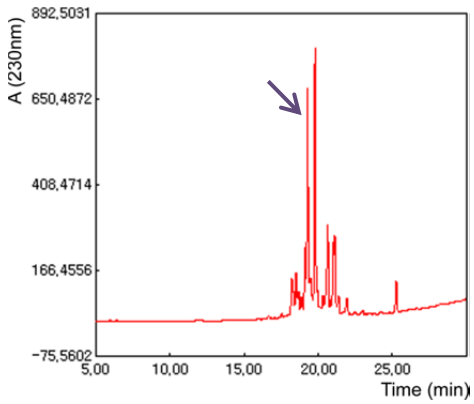

Figure 17. HPLC analysis of β_2M(59–71) synthesized from (a) IL resin (**3d**), (b) IL resin (**3e**), and (c) AM PS resin.

3.2.3. Synthesis of JR 10-mer

To further investigate the clear differences on the effect of anions and the IL environment in SPPS, Jung-Redemann 10-mer[170] (JR 10-mer, H-WFTTLISTIM-NH_2), which was known as one of the most difficult sequence to be synthesized, was synthesized on IL resins using Fmoc/t-Bu chemistry. JR 10-mer is a suitable peptide model for examining the efficiency of solid support in SPPS.[171] The results showed that JR 10-mer was obtained in higher purities from IL resins (**3a–3e**) than from AM PS resin (Table 9). In particular, the best resin for SPPS was IL[$TFSI^-$] resin (Figure 18a, 57% purity). The performance of IL resins appeared to depend on the swelling properties, especially the loading of the first amino acid on the resin. Despite having a similar swelling property to **3d** resin, AM PS resin exhibited the lowest performance in SPPS (Figure 18b). These results may be attributed to not only the swelling property of resins but also the IL spacer which can furnish the growing peptide with an adequate environment within the polymer matrix and may inhibit the peptide on the resin from self-aggregation. Based on this, we demonstrate that the IL spacer could create a proper environment for efficient SPPS.

(a)

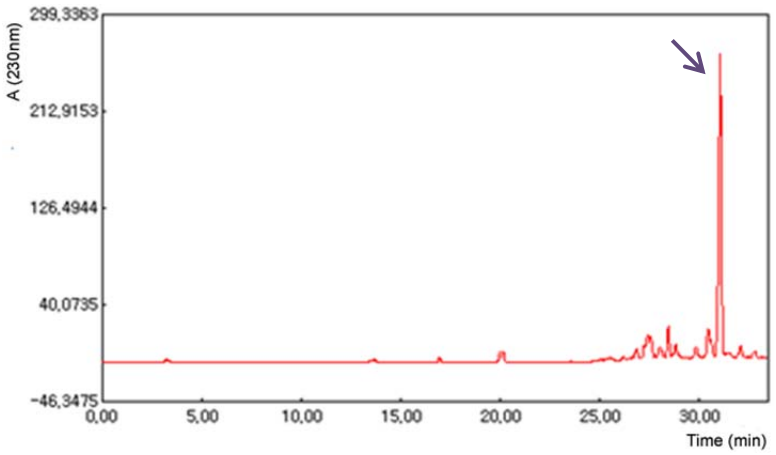

(b)

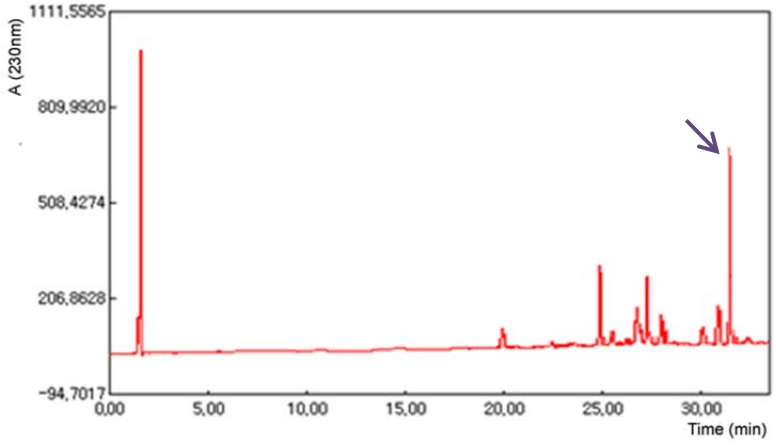

Figure 18. HPLC analysis of JR 10-mer synthesized from (a) IL resin (**3e**) and (b) AM PS resin.

Table 9. Crude Purity of Peptides (Leu-enkephalin, β_2M(59–71), and JR 10-mer) Synthesized from the IL Resins and AM PS Resin

resin	purity of peptides (%)		
	Leu-enkephalin	β_2M(59–71)	JR 10-mer
3a (Cl^-)	87	21	42
3b (BF_4^-)	95	23	48
3c (OTf^-)	93	26	43
3d (PF_6^-)	94	28	51
3e ($TFSI^-$)	94	27	57
AM PS resin	90	21	33

4. Conclusion

We prepared IL resins with Cl^-, BF_4^-, OTf^-, PF_6^-, and $TFSI^-$ anions by introducing amine functionalized an imidazolium group to PS resin. By changing the anions of the IL, IL resins revealed different properties depending on the characteristics of each IL spacer group. In particular, IL resins with PF_6^- and $TFSI^-$ anions swelled the most in NMP and performed well in the loading of the first amino acids. They also achieved higher purity in solid-phase peptide synthesis than AM PS resin. These results are related to not only the swelling property of resins but also the IL spacer group which can afford an adequate ionic environment to the glowing peptide during peptide synthesis. Therefore, IL resin with versatile properties caused by IL spacer enables efficient SPPS, even in the synthesis of difficult sequences peptide.

Chapter IV

Core–Shell-Type Resin for Solid-Phase Peptide Synthesis

1. Introduction

The synthesis of highly aggregative peptides, which are responsible for various diseases such as Alzheimer's, "Mad cow", Parkinson's, and Huntington's diseases, is important to identify the causes of the diseases and to develop therapeutic agents.[172–174] Chemical and recombinant methods have been proposed to synthesize these difficult peptide sequences. Among them, SPPS have attracted a lot of attention due to its convenient work-up and purification procedures. Therefore, since Merrifield introduced solid-phase peptide synthesis (SPPS) method,[6] various attempts have been made to synthesize difficult peptide sequences and complicated structural molecules, such as the development of a new synthetic strategy, new coupling reagents, new polymer supports, and the use of microwave reactors.[7]

One of the most pivotal factors for the success of solid-phase synthesis is choosing a proper solid support. The performance of the solid support is closely related to its swelling property, accessibility, and compatibility with the solvent, reagents, and synthesized peptide.[175,176] Polystyrene (PS) resin beads, which have been most commonly used as a solid support, are composed of a hydrophobic backbone and, therefore, are not compatible with peptides and biomolecules. Because of the many disadvantages of a hydrophobic polymer matrix, there have been needs for development of amphiphilic or hydrophilic polymer beads with both high stability and good swellability in various solvents.

As an alternatives to hydrophobic PS resin, various gel-type, such as TentaGel (PEG-PS), NovaGel (PEG-PS), and ArgoGel (PEG/PS), and polymer grafted pins, such as SynPhase Lanterns, have been introduced (Figure 19).[153,177–182] To obtain a more hydrophilic PEG-based resin without PS backbone, PEGA resin,[183,184] CLEAR resin,[185] SPOCC resin,[186,187] and ChemMatrix resin[188] have been developed for enzymatic reaction and for the synthesis of highly complex peptides (Figure 19). However, preparing PEG-based resins has several shortcomings such as difficult synthetic procedures and high production costs. Therefore, the development of highly efficient and inexpensive solid supports still remains a challenge in peptide chemistry field.

For efficient SPPS, we have proposed several core–shell-type polymer beads in which functional groups are mainly distributed on the outer layer of the resin.[16–18,26–28,33] The core–shell structure was designed to overcome the diffusion problem of reagents and for increased accessibility. Because of this distinctive structural feature, the core–shell-type resins afford high performance in peptide synthesis and photolytic cleavage reactions. But preparing the core–shell structure on polymer beads requires complicated procedures and sometimes harsh conditions. As a result, core–shell polymer beads are not prepared reliably and consistently and they do not always show good performance in SPPS.

Here, we describe a robust method for preparing a core–shell-type resin, which can be facilely and inexpensively prepared from aminomethyl polystyrene (AM PS)

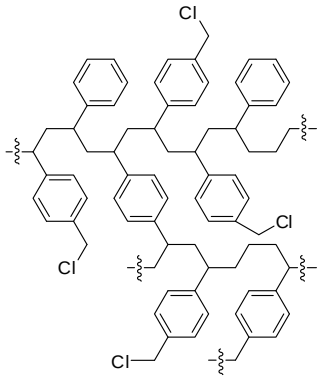

CM PS resin

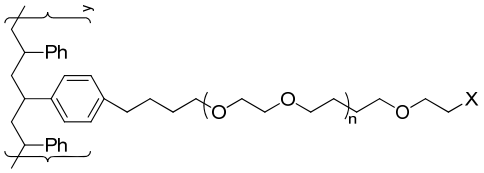

TentaGel®

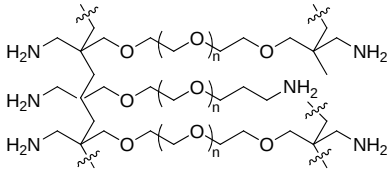

ChemMatrix® resin

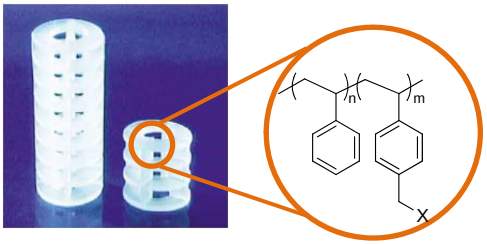

SynPhase™ Lantern

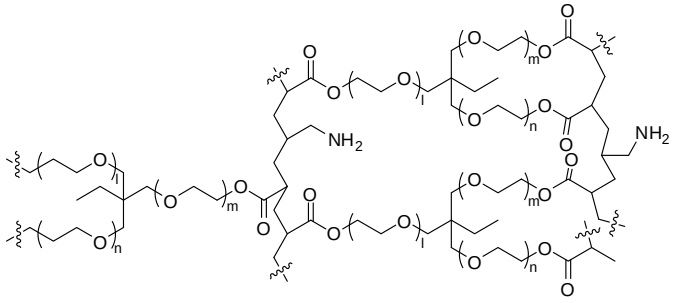

CLEAR®

Figure 19. Representative solid supports for SPPS.

resin using a bi-phasic functionalization method which was developed by Lam.[29–31] The resulting resin possesses good swelling properties and a clear core–shell-type structure which can be easily controlled and reproduced. To evaluate the performance of the core–shell-type resin, difficult peptide sequences, a disulfide-bridged cyclic peptide, and a peptide nucleic acid (PNA) were synthesized, and the results were compared with those of noncore–shell-type AM PS resin, TentaGel resin, and CLEAR resin, which are widely used for SPPS as controls. Furthermore, a long peptide sequence which contains many hydrophobic sequences was synthesized by a microwave-assisted method, and the results were compared with those of AM PS resin and ChemMatrix resin.

2. Experimental Section

2.1. Preparation of Solid Support

2.1.1. Preparation of Core–Shell-Type Resin

Aminomethyl polystyrene resin (10 g, 2.3 mmol/g) was treated with 1 *N* HCl/THF (80 mL, 1/1, v/v) for 2 h, and the resin was washed with water (8 × 100 mL). After the water was removed by filtration, Fmoc-OSu (2.87 g, 8.5 mmol) and DIPEA (1.48 mL, 8.5 mmol) dissolved in CH_2Cl_2 (80 mL) were added to the resin with vigorous shaking overnight at room temperature. The resin was washed with DMF, CH_2Cl_2, and MeOH (3 × 100 mL, each). To cap the amino group in the core part of the resin, the resin was treated with acetic anhydride (4.25 mL, 45 mmol) and DIPEA (7.84 mL, 45 mmol) in DMF for 2 h at room temperature. The Fmoc group was removed with 20% piperidine/DMF for 1 h. The resin was washed with DMF (3×), CH_2Cl_2 (3×), and MeOH (3×) and were dried in vacuo. The loading level of the resin was determined to be 0.67 mmol/g by Fmoc titration.[127] To identify the surface uniformity and morphology of the resin, core–shell-type resin was examined by FE-SEM operated at an accelerating voltage of 5 kV. For high-resolution images, the resin was placed on carbon tape and was coated with Pt via sputtering.

2.1.2. Coupling FITC on Core–Shell-Type Resin for CLSM Analysis

FITC (2 equiv) and DIPEA (4 equiv) were dissolved in DMF (2 mL) and added to the core–shell-type resin (50 mg) which was swollen in DMF. After shaking for 2 h at room temperature, the resin was washed with DMF (3×), CH_2Cl_2 (3×), and MeOH (3×) to remove residual FITC, and then dried in vacuo. As a control group, AM PS resin was coupled with FITC using the same procedure as the core–shell-type resin. To investigate the distribution of amino groups of the resins by CLSM, the fluorescent-labeled resins were placed on a standard microscope glass slide. These resins were examined on CLSM (Carl Zeiss LSM-510) with a 20× power lens using an argon ion (λ = 488 nm) for excitation.

2.2. Peptides Synthesis

2.2.1. ACP(65–74) (H-VQAAIDYING-NH_2)

ACP fragment 65–74 was synthesized manually on Fmoc-Rink-resins (core–shell-type resin: 0.25, 0.51 mmol/g, AM PS resin: 0.28, 0.48 mmol/g) using Fmoc/tBu solid-phase procedure. For this, Fmoc-Rink amide linker (3 equiv) was coupled on the core–shell-type resins (50 mg) with HBTU (3 equiv), HOBt (3 equiv), and DIPEA (3 equiv) for 2 h. In the case of AM PS resin, Fmoc-Rink amide linker (0.8 mmol) was coupled on AM PS (1 g, 2.3 mmol/g) with HBTU (0.8 mmol), HOBt (0.8 mmol), and DIPEA (0.8 mmol) in DMF (15 mL) for 2 h. The remaining amino group was capped with excess acetic anhydride and DIPEA for 2 h. The loading level of Fmoc-Rink-AM PS resin was determined to be 0.48 mmol/g. After Fmoc deprotection with 20% piperidine/NMP for 1 h, the resins (core–shell-type resin: 0.25, 0.51 mmol/g, AM PS resin: 0.28, 0.48 mmol/g, 50 mg each) were treated with preactivated amino acid solution, which was prepared with Fmoc-amino acid (3 equiv), HBTU (3 equiv), HOBt (3 equiv), and DIPEA (6 equiv) in NMP (2 mL). All amino acid couplings were performed for 1 h at 25 ºC. After the coupling reaction, the resin was washed with NMP (5×). The Fmoc group was removed using 20% piperidine/NMP (2 mL, 5 min + 10 min). Completion of each coupling step was monitored by the Kaiser test. The final peptide was cleaved with TFA/TIS/H_2O (95:2.5:2.5) solution for 1 h and was recovered as white solids by ether precipitation.

The crude yield was calculated based on the initial loading level of resins. For the HPLC analysis, condition B was used with a SPIRIT PEPTIDE 120 C18 column. ACP(65–74) was analyzed by MALDI-TOF (calculated exact mass = 1061.6 for $C_{47}H_{75}N_{13}O_{15}$ (ACP(65–74)), $[M + Na]^+$, found 1084.6).

2.2.2. JR 10-mer (H-WFTTLISTIM-NH_2)

JR 10-mer was synthesized by the same procedure as used for ACP(65–74). The peptide was cleaved from the resin by TFA/thioanisole/1,2-ethanedithiol/anisole (90:5:3:2) solution for 1 h, and was recovered as white solids by ether precipitation. For the HPLC analysis, condition B was used with a Waters symmetry C18 column. The JR 10-mer peptide was identified by MALDI-TOF (calculated exact mass = 1210.6 for $C_{58}H_{90}N_{12}O_{14}S$ (JR 10-mer), $[M + Na]^+$, found 1233.8).

2.2.3. iRGD (Fmoc-c(CRGDRGPDC)-TEG-K-NH_2)

iRGD was synthesized on an Fmoc-Rink amide core–shell-type resin and Fmoc-Rink amide TentaGel resin (0.33 mmol/g, respectively) by the same method as above. After the last amino acid coupling, the linear peptide containing the S-Acm

protecting groups was treated with 2 equivalents of $Tl(Tfa)_3$ in NMP (2 mL) for 2 h. The final cyclic peptide was cleaved from the resin with TFA/thioanisole/TIS/H_2O (85:5:5:5) solution for 1 h and was recovered as white solids by ether precipitation. For the HPLC analysis, condition B was used with a SPIRIT PEPTIDE 120 C18 column. The peptide was identified by MALDI-TOF (calculated exact mass = 1626.7 for $C_{70}H_{106}N_{20}O_{21}S_2$ (Fmoc-iRGD-TEG-K)$[M + H]^+$, found 1627.5).

2.2.4. PNA Probe for HPV 31 (Bts-ctgcaattgcaaacagtg)

Synthesis of the PNA oligomer was kindly tested by Panagene, Inc., using a Bts strategy. Briefly, Fmoc-PAL-resins were prepared by coupling the Fmoc-Gly-OH and Fmoc-PAL linker sequentially on core–shell-type and CLEAR resins. To adjust for the same loading level (0.15 mmol/g) of resins (core–shell-type resin and CLEAR resin), 0.15 mmol (per 1 g of each resin) of Fmoc-PAL linker was coupled to the resins and the remnant of amino groups were then capped with excess acetic anhydride and DIPEA. After deprotection of the Fmoc group, the resins were treated with 0.3 M solution of appropriate cyclic Bts-PNA monomer in DMF for 1.5 h at 40 ºC. The remnant amino group was capped by treatment 5% acetic anhydride and 6% lutidine in DMF for 3 min. To detach over-reacted acetyl group on the Bts-protected amine, the resin was treated with 1.0 M piperidine in DMF for 3 min. Then, the Bts protecting group was deprotected by 1 M 4-methoxybenzenethiol and

1 M DIPEA in DMF for 10 min at 40 ºC. This cycle was repeated for every Bts-PNA monomer coupling step. After the last monomer was coupled, the final PNA oligomer was cleaved from the resins with 25% *m*-cresol in TFA for 1.5 h and was characterized by HPLC.

2.2.5. MoPrP 105–125 (H-KTNLKHVAGAAAAGAVVGGLG-NH_2)

MoPrP 105–125 was synthesized using Fmoc/tBu-based strategy on a Liberty microwave-assisted peptide synthesizer (CEM). Three kinds of Rink amide linker loaded resins were prepared (core–shell-type resin: 0.40 mmol/g, AM PS: 0.45 mmol/g, ChemMatrix: 0.41 mmol/g). These resins (100 mg each) were transferred to a Teflon vessel, and peptide synthesis was carried out under nitrogen bubbling. Each coupling reaction was performed with Fmoc-amino acid (5 equiv), HBTU (5 equiv) and DIPEA (10 equiv) in DMF by irradiating at 70 °C for 300 s (maximum power 20 W). Double Fmoc deprotection with 20% piperidine/DMF was performed at 75 °C for 30 s (maximum power 40 W) for the first deprotection and 70 °C for 180 s (maximum power 35 W) for the second deprotection. After the last amino acid coupling and deprotection, the final peptide was cleaved from the resins with TFA/TIS/H_2O (95:2.5:2.5) solution for 1 h, and was recovered as white solids by ether precipitation. For the HPLC analysis, condition B was used with a SPIRIT PEPTIDE 120 C18 column. The peptide was analyzed by MALDI-TOF (calculated

exact mass = 1860.1 for $C_{81}H_{141}N_{27}O_{23}$ (MoPrP(105–125))$[M + H]^+$, found 1861.1).

3. Results and Discussion

3.1. Preparation and Characterization of Core–Shell-Type Resin

3.1.1. Preparation of Core–Shell-Type Resin

As shown in Scheme 9, AM PS resin was treated with 1 *N* HCl/THF for 2 h to prepare a hydrophilic HCl salt form. After washing with water, Fmoc-OSu in CH_2Cl_2 was added to the resin and was coupled to the amino groups on the shell layer. During this step, Fmoc groups start to couple to the amino groups on the outermost interface between the aqueous and organic phases and gradually react

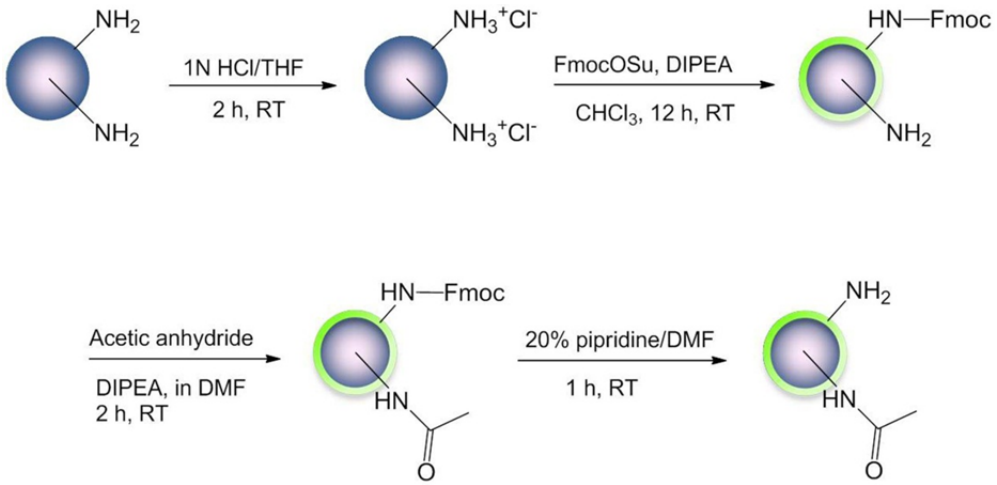

Scheme 9. Preparation of Core–Shell-Type Resin

with the amino groups at the inner part of the resin due to the movement of the interface to the inside of the resin during Fmoc coupling. Then, the remnant amino groups in the core domain of the resin were capped by acetyl groups. After deprotection of the Fmoc groups, we finally obtained the core–shell-type resin, which provided clear surface morphology without any physical changes (Figure 20a). Chemical changes from amine to amide were confirmed by FT-IR (amide band, 1652 cm^{-1}, Figure 20b).

(a) (b)

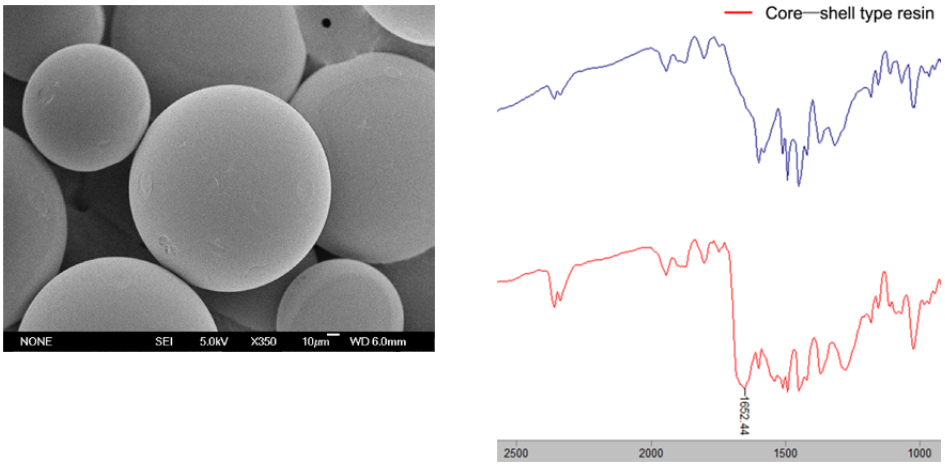

Figure 20. Characterization of core–shell-type resin: (a) SEM image showing clear surface morphology of the core–shell-type resin and (b) FT-IR spectra of AM PS resin and core–shell-type resin.

3.1.2. Swelling Properties

The swelling properties of the core–shell-type and AM PS resins were measured in various solvents (Table 10). The core–shell-type resin exhibited good swelling properties in most aprotic polar solvents. In particular, the core–shell-type resin swelled much better than AM PS resin in NMP, DMF, and CH_2Cl_2. Thus, this resin was expected to afford good coupling efficiency during the early stage of peptide synthesis.[189]

Table 10. Swelling Volume of Core–Shell-Type Resin and AM PS Resin in Various Solvents

resin	swelling volume (mL/g)							
	dry	H_2O	NMP	DMF	MeOH	THF	CH_2Cl_2	Hex
core–shell-type resin	1.7	1.5	7.5	6.6	2.3	5.5	6.2	1.9
AM PS resin	1.6	1.4	6.0	5.5	2.6	3.9	4.5	2.1

3.1.3. Core–Shell Structure

The distribution of reactive amino groups on the resin can be clearly visualized after fluorescent dye coupling.[190] After FITC (fluorescein 5(6)-isothiocyanate) was covalently attached to the resin, the FITC-labeled resin was analyzed by confocal laser scanning microscopy (CLSM) to confirm the core–shell structure. As shown in the CLSM images (Figure 21b), the core–shell-type resin revealed reactive amino groups on the shell layer, whereas the AM PS resin had reactive amino groups in the entire region of the resin (Figure 21a). In addition, the fluorescence intensity profile of the core–shell-type resin demonstrates quite clearly that the functional groups were concentrated on the shell layer (Figure 21c).

(a) (b) (c)

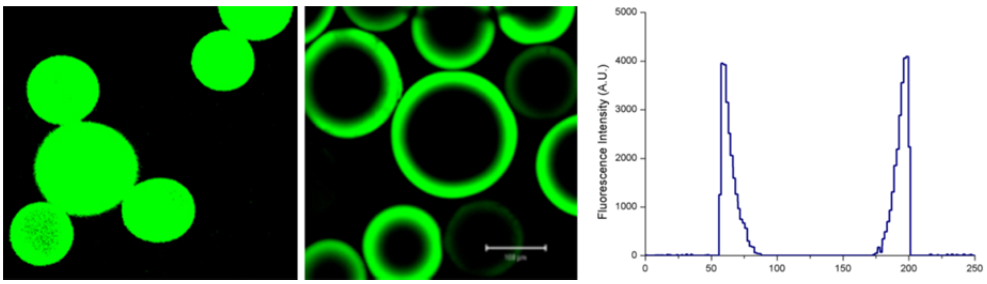

Figure 21. Distribution of amino group on resins: CLSM images of FITC coupled (a) AM PS resin and (b) core–shell-type resin; (c) Fluorescence profile graph of a line passing through the center of core–shell-type resin.

3.1.4. Control of Shell Layer Thickness

In previous approaches for the preparation of core–shell structure on PS resins led to the realization that consistent production was difficult because it required elaborate controls of the reaction under harsh conditions. However, in our new method, we can precisely control the amount of amino groups and the thickness of the shell layer by regulating the amount of Fmoc-OSu and DIPEA under mild conditions. Thus, various classes of core–shell-type resins with different loading could be obtained by varying the amount of reagents (Fmoc-OSu and DIPEA). For example, when 0.51 mmol of reagents were treated with 1 g of resin, we finally obtained 0.43 mmol/g of core–shell-type resin. From this result, we found that the loading level of the reactive amino group on the resin was linearly correlated to the amount of added reagent with ca. 82% yield (Figure 22a). The changes in the thickness of the shell layer and the distribution of amino groups on the resins were visualized by FITC. As shown in the CLSM images (Figure 22b), shell layer thickness was increased as the amine loading levels increased. These results indicate that the core–shell structure can be prepared precisely and consistently by using this method, with the whole range of amine loading levels appropriate for peptide target.

(a)

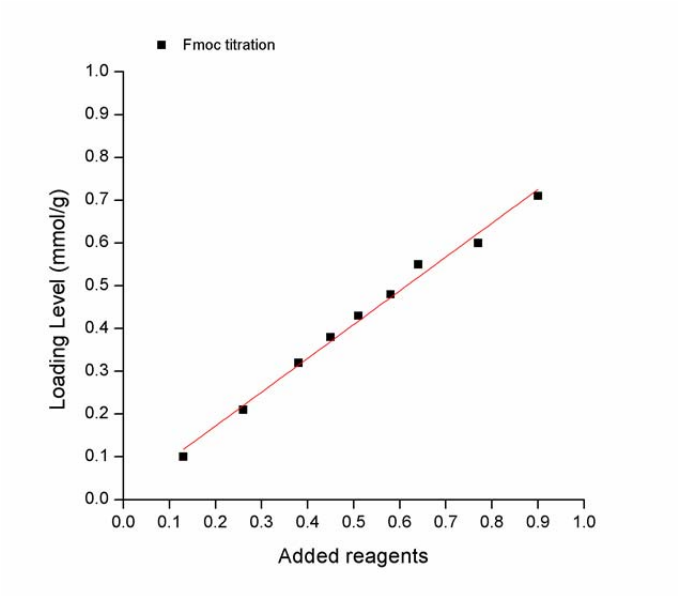

(b)

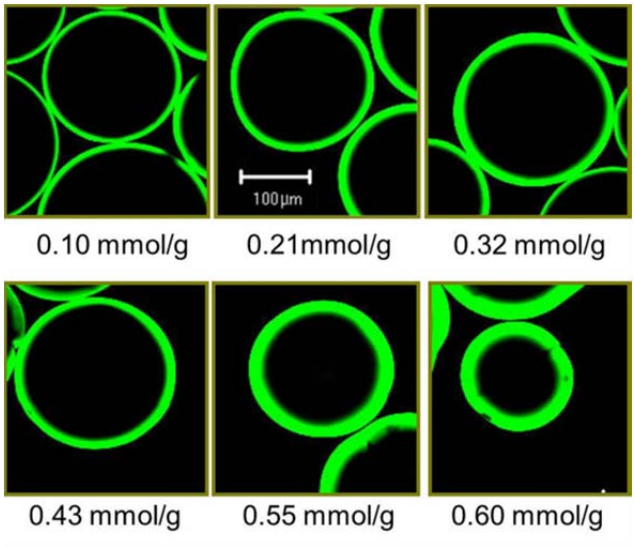

Figure 22. Controlling the thickness of the shell layer of the core–shell-type resin: (a) correlation between the amount of added reagents and the loading level of reactive amino groups on the resin, (b) CLSM images of the core–shell-type resins.

3.2. Synthesis of Peptides on Core–Shell-Type Resin

3.2.1. Synthesis of ACP(65–74) and JR 10-mer

ACP(65–74) and JR 10-mer were chosen as model peptides and were synthesized using Fmoc/tBu strategy on Rink amide linker coupled core–shell-type and AM PS resins.[155,171] The peptides are known as difficult peptide sequences due to the β-sheet structure and hence, are suitable targets for evaluating the synthetic performance of the resins in SPPS. High loaded and low loaded resins (ca. 0.50,

Table 11. Crude Yield and Purity of Peptides (ACP(65–74) and JR 10-mer) Obtained from the Core–Shell-Type Resin and AM PS Resin

loading level	resin	ACP(65–74)		JR 10-mer	
		crude yield (%)	purity (%)	crude yield (%)	purity (%)
high loading (0.50 mmol/g)	core–shell-type resin	99	88	90	45
	AM PS resin	60	28	83	35
low loading (0.25 mmol/g)	core–shell-type resin	99	88	99	54
	AM PS resin	85	37	89	51

0.25 mmol/g) were prepared to determine the differences in synthetic performance between the core–shell- and noncore–shell-type resins. The results of the peptide synthesis revealed that the core–shell-type resins afforded ACP(65–74) and JR 10-mer in higher crude yield and purity than those of the AM PS resin (Table 11). Noticeable differences in synthetic performance were exhibited on the high-loaded resin. In particular, from the results of ACP(65–74), we found that the desired product was obtained without significant deletion sequences from the core–shell-type resin, whereas many deletion sequences were detected from the AM PS resin, as shown in the high-performance liquid chromatography (HPLC) chromatogram. Although no critical differences in the purity were found from the low-loaded resins during JR 10-mer synthesis, we noticed that the core–shell-type resin provided better synthetic efficiency than the AM PS resin at a high loading level (Table 11). Based on these results, we can say that many deletion sequence peptides and side products during SPPS might come from the core domain of the resins. Therefore, it is noteworthy that the core–shell structure offered a significant advantage to overcome the diffusion problem because the accessibility of the functional groups located on the shell layer is better than that in the core domain for the incoming reagents.

3.2.2. Synthesis of Cyclic Peptide (iRGD)

A disulfide-bridged cyclic peptide, triethylene glycol (TEG) grafted iRGD (c(CRGDRGPD C)-TEG-K), was synthesized to show that the cyclic peptide could be well-prepared and -cyclized on the core–shell-type resin (0.33 mmol/g) as on TentaGel resin (0.30 mmol/g). The cyclic peptide, which is internalizing RGD (iRGD, c(CRGDRGPDC)), can bind to α_v integrin and its truncated motif interacts with neuropilin-1 to be internalized into tumor cells.[191,192] Peptide synthesis was followed by the same procedure as above, and on-resin cyclization was performed using thallium(III) trifluoroacetate ($Tl(Tfa)_3$).[193] After cleavage, the peptides were recovered in similar crude yields (40–42%) and purities (44%) from both of the resins. As shown in Figure 23, the HPLC pattern of the peptide from the core–shell-type resin looked quite similar to that from TentaGel. Linear peptide sequences containing free cysteine residues were not detected in the HPLC peaks assigned by the matrix-assisted laser desorption/ionization-time-of-flight (MALDI-TOF) mass spectrometry. The cyclization reaction was carried out effectively on the core–shell-type resin. These results indicated that the core–shell-type resin showed effective synthetic performance as good as TentaGel, even for the synthesis of a disulfide-bridged cyclic peptide. After iRGD peptide was isolated and purified from core–shell-type resin, fluorescence dye (AF 488) was conjugated on N-terminal of the peptide. Biological activity of the peptide was demonstrated by incubating it

with cancer cell lines. As a result, the dye conjugated peptide could visualize cancer cell which has both $\alpha_v\beta_3$ integrin and neurophilin-1 by being internalized into the cell (data not shown). Therefore, we can conclude that iRGD peptide was efficiently synthesized on the core–shell-type resin and it maintained its biological activity.

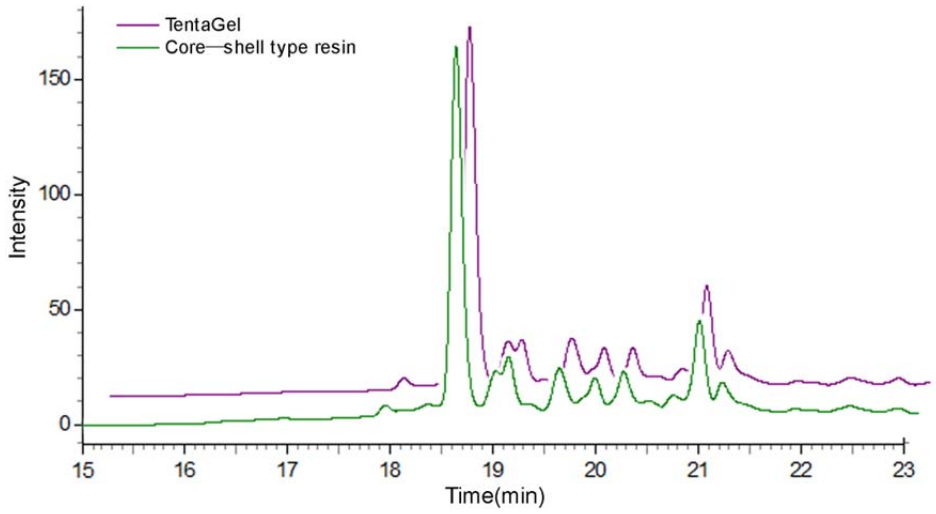

Figure 23. HPLC analysis of the crude iRGD peptide prepared on Tentagel and the core–shell-type resin.

3.2.3. Synthesis of PNA

PNA oligomer was synthesized on the core–shell-type resin, and the result was compared with that of CLEAR resin, which is generally used as a solid support in the field of PNA oligomer synthesis. The PNA probe for HPV 31 genotyping (Bts-ctgcaattgcaaacagtg), which is known as one of the difficult sequences of the HPV types, was prepared by benzothiazole-2-sulfonyl (Bts) strategy using self-activated Bts protected PNA monomer.[194] The core–shell-type resin gave similar results to the CLEAR resin (Figure 24). During synthesis, trans-acylation and other side reactions were not observed on the core–shell-type resin. PNA synthesis on the core–shell-type resin could be further optimized, and is expected to replace the CLEAR resin for the synthesis of PNA oligomers.

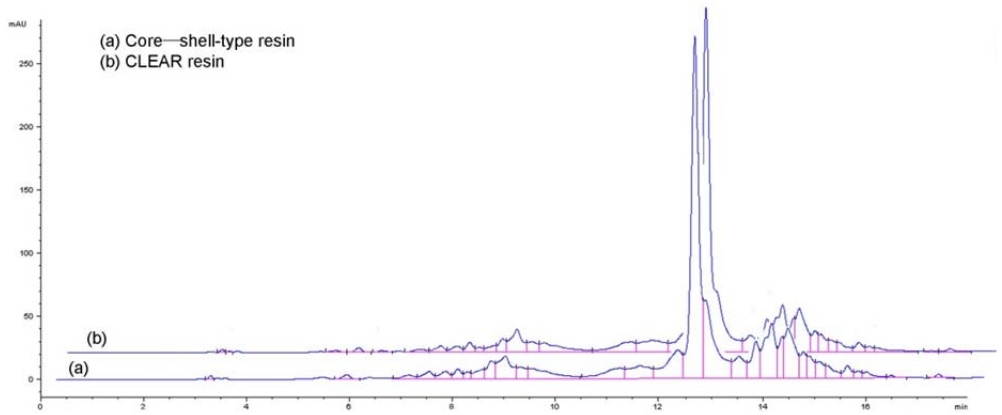

Figure 24. HPLC analysis of crude PNA probe for HPV 31 prepared on (a) core–shell-type resin and (b) CLEAR resin.

3.2.4. Synthesis of MoPrP(105–125) under Microwave Condition

Because microwave irradiation enhances coupling efficiency during SPPS,[195] several PEG-based resins, such as Tentagel, ChemMatrix and other PS-PEG resins, have provided satisfactory outcomes following microwave-assisted SPPS, due to the versatile properties of PEG. The synthesis of MoPrP(105–125) was carried out on the core–shell-type resin to ascertain whether the core–shell structure could afford better results during microwave-assisted SPPS, as compared to those of AM PS and ChemMatrix resins which have similar loading levels (0.40–0.45 mmol/g). MoPrP(105–125) (^{105}KTNLKH^{111}VAGAAAAGAVVGG LG^{125}), a peptide fragment of a mouse prion protein, has a high aggregation tendency which is caused by the presence of long hydrophobic sequences at its C-terminus (111–125).[196,197] Mild protocols (70 °C for 300 s, maximum power 20 W) were followed during microwave irradiation in every coupling and deprotection step, so as to determine the differences in performance among resins. Although the crude yields are similar among the resins (core–shell-type resin: 59%, AM PS resin: 52% and ChemMatrix resin: 61%), the HPLC pattern showed dramatic differences between the core–shell-type and noncore–shell-type resins (Figure 25). The HPLC data (Figure 25a) showed that the peptide from the AM PS resin was accompanied by many deletion sequences and that the main peak was an undesired product with a low molecular weight ([M + H] = 939.5, [M–Ala + H] = 868.5, t_R = 13.6 min). The desired product

appeared in low purity (13%, t_R = 14.1 min) next to the main peak. The HPLC data from ChemMatrix, which is similar to that from the AM PS resin, revealed a few side products due to the PEG chain, which can minimize self-aggregation of the growing peptide chains on the resin. However, it still yielded the same undesired product as the major one as the AM PS resin (Figure 25b, purity = 26%). By Edman degradation and MALDI-TOF mass analysis, we found that this undesired product was KTNKKHAGG or KTNKHAGAGG (Table 12, [M + H] = 939.5, [M–Ala + H] = 868.5), which did not possess most of the hydrophobic residues in the MoPrP(105–125) sequences. Thus, it appears that the reagents could not diffuse freely into the core domain of the resins due to the aggregated fragments formed during the initial stages of SPPS with hydrophobic sequences. Because of this, the noncore–shell-type resins led to serious deletion during MoPrP(105–125) synthesis, even on the PEG-based resin. However, the peptide synthesized on the core–shell-type resin gave higher purity than other resins and afforded the desired product as a major one (Figure 25c, purity = 31%). Because of the excellent reagent accessibility of the core–shell structure, the synthesis of hydrophobic sequences was well carried out, which led to an increased yield and higher purity. Although the unexpected side product with a deletion sequence was detected in the HPLC (Table 12, [M + H] = 1781.07 t_R = 15.0 min), we believe that this could be easily overcome by optimizing the reaction conditions, as it involved only one or two sequences. Based on these results, we can conclude that the core–shell-type resin can offset the hydrophobic environment which causes severe deletion sequences during peptide synthesis by

enhancing reagent accessibility, and can therefore enable more efficient peptide synthesis than other noncore–shell-type resins.

Table 12. Peptide Sequences of MoPrP(105–125) Peptide Fragments Analyzed by Edman Degradation

molecular weight	peptide sequences
[M+H] = 939.5 [M-Ala+H] = 868.4 (t_R = 13.6 min)	KTNKKHAGG or KTNKHAGAGG
[M+H] = 1781.07 (t_R = 15.0 min)	KTNLKKVAGAAAAGVVGGLG or KTNLKVAGAAAAGGAVVGGLG

(a)

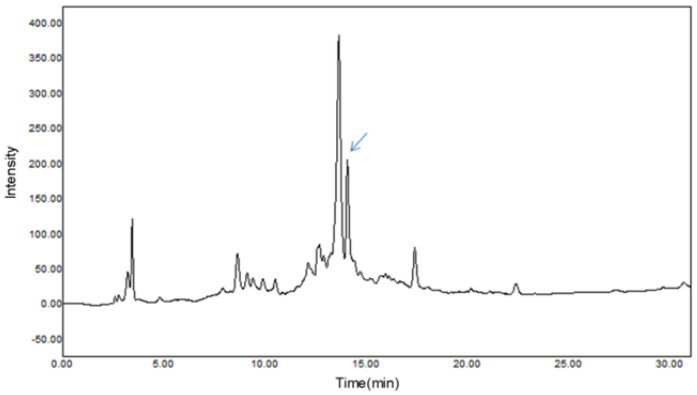

(b)

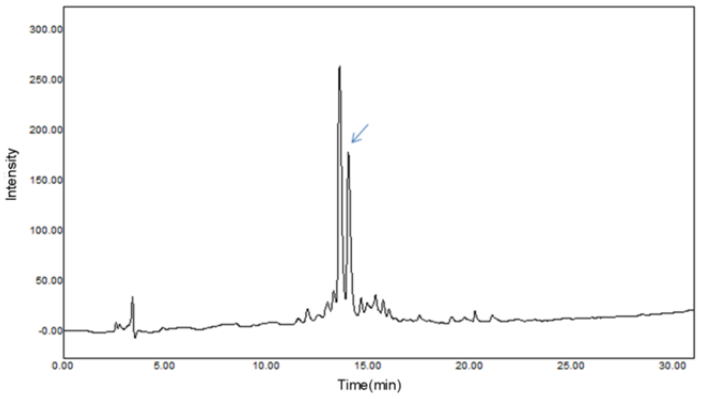

(c)

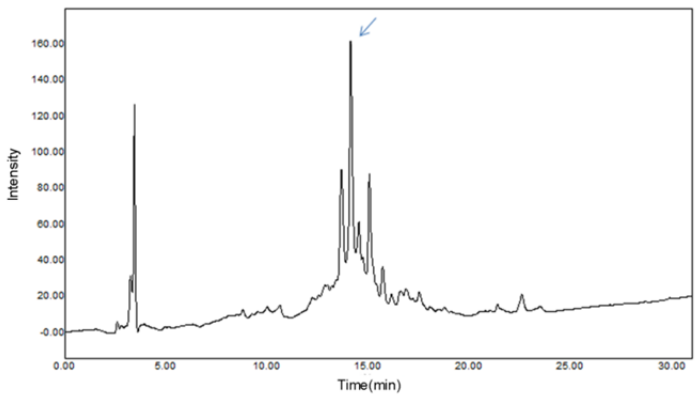

Figure 25. HPLC analysis of crude MoPrP 105–125 prepared by automatic microwave-assisted peptide synthesizer on (a) AM PS, (b) ChemMatrix resin, and (c) core–shell-type resin. Desired product is marked with an arrow.

4. Conclusion

A core–shell-type resin was prepared by a bi-phasic functionalization method under relatively mild conditions. The procedure was beneficial for controlling both the thickness of the shell layer and the loading level of the resin. The core–shell-type resin exhibited good swelling properties in various solvents and afforded a uniform core–shell structure. In SPPS, the core–shell-type resin provided effective synthetic performance during the synthesis of hydrophobic peptide sequences, a disulfide-bridged cyclic peptide, and a difficult PNA sequence. Furthermore, a highly aggregative peptide fragment was synthesized effectively on the core–shell-type resin under microwave-assisted synthesis. These results demonstrate that the core–shell-type resin can compensate for the synthetic loss caused by the hydrophobic environment by blocking the core part of the resin, which is responsible for the deletion sequences. Therefore, the core–shell-type resin has comparative advantages over other PEG-based resins in terms of synthetic performance. Furthermore, we expect that the core–shell-type resin can be applied successfully to other applications in organic synthesis as a polymer support, polymer-supported reagent, or as a polymer-supported catalyst.

References

1. McGonigle, P. *Biochemical Pharmacology* **2012**, *83*, 559.

2. Itakura, K.; Hirose, T.; Crea, R.; Riggs, A. D.; Heyneker, H. L.; Bolivar, F.; Boyer, H. W. *Science (New York, N.Y.)* **1977**, *198*, 1056.

3. Hu, G. *BioProcess Journal* **2009**, *8*, 51.

4. Kent, S. B. H. *Annual Review of Biochemistry* **1988**, *57*, 957.

5. Tsuda, Y.; Okada, Y. In *Amino Acids, Peptides and Proteins in Organic Chemistry*; Hughes, A. B. Eds.; Wiley-VCH Verlag GmbH & Co. KGaA: 2010, p 201.

6. Merrifield, R. B. *J. Am. Chem. Soc.* **1963**, *85*, 2149.

7. Kate, S. A.; Albericio, F. In *Solid Phase Synthesis: A Practical Guide*; Marcel Dekker: New York, 2000.

8. Riniker, B.; Flörsheimer, A.; Fretz, H.; Sieber, P.; Kamber, B. *Tetrahedron* **1993**, *49*, 9307.

9. Andersson, L.; Blomberg, L.; Flegel, M.; Lepsa, L.; Nilsson, B.; Verlander, M. *Biopolymers* **2000**, *55*, 227.

10. Bray, B. L. *Nature reviews. Drug discovery* **2003**, *2*, 587.

11. Hughes, L. J.; Brown, G. L. *Journal of Applied Polymer Science* **1961**, *5*, 580.

12. Li, W.-H.; Stöver, H. D. H. *Macromolecules* **2000**, *33*, 4354.

13. Grancio, M. R.; Williams, D. J. *Journal of Polymer Science Part A-1: Polymer Chemistry* **1970**, *8*, 2617.

14. Stutman, D. R.; Klein, A.; El-Aasser, M. S.; Vanderhoff, J. W. *Industrial & Engineering Chemistry Product Research and Development* **1985**, *24*, 404.

15. Winnik, M. A.; Zhao, C. L.; Shaffer, O.; Shivers, R. R. *Langmuir* **1993**, *9*, 2053.

16. Cho, J. K.; Park, B. D.; Lee, Y. S. *Tetrahedron Letters* **2000**, *41*, 7481.

17. Cho, J. K.; Park, B. D.; Park, K. B.; Lee, Y. S. *Macromolecular Chemistry and Physics* **2002**, *203*, 2211.

18. Kim, H.; Cho, J. K.; Chung, W. J.; Lee, Y. S. *Organic Letters* **2004**, *6*, 3273.

19. Kim, J.-H.; Jun, B.-H.; Byun, J.-W.; Lee, Y.-S. *Tetrahedron Letters* **2004**, *45*, 5827.

20. Kim, J.-H.; Kim, J.-W.; Shokouhimehr, M.; Lee, Y.-S. *The Journal of Organic Chemistry* **2005**, *70*, 6714.

21. Ishizu, K.; Fukutomi, T. *Journal of Polymer Science Part C: Polymer Letters* **1988**, *26*, 281.

22. Saito, R.; Ishizu, K.; Fukutomi, T. *Polymer* **1990**, *31*, 679.

23. Iijima, M.; Nagasaki, Y.; Okada, T.; Kato, M.; Kataoka, K. *Macromolecules* **1999**, *32*, 1140.

24. Thurmond, K. B.; Kowalewski, T.; Wooley, K. L. *Journal of the American Chemical Society* **1997**, *119*, 6656.

25. Ding, J.; Liu, G. *Macromolecules* **1998**, *31*, 6554.

26. Lee, T. K.; Ryoo, S. J.; Byun, J. W.; Lee, S. M.; Lee, Y. S. *Journal of Combinatorial Chemistry* **2005**, *7*, 170.

27. Lee, T. K.; Lee, S. M.; Ryoo, S. J.; Byun, J. W.; Lee, Y. S. *Tetrahedron Letters* **2005**, *46*, 7135.

28. Choi, J. H.; Lee, T. K.; Byun, J. W.; Lee, Y. S. *Tetrahedron Letters* **2009**, *50*, 4272.

29. Vagner, J.; Barany, G.; Lam, K. S.; Krchnak, V.; Sepetov, N. F.; Ostrem, J. A.; Strop, P.; Lebl, M. *Proceedings of the National Academy of Sciences of the United States of America* **1996**, *93*, 8194.

30. Liu, R. W.; Mark, J.; Lam, K. S. *Journal of the American Chemical Society* **2002**, *124*, 7678.

31. Song, A. M.; Zhang, J. H.; Lebrilla, C. B.; Lam, K. S. *Journal of the American Chemical Society* **2003**, *125*, 6180.

32. Wang, X. B.; Zhang, J. H.; Song, A. M.; Lebrilla, C. B.; Lam, K. S. *Journal of the American Chemical Society* **2004**, *126*, 5740.

33. Lee, T. K.; Choi, J. H.; Ryoo, S. J.; Lee, Y. S. *Journal of Peptide Science* **2007**, *13*, 655.

34. Klein, J.; Widdecke, H.; Bothe, N. *Die Makromolekulare Chemie* **1984**, *6*, 211.

35. Badyal, J. P.; Cameron, A. M.; Cameron, N. R.; Coe, D. M.; Cox, R.; Davis, B. G.; Oates, L. J.; Oye, G.; Spanos, C.; Steel, P. G. *Chemical Communications* **2004**, 1402.

36. Wasserscheid, P.; Welton, T. *Ionic Liquids in Synthesis*; John Wiley & Sons, 2008.

37. Gordon, C. M.; Holbrey, J. D.; Kennedy, A. R.; Seddon, K. R. *Journal of Materials Chemistry* **1998**, *8*, 2627.

38. Suarez, P., A.Z.; Einloft, S.; Dullius, J., E.L.; de Souza, R., F.; Dupont, J. *J. Chim. Phys.* **1998**, *95*, 1626.

39. Zim, D.; de Souza, R. F.; Dupont, J.; Monteiro, A. L. *Tetrahedron Letters* **1998**, *39*, 7071.

40. Dyson, P. J.; Ellis, D. J.; Welton, T.; Parker, D. G. *Chemical Communications* **1999**, 25.

41. J. Earle, M.; B. McCormac, P.; R. Seddon, K. *Green Chemistry* **1999**, *1*, 23.

42. Muldoon, M. J. *Dalton Transactions* **2010**, *39*, 337.

43. Hussey, R. L. In *Chemistry of Nonaqueous Solutions;* Mamantov, G.; Popov, A., *Ed, VCH,* Weinheim, 1994, *p* 227.

44. MacFarlane, D. R.; Forsyth, M.; Howlett, P. C.; Pringle, J. M.; Sun, J.; Annat, G.; Neil, W.; Izgorodina, E. I. *Accounts of Chemical Research* **2007**, *40*, 1165.

45. Hussey, C. L. *Pure and Applied Chemistry* **1988, 60**, 1763.

46. Carlin, R. T.; Wikes, J. S. In *Chemistry of Nonaqueous Solutions;* Mamantov, G.; Popov, A., *Ed, VCH,* Weinheim, 1994, *p* 277.

47. Huo, C. D.; Chan, T. H. *Chemical Society Reviews* **2010**, *39*, 2977.

48. Clare, B.; Sirwardana, A.; MacFarlane, D. R. In *Ionic Liquids*; Kirchner, B., Ed. 2009; Vol. 290, p 1.

49. Gabriel, S.; Weiner, J. *Berichte der deutschen chemischen Gesellschaft* **1888**, *21*, 2669.

50. Walden, P. *Bull. Acad. Imp. Sci. (St. Petersburg)* **1914**, 1800.

51. Wilkes, J. S.; Levisky, J. A.; Wilson, R. A.; Hussey, C. L. *Inorganic Chemistry* **1982**, *21*, 1263.

52. Wilkes, J. S.; Zaworotko, M. J. *Journal of the Chemical Society, Chemical Communications* **1992**, 965.

53. Davis, J. J. H. *Chemistry Letters* **2004**, *33*, 1072.

54. Visser, A. E.; Swatloski, R. P.; Reichert, W. M.; Mayton, R.; Sheff, S.; Wierzbicki, A.; Davis, J. J. H.; Rogers, R. D. *Chemical Communications* **2001**, 135.

55. Freemantle, M. *Chemical & Engineering News Archive* **1998**, *76*, 32.

56. Berthod, A; Carda-Broch, S. *The Annals of the Marie Curie Fellowships* **2004**, 3, 32.

57. Reichardt, C. *Green Chemistry* **2005**, *7*, 339.

58. Greaves, T. L.; Drummond, C. J. *Chemical Reviews* **2007**, *108*, 206.

59. Singh, T.; Kumar, A. *The Journal of Physical Chemistry B* **2008**, *112*, 12968.

60. Freemantle, M. *An Introduction to Ionic Liquids*; RSC Pub., 2009.

61. Hallett, J. P.; Welton, T. *Chemical Reviews* **2011**, *111*, 3508.

62. Seddon, K. R. *Journal of Chemical Technology & Biotechnology* **1997**, *68*, 351.

63. Elaiwi, A.; Hitchcock, P. B.; Seddon, K. R.; Srinivasan, N.; Tan, Y.-M.; Welton, T.; Zora, J. A. *Journal of the Chemical Society, Dalton Transactions* **1995**, 3467.

64. Stegemann, H.; Rohde, A.; Reiche, A.; Schnittke, A.; Füllbier, H. *Electrochimica Acta* **1992**, *37*, 379.

65. Wasserscheid, P.; Keim, W. *Angewandte Chemie International Edition* **2000**, *39*,

3772.

66. Swatloski, R. P.; Holbrey, J. D.; Rogers, R. D. *Green Chemistry* **2003**, *5*, 361.

67. Greaves, T. L.; Weerawardena, A.; Fong, C.; Krodkiewska, I.; Drummond, C. J. *The Journal of Physical Chemistry B* **2006**, *110*, 22479.

68. Bonhôte, P.; Dias, A.-P.; Papageorgiou, N.; Kalyanasundaram, K.; Grätzel, M. *Inorganic Chemistry* **1996**, *35*, 1168.

69. Mehdi, H.; Binnemans, K.; Van Hecke, K.; Van Meervelt, L.; Nockemann, P. *Chemical Communications* **2010**, *46*, 234.

70. Fannin, A. A.; Floreani, D. A.; King, L. A.; Landers, J. S.; Piersma, B. J.; Stech, D. J.; Vaughn, R. L.; Wilkes, J. S.; Williams John, L. *The Journal of Physical Chemistry* **1984**, *88*, 2614.

71. Perry, R. L.; Jones, K. M.; Scott, W. D.; Liao, Q.; Hussey, C. L. *Journal of Chemical & Engineering Data* **1995**, *40*, 615.

72. Hirao, M.; Sugimoto, H.; Ohno, H. *Journal of The Electrochemical Society* **2000**, *147*, 4168.

73. Bonhôte, P.; Dias, A.-P.; Papageorgiou, N.; Kalyanasundaram, K.; Grätzel, M. *Inorganic Chemistry* **1996**, *35*, 1168.

74. Bagno, A.; Butts, C.; Chiappe, C.; D'Amico, F.; Lord, J. C. D.; Pieraccini, D.; Rastrelli, F. *Organic & Biomolecular Chemistry* **2005**, *3*, 1624.

75. Reichardt, C. *Solvents and Solvent Effects in Organic Chemistry*, 3rd ed.; Wiley-VCH: Weinheim, Germany, **2003**.

76. Muller, P. *Pure and Applied Chemistry* **1994**, *66*, 1077.

77. Freemantle, M. *Chemical & Engineering News Archive* **1999**, *77*, 23.

78. Ott, D.; Kralisch, D.; Stark, A. In *Handbook of Green Chemistry*; Wiley-VCH Verlag GmbH & Co. KGaA: 2010.

79. Sheldon, R. *Chemical Communications* **2001**, 2399.

80. Deng, Y.; Shi, F.; Beng, J.; Qiao, K. *Journal of Molecular Catalysis A: Chemical* **2001**, *165*, 33.

81. Fraga-Dubreuil, J.; Bourahla, K.; Rahmouni, M.; Bazureau, J. P.; Hamelin, J. *Catalysis Communications* **2002**, *3*, 185.

82. Fayet, C.; Gelas, J. *Carbohydrate Research* **1983**, *122*, 59.

83. Bao, Q.; Qiao, K.; Tomida, D.; Yokoyama, C. *Catalysis Communications* **2008**, *9*, 1383.

84. Pârvulescu, V. I.; Hardacre, C. *Chemical Reviews* **2007**, *107*, 2615.

85. Olivier-Bourbigou, H.; Magna, L.; Morvan, D. *Applied Catalysis A: General* **2010**, *373*, 1.

86. Mehnert, C. P. *Chemistry – A European Journal* **2005**, *11*, 50.

87. DeCastro, C.; Sauvage, E.; Valkenberg, M. H.; Hölderich, W. F. *Journal of Catalysis* **2000**, *196*, 86.

88. Valkenberg, M. H.; deCastro, C.; Hoelderich, W. F. In *Studies in Surface Science and Catalysis*; A. Galarneau, F. F. F. D. R., Vedrine, J., Eds.; Elsevier: 2001; Vol. Volume 135, p 179.

89. Valkenberg, M. H.; deCastro, C.; Hölderich, W. F. *Topics in Catalysis* **2000**, *14*, 139.

90. Kim, D. W.; Chi, D. Y. *Angewandte Chemie International Edition* **2004**, *43*, 483.

91. Mehnert, C. P.; Mozeleski, E. J.; Cook, R. A. *Chemical Communications* **2002**, 3010.

92. Gelesky, M. A.; Chiaro, S. S. X.; Pavan, F. A.; dos Santos, J. H. Z.; Dupont, J. *Dalton Transactions* **2007**, 5549.

93. Mehnert, C. P.; Cook, R. A.; Dispenziere, N. C.; Afeworki, M. *Journal of the American Chemical Society* **2002**, *124*, 12932.

94. Autenrieth, B.; Frey, W.; Buchmeiser, M. R. *Chemistry – A European Journal* **2012**, *18*, 14069.

95. Miao, W.; Chan, T. H. *Advanced Synthesis & Catalysis* **2006**, *348*, 1711.

96. Yin; Liebscher, J. *Chemical Reviews* **2006**, *107*, 133.

97. Hirao, M.; Ito, K.; Ohno, H. *Electrochimica Acta* **2000**, *45*, 1291.

98. Shi, F.; Zhang, Q.; Li, D.; Deng, Y. *Chemistry – A European Journal* **2005**, *11*, 5279.

99. Polshettiwar, V.; Hesemann, P.; Moreau, J. J. E. *Tetrahedron Letters* **2007**, *48*, 5363.

100. Choi, J.; Yang, H. Y.; Kim, H. J.; Son, S. U. *Angewandte Chemie International Edition* **2010**, *49*, 7718.

101. Minami, H.; Fukaumi, H.; Okubo, M.; Suzuki, T. *Colloid Polym Sci* **2012**, 1.

102. Palomar, J.; Lemus, J.; Alonso-Morales, N.; Bedia, J.; Gilarranz, M. A.; Rodriguez, J. J. *Chemical Communications* **2012**, *48*, 10046.

103. Dupont, J.; Pfeffer, M. *Palladacycles*; Wiley, 2008.

104. Cope, A. C.; Siekman, R. W. *Journal of the American Chemical Society* **1965**, *87*, 3272.

105. Cope, A. C.; Friedrich, E. C. *Journal of the American Chemical Society* **1968**, *90*, 909.

106. Herrmann, W. A.; Brossmer, C.; Öfele, K.; Reisinger, C.-P.; Priermeier, T.; Beller, M.; Fischer, H. *Angewandte Chemie International Edition in English* **1995**, *34*, 1844.

107. Beller, M.; Fischer, H.; Herrmann, W. A.; Öfele, K.; Brossmer, C. *Angewandte Chemie International Edition in English* **1995**, *34*, 1848.

108. Alonso, D. A.; Nájera, C.; Pacheco, M. C. *Organic Letters* **2000**, *2*, 1823.

109. Onoue, H.; Minami, K.; Nakagawa, K. *Bulletin of the Chemical Society of Japan* **1970**, *43*, 3480.

110. Alonso, D. A.; Botella, L.; Nájera, C.; Pacheco, C. *Synthesis-Stuttgart* **2004**, 1713.

111. Alacid, E.; Alonso, D. A.; Botella, L.; Nájera, C.; Pacheco, M. C. *The Chemical Record* **2006**, *6*, 117.

112. Alonso, D. A.; Nájera, C. *Chemical Society Reviews* **2010**, *39*, 2891.

113. Alonso, D. A.; Nájera, C.; Pacheco, M. C. *Advanced Synthesis & Catalysis* **2002**, *344*, 172.

114. Iyer, S.; Jayanthi, A. *Synlett* **2003**, 1125.

115. Iyer, S.; Kulkarni, G. M.; Ramesh, C. *Tetrahedron* **2004**, *60*, 2163.

116. Baleizão, C.; Corma, A.; Garcia, H.; Leyva, A. *Chemical Communications* **2003**, 606.

117. Corma, A.; Das, D.; García, H.; Leyva, A. *Journal of Catalysis* **2005**, *229*, 322.

118. Baleizão, C.; Corma, A.; García, H.; Leyva, A. *The Journal of Organic Chemistry* **2003**, *69*, 439.

119. Corma, A.; García, H.; Leyva, A. *Tetrahedron* **2004**, *60*, 8553.

120. Corma, A.; García, H.; Leyva, A. *Tetrahedron* **2005**, *61*, 9848.

121. Alacid, E.; Nájera, C. *Synlett* **2006**, 18, 2959.

122. Alacid, E.; Nájera, C. *European Journal of Organic Chemistry* **2008**, 3102.

123. Alacid, E.; Nájera, C. *Journal of Organometallic Chemistry* **2009**, *694*, 1658.

124. Liu, Q. P.; Chen, Y. C.; Wu, Y.; Zhu, J.; Deng, J. G. *Synlett* **2006**, 1503.

125. Mennecke, K.; Solodenko, W.; Kirschning, A. *Synthesis-Stuttgart* **2008**, 1589.

126. Kaiser, E.; Colescott, R. L.; Bossinger, C. D.; Cook, P. I. *Analytical Biochemistry* **1970**, *34*, 595.

127. Fields, G. B.; Tian, Z.; Barany, G. In *Synthetic Peptides: A User's Guide*; Grant, G. A., Eds.; W. H. Freeman & Co.: New York, 1992; pp 77−183.

128. Dyker, G. *Chemische Berichte* **1997**, *130*, 1567.

129. Herrmann, W. A.; Böhm, V. P. W.; Reisinger, C.-P. *Journal of Organometallic Chemistry* **1999**, *576*, 23.

130. Albisson, D. A.; Bedford, R. B.; Scully, P. N.; Lawrence, S. E. *Chemical Communications* **1998**, 2095.

131. Bedford, R. B.; Cazin, C. S. J.; Hazelwood, S. L. *Angewandte Chemie*

International Edition **2002**, *41*, 4120.

132. Ohff, M.; Ohff, A.; Milstein, D. *Chemical Communications* **1999**, 357.

133. Nowotny, M.; Hanefeld, U.; Koningsveld, H. v.; Maschmeyer, T. *Chemical Communications* **2000**, 1877.

134. Gruber, A. S.; Zim, D.; Ebeling, G.; Monteiro, A. L.; Dupont, J. *Organic Letters* **2000**, *2*, 1287.

135. Paz Muñoz, M.; Martín-Matute, B.; Fernández-Rivas, C.; Cárdenas, Diego J.; Echavarren, Antonio M. *Advanced Synthesis & Catalysis* **2001**, *343*, 338.

136. Leadbeater, N. E.; Marco, M. *Chemical Reviews* **2002**, *102*, 3217.

137. Anastas, P. T.; Kirchhoff, M. M. *Accounts of Chemical Research* **2002**, *35*, 686.

138. Martin, R.; Buchwald, S. L. *Accounts of Chemical Research* **2008**, *41*, 1461.

139. Fortman, G. C.; Nolan, S. P. *Chemical Society Reviews* **2011**, *40*, 5151.

140. Hartwig, J. F.; Richards, S.; Barañano, D.; Paul, F. *Journal of the American Chemical Society* **1996**, *118*, 3626.

141. Grasa, G. A.; Viciu, M. S.; Huang, J.; Zhang, C.; Trudell, M. L.; Nolan, S. P. *Organometallics* **2002**, *21*, 2866.

142. Walker, S. D.; Barder, T. E.; Martinelli, J. R.; Buchwald, S. L. *Angewandte Chemie International Edition* **2004**, *43*, 1871.

143. Culkin, D. A.; Hartwig, J. F. *Organometallics* **2004**, *23*, 3398.

144. Kantchev, E. A. B.; O'Brien, C. J.; Organ, M. G. *Aldrichimica Acta* **2006**, *39*, 97.

145. Su, M.; Buchwald, S. L. *Angewandte Chemie International Edition* **2012**, *51*, 4710.

146. Yanagisawa, H.; Takamura, M.; Yamada, E.; Fujita, S.; Fujiwara, T.; Yachi, M.; Isobe, A.; Hagisawa, Y. *Bioorganic & Medicinal Chemistry Letters* **2000**, *10*, 373.

147. DeGrado, W. F.; Kaiser, E. T. *The Journal of Organic Chemistry* **1980**, *45*, 1295.

148. Kumar, G.; Blackburn, J. R.; Albridge, R. G.; Moddeman, W. E.; Jones, M. M. *Inorganic Chemistry* **1972**, *11*, 296.

149. Sharp, M. J.; Snieckus, V. *Tetrahedron Letters* **1985**, *26*, 5997.

150. Gronowitz, S.; Peters, D. *Heterocycles* **1990**, *30*, 645.

151. Bussolari, J. C.; Rehborn, D. C. *Organic Letters* **1999**, *1*, 965.

152. Mora, M.; Jimenez-Sanchidrian, C.; Ruiz, J. R. *Applied Organometallic Chemistry* **2008**, *22*, 122.

153. Bayer, E. *Angewandte Chemie International Edition* **1991**, *30*, 113.

154. Wang, Y.; Zhang, G.; Yan, H.; Fan, Y.; Shi, Z.; Lu, Y.; Sun, Q.; Jiang, W.; Zheng, Y.; Li, S.; Liu, Z. *Tetrahedron* **2006**, *62*, 4948.

155. Atherton, E.; Clive, D. L. J.; Sheppard, R. C. *Journal of the American Chemical Society* **1975**, *97*, 6584.

156. Moss, J. A.; Dickerson, T. J.; Janda, K. D. *Tetrahedron Letters* **2002**, *43*, 37.

157. Vallette, H.; Ferron, L.; Coquerel, G.; Gaumont, A. C.; Plaquevent, J. C. *Tetrahedron Letters* **2004**, *45*, 1617.

158. Chen, L.; Zheng, M. F.; Zhou, Y.; Liu, H.; Jiang, H. L. *Synthetic Communications* **2008**, *38*, 239.

159. Maiti, B.; Chanda, K.; Sun, C. M. *Organic Letters* **2009**, *11*, 4826.

161. Plaquevent, J. C.; Levillain, J.; Guillen, F.; Malhiac, C.; Gaumont, A. C. *Chemical Reviews* **2008**, *108*, 5035.

162. Huang, J. L.; Noss, M. E.; Schmidt, K. M.; Murray, L.; Bunagan, M. R. *Chemical Communications* **2011**, *47*, 8007.

163. Shin, J. Y.; Lee, B. S.; Jung, Y.; Kim, S. J.; Lee, S. G. *Chemical Communications* **2007**, 5238.

164. Schwarz, J.; Bohm, V. P. W.; Gardiner, M. G.; Grosche, M.; Herrmann, W. A.;

Hieringer, W.; Raudaschl-Sieber, G. *Chemistry-a European Journal* **2000**, *6*, 1773.

165. Lu, J. M.; Yan, F.; Texter, J. *Progress in Polymer Science* **2009**, *34*, 431.

166. Bower, J. D.; Guest, K. P.; Morgan, B. A. *Journal of the Chemical Society, Perkin Transactions 1* **1976**, 2488.

167. Miao, W. S.; Chan, T. H. *The Journal of Organic Chemistry* **2005**, *70*, 3251.

168. McParland, V. J.; Kad, N. M.; Kalverda, A. P.; Brown, A.; Kirwin-Jones, P.; Hunter, M. G.; Sunde, M.; Radford, S. E. *Biochemistry* **2000**, *39*, 8735.

169. Jones, S.; Manning, J.; Kad, N. M.; Radford, S. E. *Journal of Molecular Biology* **2003**, *325*, 249.

170. Redemann, T.; Jung, G. Peptides 1996. In *Proceedings of the 24th European Peptide Symposium*; Ramage, R., Epton, R., Eds.; Mayflower Scientific Ltd: Kingswinford, UK, 1998; p 749.

171. Carpino, L. A.; Krause, E.; Sferdean, C. D.; Schumann, M.; Fabian, H.; Bienert, M.; Beyermann, M. *Tetrahedron Letters* **2004**, *45*, 7519.

172. Taylor, J. P.; Hardy, J.; Fischbeck, K. H. *Science* **2002**, *296*, 1991.

173. Brody, D. L.; Holtzman, D. M. *Annual Review of Neuroscience* **2008**, *31*, 175.

174. Caughey, B.; Lansbury, P. T. *Annual Review of Neuroscience* **2003**, *26*, 267.

175. Meldal, M. Solid-Phase Peptide Synthesis. In *Methods in Enzymology*; Gregg, B. F., Ed.; Academic Press: New York, 1997; Vol. 289, pp 83−104.

176. Barany, G.; Kempe, M. The Context of Solid-Phase Synthesis. In *A Practical Guide to Combinatorial Chemistry*; Czarnik, A. W., Dewitt, S. H., Eds.; American Chemical Society Books: Washington, DC, 1997; pp 51−97.

177. Zalipsky, S.; Chang, J. L.; Albericio, F.; Barany, G. *Reactive Polymers* **1994**, *22*, 243.

178. Adams, J. H.; Cook, R. M.; Hudson, D.; Jammalamadaka, V.; Lyttle, M. H.; Songster, M. F. *Journal of Organic Chemistry* **1998**, *63*, 3706.

179. Gooding, O. W.; Baudart, S.; Deegan, T. L.; Heisler, K.; Labadie, J. W.;

Newcomb, W. S.; Porco, J. A.; van Eikeren, P. *Journal of Combinatorial Chemistry* **1999**, *1*, 113.

180. Maeji, N. J.; Valerio, R. M.; Bray, A. M.; Campbell, R. A.; Geysen, H. M. *Reactive Polymers* **1994**, *22*, 203.

181. Ede, N. J. *Journal of Immunological Methods* **2002**, *267*, 3.

182. Ercole, F.; FitzGerald, M.; Perera, S.; Ede, N.; Riley, P.; Campbell, R. *Journal of Applied Polymer Science* **2003**, *89*, 3371.

183. Meldal, M. *Tetrahedron Letters* **1992**, *33*, 3077.

184. Renil, M.; Ferreras, M.; Delaisse, J. M.; Foged, N. T.; Meldal, M. *Journal of Peptide Science* **1998**, *4*, 195.

185. Kempe, M.; Barany, G. *Journal of the American Chemical Society* **1996**, *118*, 7083.

186. Rademann, J.; Grotli, M.; Meldal, M.; Bock, K. *Journal of the American Chemical Society* **1999**, *121*, 5459.

187. Miranda, L. P.; Lubell, W. D.; Halkes, K. M.; Groth, T.; Grotli, M.; Rademann, J.; Gotfredsen, C. H.; Meldal, M. *Journal of Combinatorial Chemistry* **2002**, *4*, 523.

188. Garcia-Martin, F.; Quintanar-Audelo, M.; Garcia-Ramos, Y.; Cruz, L. J.; Gravel, C.; Furic, R.; Cote, S.; Tulla-Puche, J.; Albericio, F. *Journal of Combinatorial Chemistry* **2006**, *8*, 213.

189. Tam, J. P.; Lu, Y. A. *Journal of the American Chemical Society* **1995**, *117*, 12058.

190. Rademann, J.; Barth, M.; Brock, R.; Egelhaaf, H. J.; Jung, G. *Chemistry-a European Journal* **2001**, *7*, 3884.

191. Sugahara, K. N.; Teesalu, T.; Karmali, P. P.; Kotamraju, V. R.; Agemy, L.; Girard, O. M.; Hanahan, D.; Mattrey, R. F.; Ruoslahti, E. *Cancer Cell* **2009**, *16*, 510.

192. Sugahara, K. N.; Teesalu, T.; Karmali, P. P.; Kotamraju, V. R.; Agemy, L.; Greenwald, D. R.; Ruoslahti, E. *Science* **2010**, *328*, 1031.

193. Fujii, N.; Otaka, A.; Funakoshi, S.; Bessho, K.; Watanabe, T.; Akaji, K.; Yajima, H. *Chemical & Pharmaceutical Bulletin* **1987**, *35*, 2339.

194. Lee, H. N.; Jeon, J. H.; Lim, J. C.; Choi, H.; Yoon, Y. H.; Kim, S. K. *Organic Letters* **2007**, *9*, 3291.

195. Yu, H. M.; Chen, S. T.; Wang, K. T. *Journal of Organic Chemistry* **1992**, *57*, 4781.

196. Shmerling, D.; Hegyi, I.; Fischer, M.; Blattler, T.; Brandner, S.; Gotz, J.; Rulicke, T.; Flechsig, E.; Cozzio, A.; von Mering, C.; Hangartner, C.; Aguzzi, A.; Weissmann, C. *Cell* **1998**, *93*, 203.

197. Li, A. M.; Christensen, H. M.; Stewart, L. R.; Roth, K. A.; Chiesa, R.; Harris, D. A. *Embo Journal* **2007**, *26*, 548.

Appendix

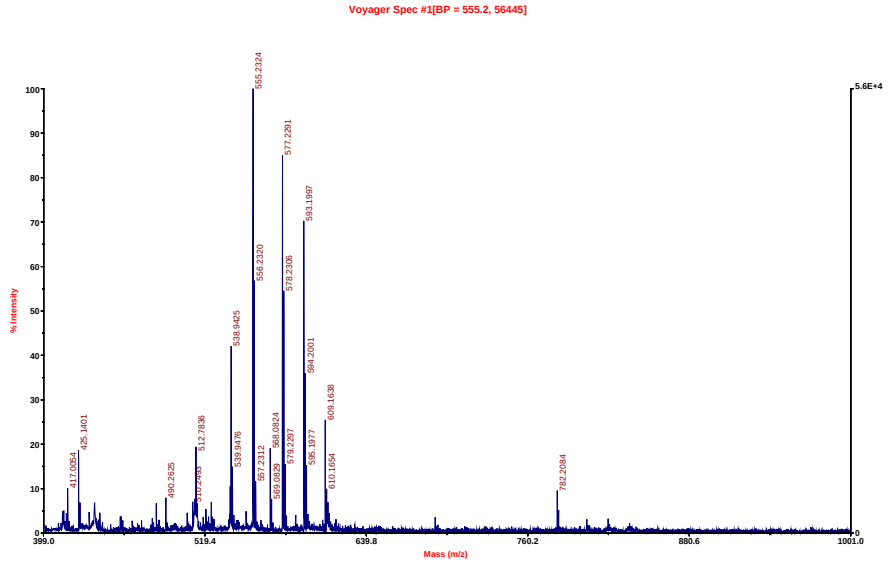

Figure A. 1. Mass analysis of Leu-enkephalin (calcd 555.65 for $C_{28}H_{39}N_6O_6$ (YGGFL-NH_2) [M+H]+, found 555.2)

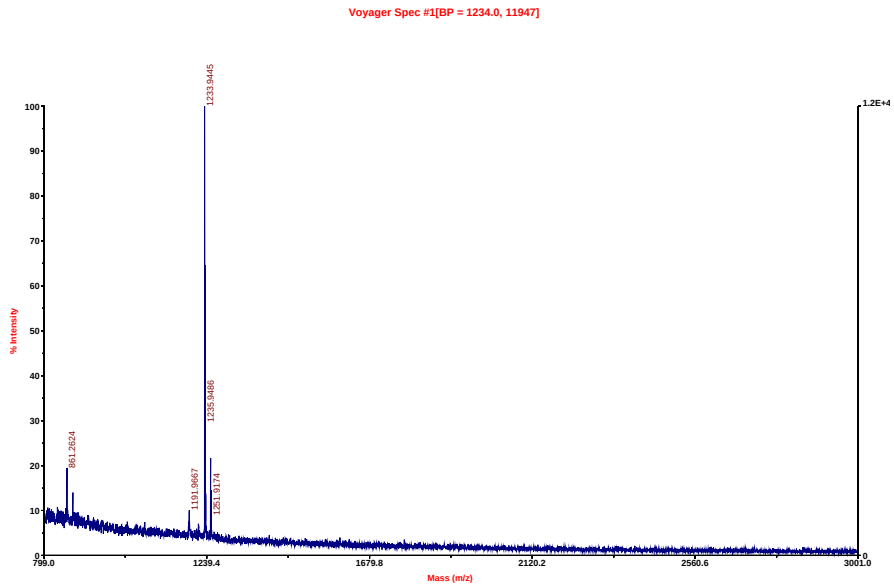

Figure A. 2. Mass analysis of JR 10-mer (calcd 1234.46 for $C_{58}H_{90}N_{12}NaO_{14}S$ (JR 10-mer)[M+Na]+, found 1234.0)

(a)

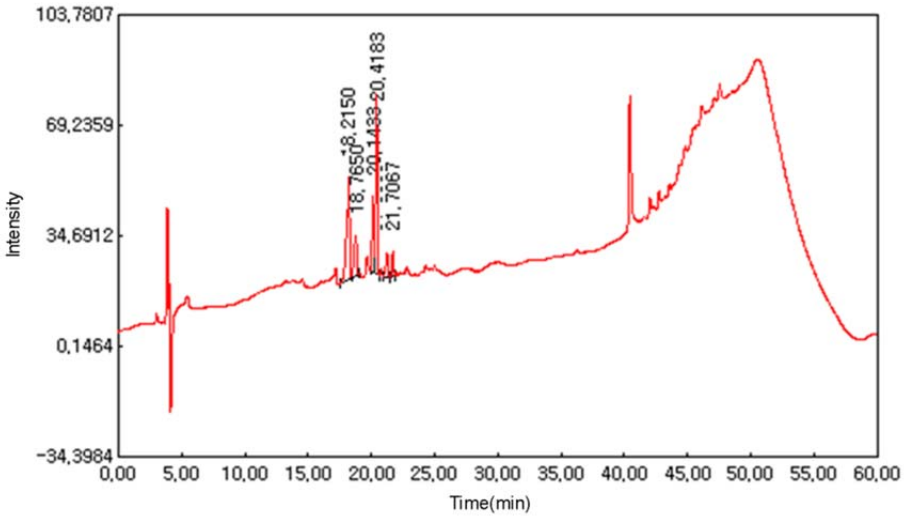

(b)

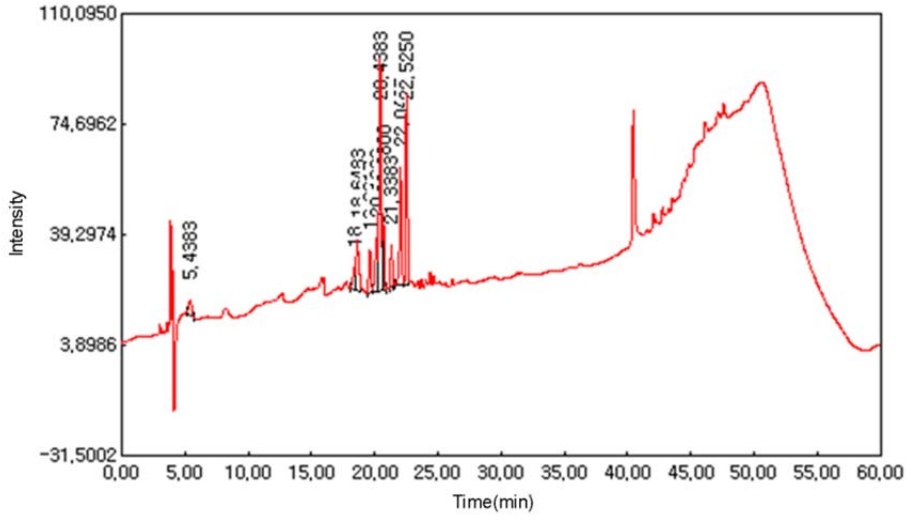

Figure A. 3. HPLC analysis of the crude ACP (65−74) peptide prepared on (a) low loaded AM PS resin and (b) high loaded AM PS resin.

(a)

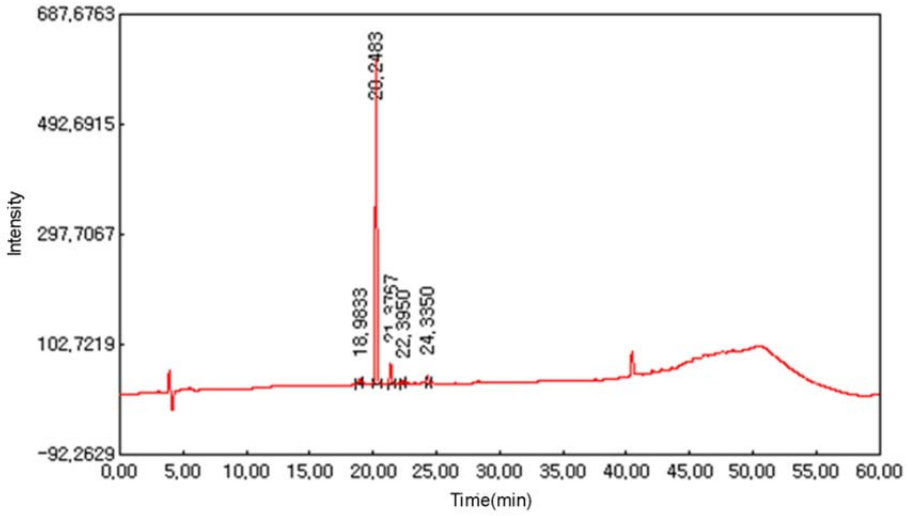

(b)

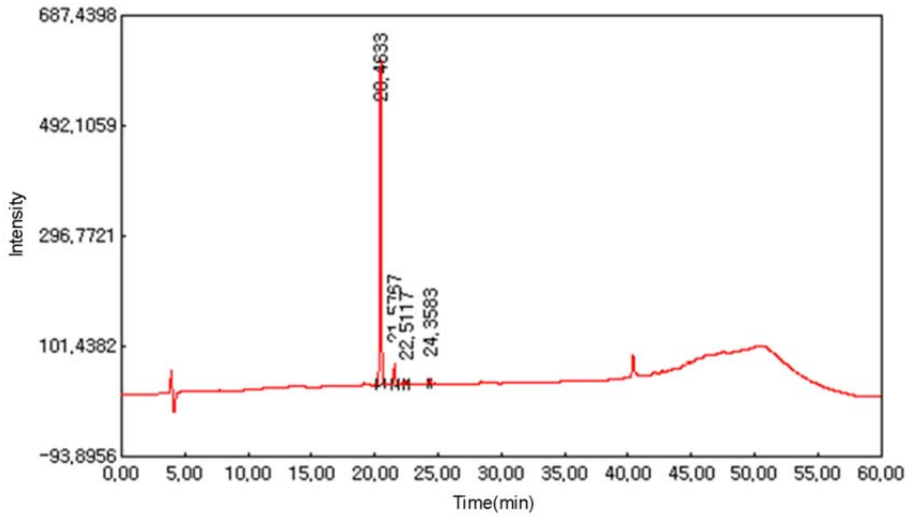

Figure A. 4. HPLC analysis of the crude ACP (65–74) peptide prepared on (a) low loaded core–shell type resin and (b) high loaded core–shell type resin.

(a)

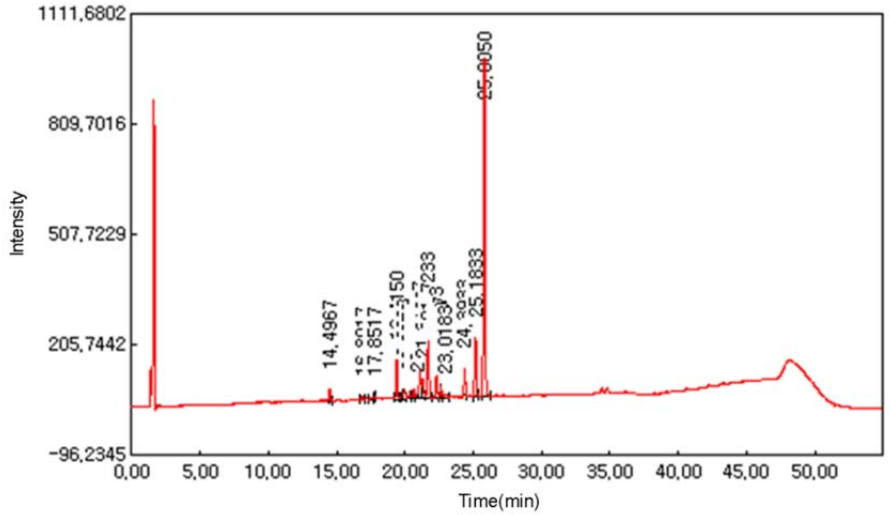

(b)

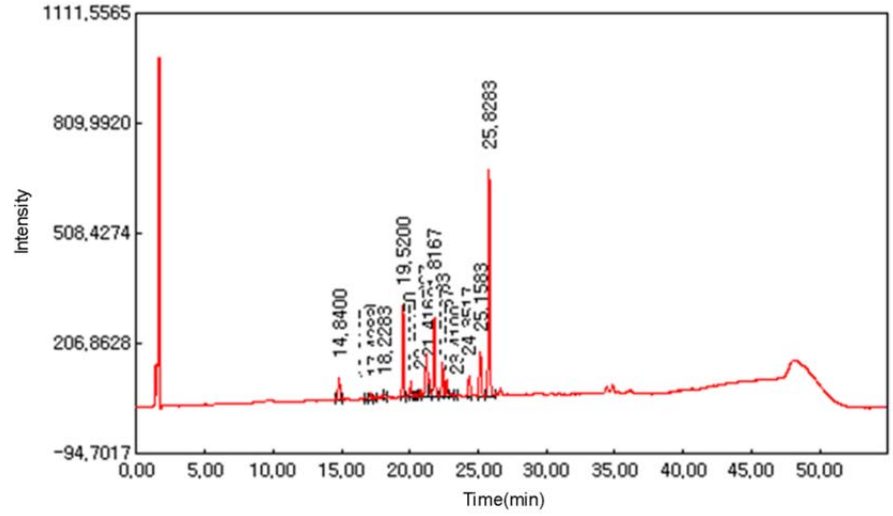

Figure A. 5. HPLC analysis of the crude JR 10-mer peptide prepared on (a) low loaded AM PS resin and (b) high loaded AM PS resin.

(a)

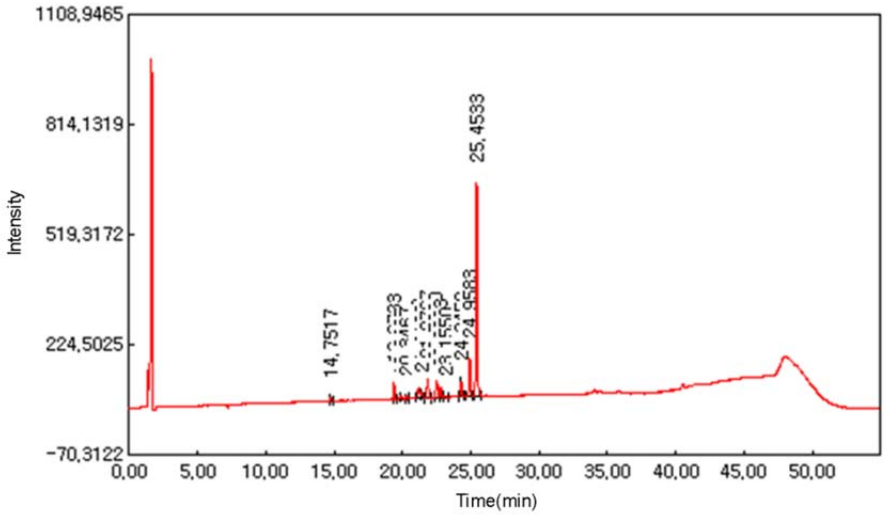

(b)

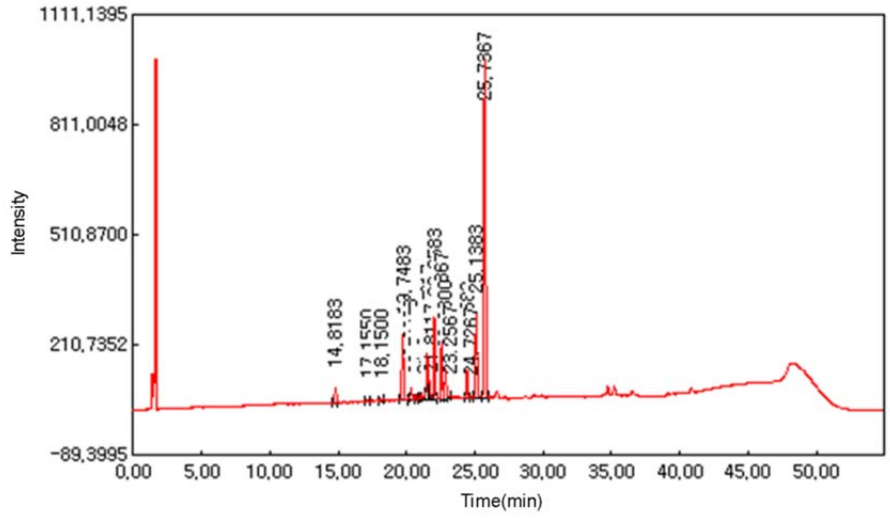

Figure A. 6. HPLC analysis of the crude JR 10-mer peptide prepared on (a) low loaded core–shell type resin and (b) high loaded core–shell type resin.

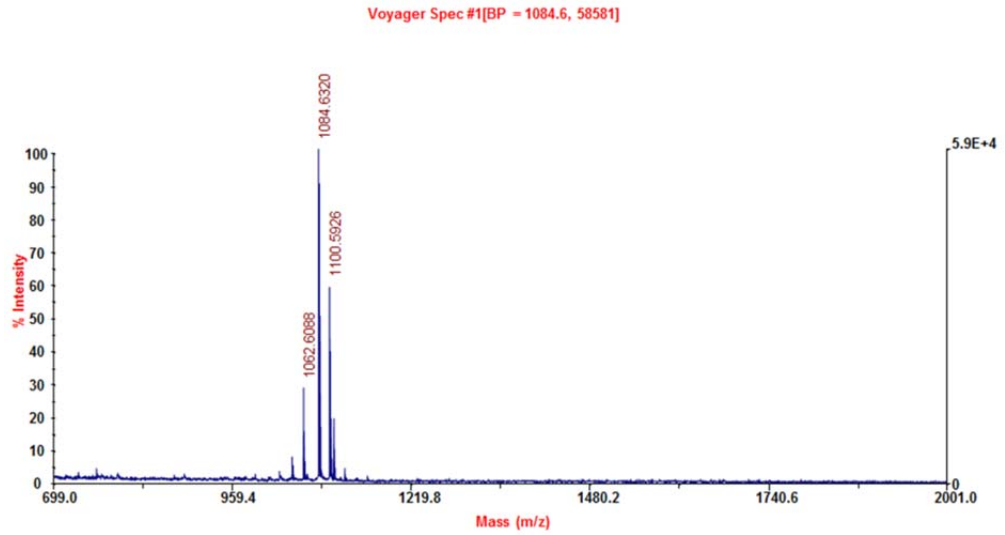

Figure A. 7. MALDI-TOF mass analysis of ACP (65–74) peptide ([M+Na] = 1084.6).

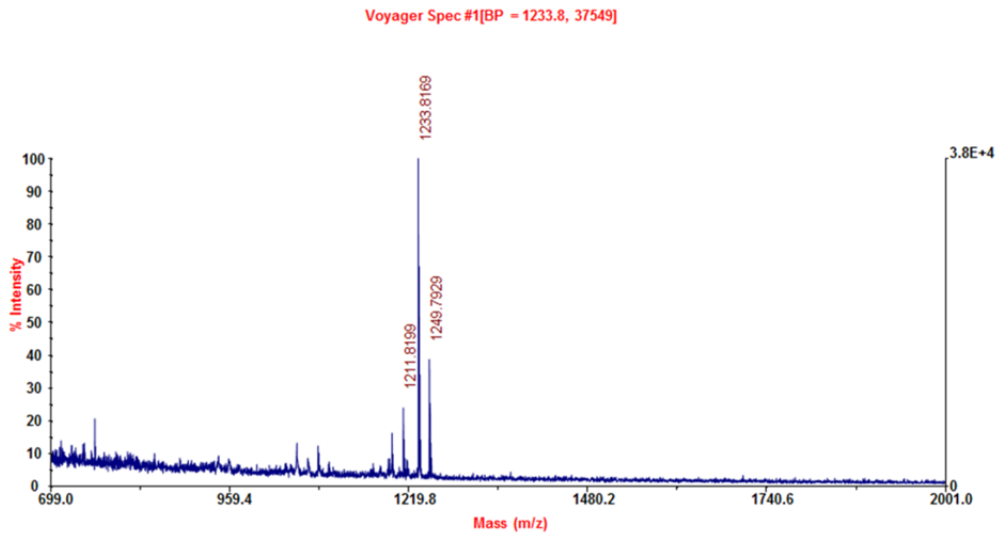

Figure A. 8. MALDI-TOF mass analysis of JR 10-mer peptide ([M+Na] = 1233.8).

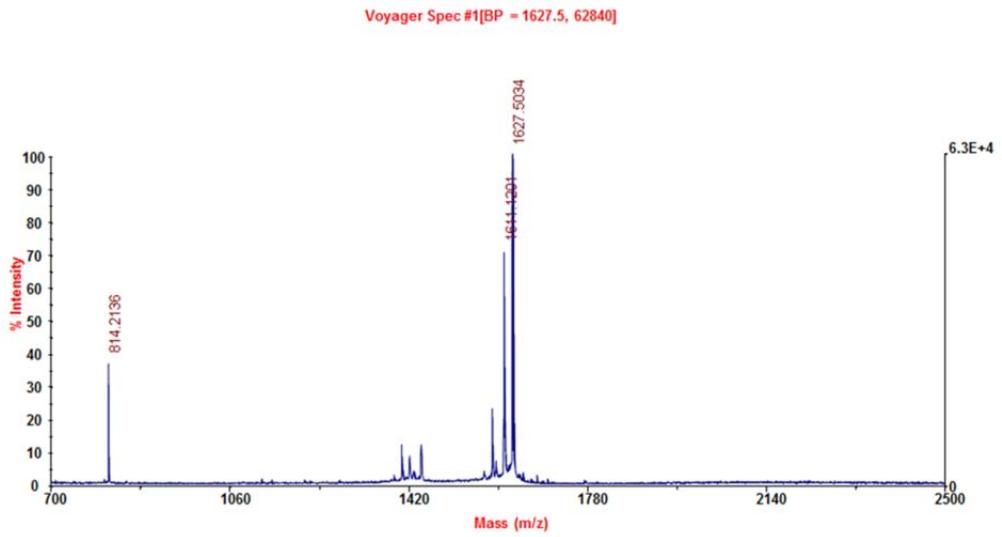

Figure A. 9. MALDI-TOF mass analysis of Fmoc-iRGD peptide ([M+H] = 1627.5).

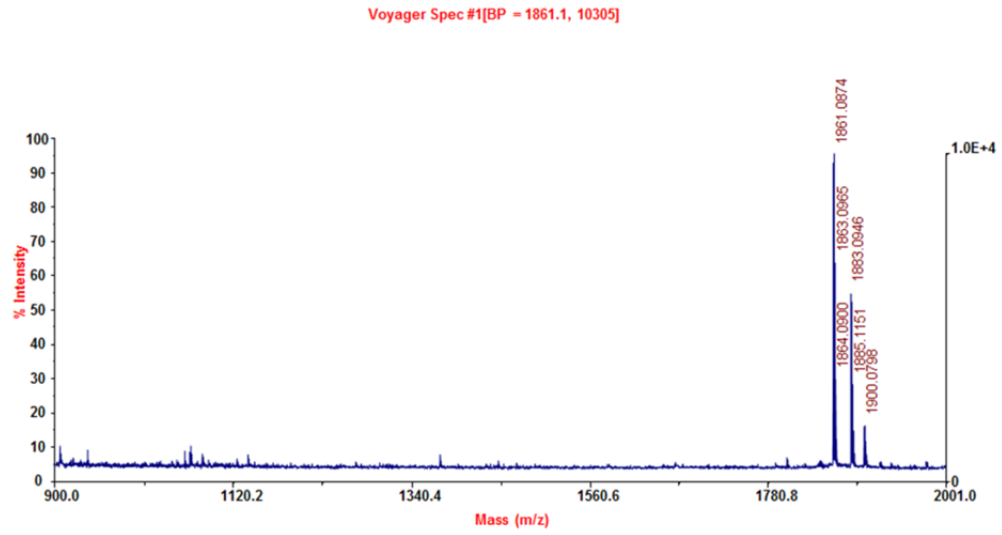

Figure A. 10. MALDI-TOF mass analysis of MoPrP(105–125) peptide ([M+H] = 1861.1).

(a)

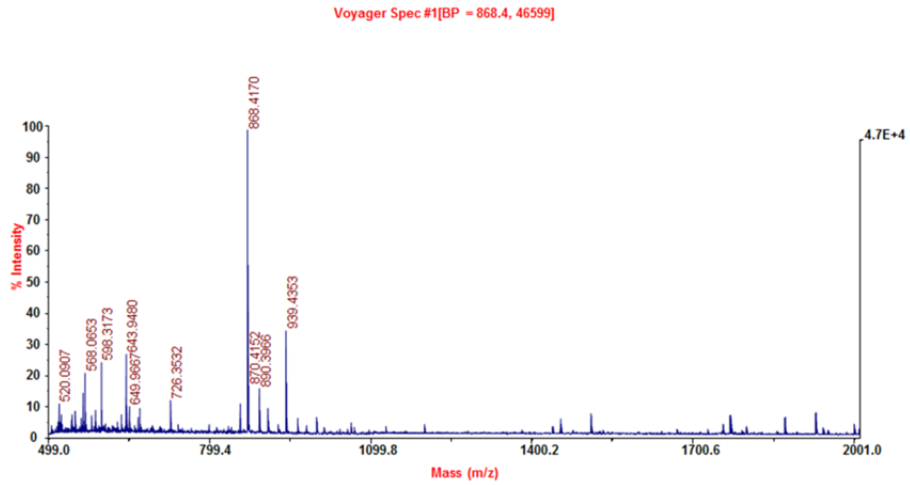

(b)

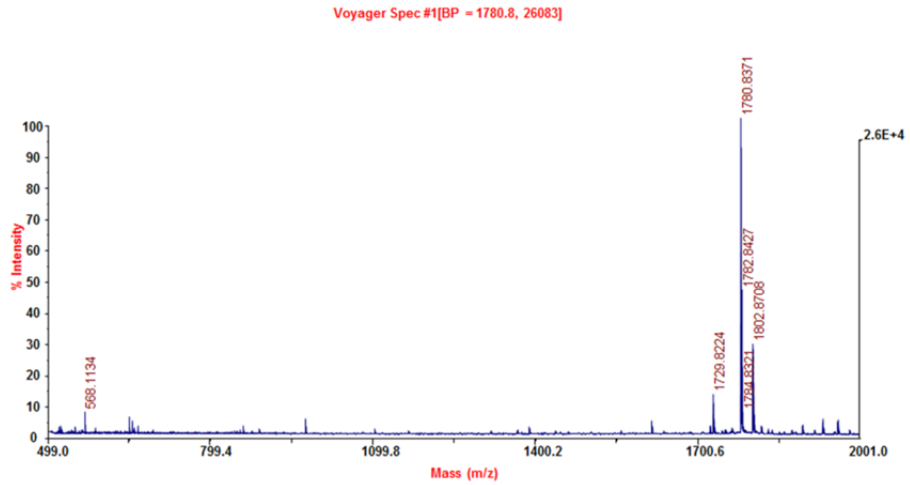

Figure A. 11. MALDI-TOF mass analysis of MoPrP(105–125) peptide fragments (a) [M+H] = 939.4, [M-Ala+H] = 868.4, t_R = 13.6 min and (b) [M+H] = 1780.8, t_R = 15.0 min.

요 약

고분자 지지체는 유기 합성이나 화학 공정에서 아주 유용하게 사용되는 물질이다. 금속 또는 유기 촉매가 고정화된 고분자 지지체는 비균일계 촉매로서 많이 사용되고, 기능기가 도입된 고분자 지지체는 고체상 펩타이드 합성이나 고체상 유기 합성에 많이 사용되고 있다. 이러한 고분자 지지체를 이용하면 간단한 여과로 이 지지체를 쉽게 회수할 수 있으며 여러 번 재사용이 가능하다. 또한 반복적인 반응과 여과과정이 포함된 간단한 화학 공정을 만들어낼 수 있다. 이러한 장점들에도 불구하고, 고분자 지지체를 사용하는 반응은 고체와 액체 사이에서 반응이 일어나기 때문에 여러 문제점들이 존재한다. 따라서 불균일계 촉매 분야나 고체상 펩타이드 합성분야에서는 여전히 효과적인 고분자 지지체를 개발하는 것이 요구 되고 있다.

본 논문에서는 세가지 다른 종류의 고분자 지지체를 개발하여 효과적인 스즈키 반응과 고체상 펩타이드 합성에 적용하였다.

첫 번째로 스즈키 커플링 반응에 불균일계 촉매로 사용할 여러 가지 옥심 팔라다싸이클 수지를 개발하였다. 기존에 사용되고 있는 카이저 옥심 수지와 다르게 전자가 풍부한 옥심 수지는 팔라듐 복합체를 아주 효과적

이고 안정하게 형성하였다. 리간드의 전자 밀도는 메톡시기의 숫자에 따라 조절되었다. 탄소-탄소 커플링 반응에서 옥심 리간드의 전자 효과는 제조된 옥심 팔라듐 촉매를 여러 가지 할로젠화 아릴과 페닐보론 산의 반응에 적용함으로써 알아볼 수 있었다. 가장 전자가 풍부한 옥심 수지를 이용하면 스즈키 커플링 반응을 아주 좋은 수율로 보낼 수 있었고 높은 전환수를 심한 팔라듐 금속의 해리 없이 얻을 수 있었다. 재사용 실험에서도 메톡시기 두개를 가진 옥심 팔라듐 수지 촉매가 좋은 촉매 활성을 유지한 채로 5번까지 재사용이 가능함을 보여주었다.

두 번째로, 여러 가지 이온성 액체 수지들은 각 이온성 액체를 폴리스티렌 수지에 고정화함으로써 제조할 수 있었다. 이온성 액체 수지들의 성질은 각각의 이온성 액체에 따라서 급격하게 변화되었다. 초기 아미노산의 커플링 반응과 펩타이드 합성을 통하여 이 이온성 액체 수지들의 성능을 확인하였다. PF_6^-와 $TFSI^-$ 음이온을 가진 이온성 액체 수지에서 첫 번째 아미노산 커플링 반응이 아주 효과적으로 진행됨을 알 수 있었고, 이 수지들을 이용하여 펩타이드 합성을 시도한 결과 아미노폴리스티렌 수지에서 보다 높은 순도의 펩타이드를 얻을 수 있었다.

세 번째로, 간단하고 온화한 조건에서 저비용으로 코어-쉘 구조의 수지를 개발하였다. 코어-쉘 구조는 Fmoc-Osu을 아미노폴리스티렌 수지의 바깥쪽 부분에만 결합시킴으로써 만들었다. 이 방법을 사용하여 껍질부

분의 두께를 온화한 조건으로 조절이 가능하였다. 이 코어-쉘 수지의 성능은 고체상 펩타이드 합성 방법을 이용하여 여러 가지 펩타이드를 합성함으로써 상용화된 아미노폴리스티렌 수지나 폴리에틸렌글리콜로 만들어진 수지와 비교하여 평가하였다. 이 코어-쉘 수지를 이용하여 합성하기 어려운 펩타이드, 이황화물을 포함한 고리형 펩타이드, 그리고 펩타이드 핵산을 효과적으로 합성하였다. 또한 소수성 펩타이드 서열을 많이 가지고 있는 마우스 프리온 펩타이드 합성에 적용한 결과 기존에 사용되고 있는 아미노폴리스티렌 수지나 켐메트릭스 수지 보다 코어-쉘 수지에서 더욱 효과적으로 합성 됨을 확인하였다.

주요어: 스즈키 커플링 반응, 불균일계 촉매, 옥심 팔라다싸이클 수지, 고체상 펩타이드 합성, 이온성 액체 수지, 표피형 구조 수지

학번: 2007-21226